Charles University
Second Faculty of Medicine

Doctoral study programme: Neurosciences

Mgr. Ingrid Vargová

Study of mechanisms influencing inflammatory and neurodegenerative processes and their subsequent treatment in models of ALS and spinal cord injury

Studium mechanismů ovlivňujících zánětlivé a neurodegenerativní procesy a jejich následná léčba na modelech ALS a míšního poranění

Dissertation thesis

Supervisor: doc. RNDr. Pavla Jendelová, Ph.D.

Prague, 2022

Prohlášení

Prohlašuji, že jsem disertační práci zpracovala samostatně a že jsem řádně uvedla a citovala všechny použité prameny a literaturu. Současně prohlašuji, že práce nebyla využita k získání jiného nebo stejného titulu.

Souhlasím s trvalým uložením elektronické verze mé práce v databázi systému meziuniverzitního projektu Theses.cz za účelem soustavné kontroly podobnosti kvalifikačních prací.

V Praze, 30.05.2022

Ingrid Vargová

……

Podpis autora

Acknowledgment

I would like to express my gratitude to Assoc. Prof. Pavla Jendelová, PhD. for supervising my studies. I am also sincerely grateful to Prof. James W. Fawcett and Dr. Jessica C.F. Kwok for their mentorship and guidance. I would also like to thank my colleagues from the Department of Neuroregeneration, close friends and family for their support throughout my studies.

ABSTRACT

Study of mechanisms influencing inflammatory and neurodegenerative processes and their subsequent treatment in models of ALS and spinal cord injury

The mechanisms of neurodegeneration during spinal cord injury (SCI) and amyotrophic lateral sclerosis (ALS) are complex and poorly understood, which is why it's troublesome to counteract them with effective therapies. This thesis explores the pathways of autophagy, endoplasmic reticulum (ER) stress, and the mammalian target of rapamycin (mTOR) pathway that regulates these mechanisms in models of both SCI and ALS. Upregulation of autophagy and the mTOR pathway in an *in vivo* contusion SCI injury model was confirmed. The mTOR inhibition led to upregulation of autophagy, reduction of inflammation, and recovery in acute SCI. Upregulated autophagy was discovered in the $SOD1^{G93A}$ rat model of ALS. By treating the ALS rats with human mesenchymal stem cells, prolonged survival of the animals and preservation of motor neurons (MNs) possibly occurred through modulation of autophagy. The involvement of the mTOR pathway in the degeneration of MNs was further explored in the context of astrocytes. Pleckstrin homology like domain family A member 3 (PHLDA3), a newly discovered repressor of the mTOR pathway, was found to lead to ER stress if overexpressed in astrocytes and can lead to the death of MNs *in vitro*. Finally, the mTOR pathway was shown to be involved in the maturation of a newly developed model of primary spinal cord neurons. Primary neurons isolated from embryonic mice mature *in vitro* and lose their regenerative ability, making the model useful for further exploration of mechanisms involved in degeneration and regeneration of the spinal cord neurons. Together these results broaden the knowledge of the complex processes that take place in the spinal cord during the pathology and treatment of SCI and ALS.

Keywords

spinal cord injury, amyotrophic lateral sclerosis, neurodegeneration, inflammation, autophagy, ER stress, mTOR, PHLDA3, *in vitro* model

ABSTRAKT

Studium mechanismů ovlivňujících zánětlivé a neurodegenerativní procesy a jejich následná léčba na modelech ALS a míšního poranění

Neurodegenerativní mechanismy probíhající během poranění míchy (MP) a amyotrofické laterální sklerózy (ALS) jsou složité a nedostatečně prozkoumané, a proto je problematické jim čelit účinnými terapiemi. Tato práce zkoumá dráhy autofagie, stresu endoplazmatického retikula (ER) a dráhu savčího cíle rapamycinu (mTOR), která tyto mechanismy reguluje, v modelech MP i ALS. Potvrdili jsme zvýšenou aktivitu mTOR dráhy v *in vivo* modelu MP. Inhibice mTOR dráhy vedla k upregulaci autofagie, snížení zánětu a k částečnému zotavení při akutním MP. Upregulace autofagie byla objevena na $SOD1^{G93A}$ potkaním modelu ALS. Podání lidských mezenchymálních kmenových buněk ALS potkanům vedlo k prodloužení přežití zvířat a zachování motorických neuronů, částečně prostřednictvím modulace autofagie. Účast mTOR dráhy na degeneraci motorických neuronů byla blíže zkoumána z hlediska astrocytů. Zjistilo se, že nově objevený represor mTOR dráhy, PHLDA3 (z angl. *pleckstrin homology like domain family A member 3*), vede ke stresu ER, je-li nadměrně exprimován v astrocytech a může vést ke smrti motorických neuronů *in vitro*. Nakonec jsme ukázali, že mTOR dráha se podílí na zrání nově vyvinutého modelu primárních neuronů míchy. Primární neurony izolované z embryonálních myší dozrávají *in vitro* a ztrácejí svou regenerační schopnost, díky čemuž je model užitečný k dalšímu zkoumání mechanismů zapojených do degenerace a regenerace neuronů míchy. Tyto výsledky společně rozšiřují poznatky o složitých procesech, které probíhají v míše během patologie a léčby MP a ALS.

Klíčová slova

míšní poranění, amyotrofická laterální skleróza, neurodegenerace, zánět, autofagie, ER stres, mTOR, PHLDA3, *in vitro* model

LIST OF ABBREVIATIONS

4E-BP	eukaryotic translation initiation factor 4E -binding protein
βIIIt	βIII-tubulin
ACM	astrocyte conditioned medium
AL	autolysosome
ALS	amyotrophic lateral sclerosis
AP	autophagosome
ATF4	activating transcription factor 4
ATF6	activating transcription factor 6
BDNF	brain-derived neurotrophic factor
BiP	immunoglobulin-binding protein
BSA	bovine serum albumin
CACM	CMV astrocyte conditioned medium
CCL	C-C motif chemokine ligand
ChAT	choline acetyltransferase
CHOP	CAAT/enhancer-binding protein homologous protein
C_m	membrane capacitance
CNS	central nervous system
CXCL	C-X-C motif chemokine ligand
DBC	doublecortin
DIV	day *in vitro*
DRG	dorsal root ganglia
eIF2α	eukaryotic translation initiation factor 2 α
E_m	resting membrane potential
EphB1	ephrin type-B receptor 1
ER	endoplasmic reticulum
FBS	fetal bovine serum
FUS	encoding RNA binding protein FUS
GADD34	growth arrest and DNA damage-inducible 34
GAP43	growth-associated protein 43
GDNF	glial cell-derived neurotrophic factor
GFAP	glial fibrillary acidic protein

GFP	green fluorescent protein
GFRα1	GDNF family receptor alpha-1
hMSC	human mesenchymal stem cells
HSCs	hematopoietic stem cell
ICC	immunocytochemistry
IFN	interferon
IHC	immunohistochemistry
I_{Na+}	sodium currents
IL	interleukin
IR	input resistance
IRE1	inositol-requiring enzyme 1
IRS-1	insulin receptor substrate-1
JAK1	Janus kinase 1
JNK	c-Jun N-terminal kinase
LC3	microtubule-associated protein 1A/1B-light chain 3
LDH	lactate dehydragenase
MN	motor neuron
MP	míšní poranění (spinal cord injury)
mRNA	messenger ribonucleic acid
MSCs	mesenchymal stem cells
mTOR	mammalian target of rapamycin
mTORC1	mammalian target of rapamycin complex 1
mTORC2	mammalian target of rapamycin complex 2
NAR	nicotinic acetylcholine receptor α-7 (NAR)
ND	neurodegenerative disease
NF70	neurofilament 70kDa
NF-κB	nuclear factor kappa-light-chain-enhancer of activated B cells
NMJ	neuromuscular junction
NSCs	neural stem cells
PACM	PHLDA3 astrocyte conditioned medium
PBS	phosphate buffer saline
PERK	protein kinase RNA-activated-like ER kinase

PFA	paraformaldehyde
PHLDA3	pleckstrin homology like domain family A member 3
PI3K	phosphatidylinositol 3-kinase
PI3P	phosphatidylinositol 3,4,5-triphosphate
PIP	phosphatidylinositol phosphates
PKCγ	protein kinase C gamma
PTEN	phosphatase and tensin homolog
PV	parvalbumin
Rab	Ras-associated binding protein
RANTES	regulated on activation, normal T cell expressed and secreted
RAPA	rapamycin
RFP	red fluorescent protein
RNase	endoribonuclease
ROS	reactive oxygen species
S6	ribosomal protein S6
S6K	ribosomal protein S6 kinase
SCI	spinal cord injury
SOD1	superoxide dismutase 1
SpINs	spinal interneurons
SQSTM1	sequestosome 1
STAT3	signal transducer and activator of transcription 3
Syn	synaptophysin
TBST	Tris-buffered saline/Tween-20
TDP-43	TAR DNA-binding protein 43
Tg	transgenic
TGF- β1	transforming growth factor β1
TNF	tumor necrosis factor
TUNEL	terminal deoxynucleotidyl transferase-mediated dUTP biotin nick-end labeling
ULK1	Unc-51 Like Autophagy Activating Kinase 1 complex
UPR	unfolded protein response
VEGF	vascular endothelial growth factor
VGAT	vesicular gamma-aminobutyric acid transporter

VGLUT1	vesicular glutamate transporter 1
WIPI2	WD repeat domain phosphoinositide-interacting protein 2
WT	wild type
XBP1	X-box-binding protein 1

TABLE OF CONTENTS

1. INTRODUCTION

Neurodegeneration is a pathological process during which loss of nervous system function and structure occurs. In principle, neurodegenerative diseases (NDs) are a large group of disorders with diverse pathologies, involving neurons in particular anatomic structures. Their etiology is complex, not well understood and their progression is usually inevitable. and relentless (Przedborski et al., 2003). On the other hand, even though the causes of edema, hemorrhage, or trauma of the nervous system are known, they similarly lead to extensive neuronal degeneration, which mechanisms are still not yet fully elucidated.

A major reason it has been so difficult to describe and treat neurodegenerative diseases and injury of the central nervous system (CNS) is the special and complex characteristics of neurons. Neurons are postmitotic, which means they do not exhibit cell division after fetal development and generally cannot be substituted when lost. Furthermore, the morphology of neurons is also a cause of their vulnerability (Wolfe, 2018). To facilitate the flow of information coded into electric signals in the nervous system, neurons possess dendrites - short processes and axons - long processes that can extend over great distances to connect with other neurons. These connections and their maintenance are crucial for the health of neurons and if they are disrupted, it can lead to neuronal dysfunction and death (Bell and Hardingham, 2011). Although neurogenesis and formation of new circuits in adult CNS do occur (Darian-Smith, 2009; Bergmann et al., 2015) and we do no longer fully agree with the opinion that the CNS is “fixed and immutable” as was believed in the twentieth century (Cajal, 1991), regenerative processes that are present are too limited to compensate the neuronal death that happens as a consequence of injury or disease. It is therefore of utmost importance to study the cellular mechanisms that lead to neuronal degeneration and how proposed treatments counteract it.

1.1. Cellular processes involved in neurodegeneration

There are numerous fundamental pathologic mechanisms associated with progressive neuronal death, that are shared by many NDs, as well as CNS trauma. These include abnormal protein dynamics and misfolding, accompanied by endoplasmic reticulum (ER) stress, abnormalities in autophagy, mitochondrial dysfunction, disruption of cellular and axonal transport, induction of oxidative stress, and neuroinflammatory processes (Jellinger, 2010).

1.2. Autophagy

Autophagy is an evolutionary conserved intracellular degradation and trafficking pathway that takes in various substrates including organelles or cytoplasm contents and passes them to lysosomes. Double-membrane vesicles used for trafficking substrates in autophagy are named autophagosomes (AP). These vesicles are formed throughout the cell of most mammalian cells and are transported via dynein machinery on microtubules towards lysosomes, with which they fuse, forming autolysosomes (AL). The cargo contained within the AL can then be degraded by lysosomal proteases. The main role of autophagy is to maintain cellular homeostasis which requires constant turnover of defective organelles and proteins. It is essential in protecting the cells against stressors such as starvation, protein aggregation, infectious agents, defective organelles, and inflammation (Bento et al., 2016). Basal levels of autophagy are especially crucial for the homeostasis of terminally differentiated cells such as oligodendrocytes and neurons, as these cells cannot dispose of aggregate proteins via cell division (Lipinski et al., 2015). This renders neurons dependent on higher levels of constant, basal autophagy which can make them vulnerable to deficiencies in autophagy. The lack of efficient clearance of accumulated proteins is a hallmark of various neurodegenerative diseases (Cai et al., 2016). The exact role of autophagy in neurons is however, still not elucidated (Maday, 2016).

Autophagy impairment is not the only way how this cellular mechanism is connected to cell damage. In contrast to its' cytoprotective roles, unimpaired autophagy has been extensively connected to the induction of cell death (Noguchi et al., 2020). Its' relationship with cell death can have different aspects, as it can coincide with apoptosis or even trigger it, but it can also induce autophagy-dependent cell death a special mechanism of cell death that is independent of other known mechanisms (Denton and Kumar, 2019). Autophagy-dependent cell death has been observed during development, but also in pathophysiological conditions, especially following cerebral or myocardial ischemia (Bialik et al., 2018). The mechanism of autophagy-dependent cell death remains poorly understood. Compared to starvation-induced autophagy, cells undergoing autophagy-mediated cell death contain larger and more numerous AP (Arakawa et al., 2017). Additionally, disruption of autophagy inhibition feedback loop was found to lead to autophagy upregulation and cell death (Füllgrabe et al., 2013). Together, these results indicate that upregulation of autophagy can promote cell death.

A complex connection between autophagy and inflammation has been described (Qian et al., 2017b). Autophagy modulates the homeostasis and survival of cells propagating inflammation such as neutrophils, macrophages, and lymphocytes, and therefore indirectly influences development and pathogenesis of inflammation. Autophagy influences not only cellular inflammatory pathways but also interacts directly with immune signaling molecules (Saitoh and Akira, 2010). The interaction is bidirectional – autophagy can influence the release of cytokines, as well as cytokines can influence induction and inhibition of autophagy. It was recently established that autophagy plays an important role in acute and chronic inflammatory diseases such as Crohn's disease, pulmonary hypertension, and cystic fibrosis (Qian et al., 2017b), but its role in inflammation after CNS trauma is not yet fully understood.

More than 30 proteins act as key regulators of the autophagy mechanism, which are collectively referred to as autophagy-related genes (ATG). Each ATG plays a specific role in various phases of AP lifecycle, which can be for simplicity divided into five stages (Mannack and Lane, 2015): initiation, elongation, maturation, and fusion (Fig. 1).

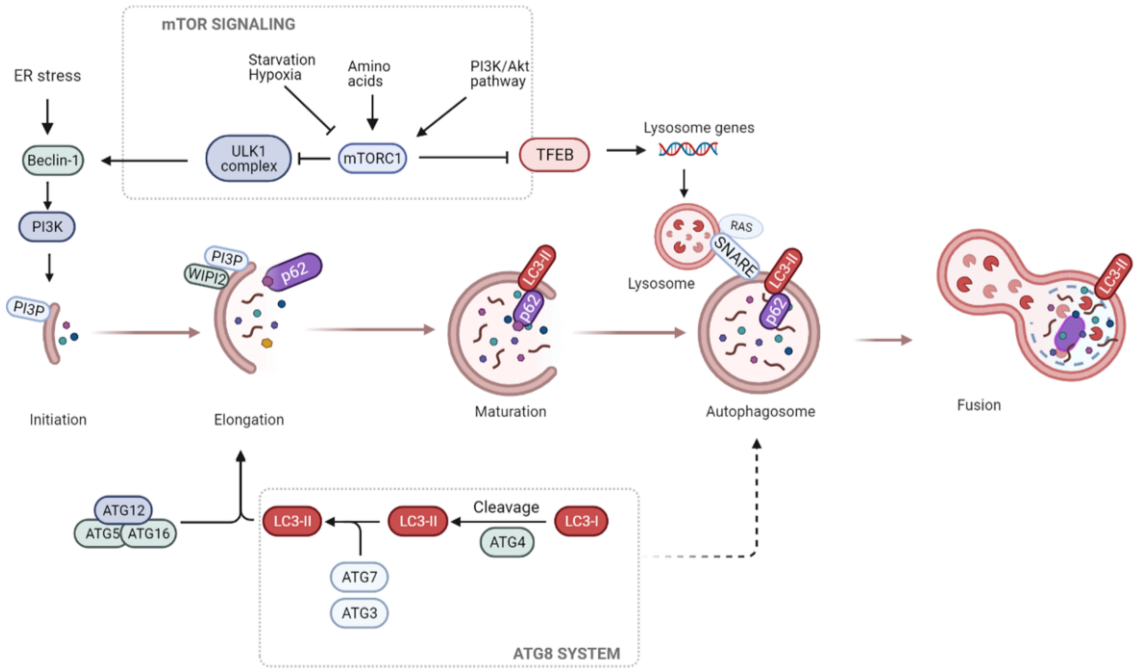

Fig. 1 Autophagy pathway consists of five stages. The mammalian target of rapamycin complex 1 (mTORC1) is a major negative regulator of autophagy. In physiological conditions, during nutrient availability, amino acids activate mTORC1. Phosphatidylinositol 3-kinase (PI3K)/Akt pathway, which transduces the signals from membrane receptors also activates mTORC1, effectively inhibiting autophagy. During starvation or hypoxia, mTORC1 is deactivated, which allows Unc-51 Like Autophagy Activating Kinase 1 complex (ULK1) to be activated. ULK1 activates Beclin-1, which can be in addition activated independently during endoplasmic reticulum (ER) stress. Beclin-1 activates PI3K, which forms phosphatidylinositol 3,4,5-triphosphate (PI3P) on a membrane that

will become an autophagosome. PI3P is needed for the elongation stage, for recruitment of WD repeat domain phosphoinositide-interacting protein 2 (WIPI2) and other autophagy-related genes (ATGs). Maturation of autophagosome is facilitated by receptor proteins, such as p62, which bring in cargo that needs to be degraded. Receptor proteins bind to microtubule-associated protein 1A/1B-light chain 3 (LC3) -II, which is integrated into the autophagosome membrane. Lysosome is fused with autophagosome with help of SNARE proteins and Ras-associated binding protein (Rab) family of GTPases. Lysosome enzymes digest the cargo within the autophagosome. Lysosome production can be inhibited by mTORC1 through transcription factor EB (TFEB) (Illustration created using BioRender.com).

1.2.1. **Initiation**

AP initiation is the first stage of autophagy. In mammalian cells, AP biogenesis is induced by cellular stressors, such as nutrient deprivation which leads to the suppression of mammalian target of rapamycin complex 1 (mTORC1) kinase. mTORC1 is a negative regulator of autophagy and once its suppressed, induction of autophagy can begin through Unc-51 Like Autophagy Activating Kinase 1 complex (ULK1) (Karanasios et al., 2016). Active ULK1 is translocated to the ER, where the formation of isolation lipid bilayer membrane – phagophore takes place. Although phagophore is initially formed on the ER, its growth around cargo in the cytoplasm is dependent on almost all intracellular membrane sources, including the plasma membrane, Golgi, the ER, mitochondria, and recycling endosomes (Hailey et al., 2010; Ravikumar et al., 2010; van der Vaart et al., 2010; Biazik et al., 2015). ULK1 recruits class III phosphatidylinositol 3-kinase (PI3K) complex to the site of phagophore biosynthesis and activates it through phosphorylation of Beclin-1 (Russell et al., 2013). PI3K generates phosphatidylinositol 3,4,5-triphosphate (PI3P), which recruits proteins required for the next step of autophagy – phagophore elongation.

1.2.2. **Elongation**

Along with others, PI3P is recruiting WD repeat domain phosphoinositide-interacting protein 2 (WIPI2) to the phagophore initiation site. WIPI2 then facilitates recruitment of ATG5/12/16 complex, which is needed for lipidation of ATG8 family, including microtubule-associated protein 1A/1B-light chain 3 (LC3) (Dooley et al., 2014). LC3 protein is initially present in cytosol, in its form LC3-I is conjugated to phosphatidylethanolamine to form LC3-II which is then required to form the AP membrane. Levels of LC3 isoform, LC3b, and especially the lapidated LC3b-II form are routinely used for monitoring autophagy (Tanida et al., 2008; Klionsky et al., 2021). ATG5/12/16 complex is considered to act as a scaffold for the growing AP and is one of the two ubiquitin-like complexes

mediating elongation. The second complex is mediating the processing of the ATG8 by Atg4, Atg7, and Atg3.

In nonselective, so-called bulk autophagy, contents of the cytoplasm are randomly enveloped within the elongating AP. However, this is not the only mechanism of how the cargo is packed into the AP. Specific cargos tagged by receptors can be sent to the APs during selective autophagy. Receptor proteins such as sequestosome 1 (SQSTM1) also known as p62, NIX of Optineurin identify and deliver damaged organelles or misfolded proteins to AP for degradation. These receptors have motifs that interact with LC3 bound to the phagophore membrane, which enables the anchoring of the cargo to the growing AP (Pankiv et al., 2007; Novak et al., 2010; Richter et al., 2016). Monitoring of autophagy and autophagic flux can be effectively performed by comparing the LC3b-II and p62 protein levels (Klionsky et al., 2021). While LC3b-II reflects the number of APs, the upregulation of LC3-II does not estimate the reasons behind autophagic activity. The number of APs can increase due to both autophagy activation and inhibition of AP degradation – a blockage in autophagic flux. AP degradation can be assessed by p62/SQSTM1 levels because this protein is degraded together with the AP cargo. Upregulation of both proteins, therefore, points to disruption of autophagy flux, rather than activation of autophagy (Yoshii and Mizushima, 2017).

1.2.3. **Maturation**

After the contents of the AP are gathered, the membrane must be sealed by merging with itself, producing a bilayer membrane enclosing the contents. The mechanism of membrane fusion is not yet fully understood, but ATG8 involvement has been implicated (Tsuboyama et al., 2016). At this stage, machinery needed for initiation and elongation, apart from ATG8 dissociate from the newly formed AP (Stavoe and Holzbaur, 2019).

1.2.4. **Fusion**

Once an AP is formed, it's carried along microtubules using a dynein motor toward the perinuclear area for fusion with the lysosome (Maday et al., 2012). The fusion mechanism requires coordination of three protein families involved in intracellular membrane trafficking: Ras-associated binding protein (Rab) family of GTPases, membrane-tethering complexes, and SNARE proteins (Bento et al., 2016). Upon fusion with the lysosome, the pH of the autophagic vesicle is decreased through the action of proton pumps.

Lysosomal enzymes are activated once the pH drops, digesting engulfed cargos after which the degradation products are released into the cytoplasm (Glick et al., 2010). Generation of new lysosomes is dependent on transcription factor EB (TFEB). TFEB activity is repressed by mTORC1, which is another pathway through which this complex is regulating autophagy (Martina et al., 2012).

1.3. ER stress

The ER is an essential organelle present in all eukaryotic cells. It has many essential functions such as regulation of calcium homeostasis, RNA metabolism, protein and lipid synthesis, regulation of trafficking pathways, and many more (Li et al., 2020). Particularly interesting is the role of ER in protein folding. The ER possesses a surveillance system that detects proteins that have failed to properly fold or assemble via ER-based chaperones and special oligosaccharide tags. Such proteins are then transported from ER to the cytosol and subsequently degraded via autophagy pathway (Alberts et al., 2002). This process is vital to the preservation of cellular health and function and prevents unwanted protein aggregation. However, the capacity of the ER to cope with misfolded proteins can be exceeded under certain conditions. Accumulation of oxygen species, pH imbalance, nutrient deprivation, hypoxia, changes in cellular calcium levels all contribute to ER stress. (Malhotra and Kaufman, 2007; Liu and Du, 2015; Bahar et al., 2016; Dong et al., 2017). Accumulation of abnormal aggregated and misfolded proteins is a common pathological trait of numerous neurodegenerative diseases, including Alzheimer's disease, Parkinson's disease, Huntington's disease, and amyotrophic lateral sclerosis (ALS) (Hetz and Saxena, 2017). Under conditions of prolonged ER stress, a mechanism of unfolded protein response (UPR) is activated. There are three parallel pathways of the UPR activated by proteins that act as ER stress sensors:

1) inositol-requiring enzyme 1 (IRE1);
2) protein kinase RNA-activated-like ER kinase (PERK);
3) activating transcription factor 6 (ATF6) (Fig. 2).

IRE1 is a transmembrane protein with an ER-luminal sensor with serine/threonine kinase activity that is stimulated during the accumulation of unfolded proteins (Bertolotti et al., 2000). Activation of IRE1 also triggers its endoribonuclease (RNase) activity in the C-terminal domain located in the cytosol (Tirasophon et al., 1998; Kadowaki and Nishitoh, 2013), which causes cytosolic splicing of multiple target messenger ribonucleic acids

(mRNAs). One significant target is the mRNA of X-box-binding protein 1 (XBP1) (Calfon et al., 2002). Alternatively spliced XBP1 becomes a transcription factor that stimulates the expression of numerous target genes involved in the UPR (Lee et al., 2003). Additionally, IRE1 is responsible for a distinct mechanism named regulated IRE1-dependent decay, where ER-targeted mRNAs are degraded to decrease protein load on the ER (Coelho and Domingos, 2014). Chronic activation of this mechanism, however, can lead to cell death (Wang and Kaufman, 2012). IRE1 activity can furthermore lead to neuronal apoptosis through activation of the c-Jun N-terminal kinase (JNK) pathway (Nishitoh et al., 2002).

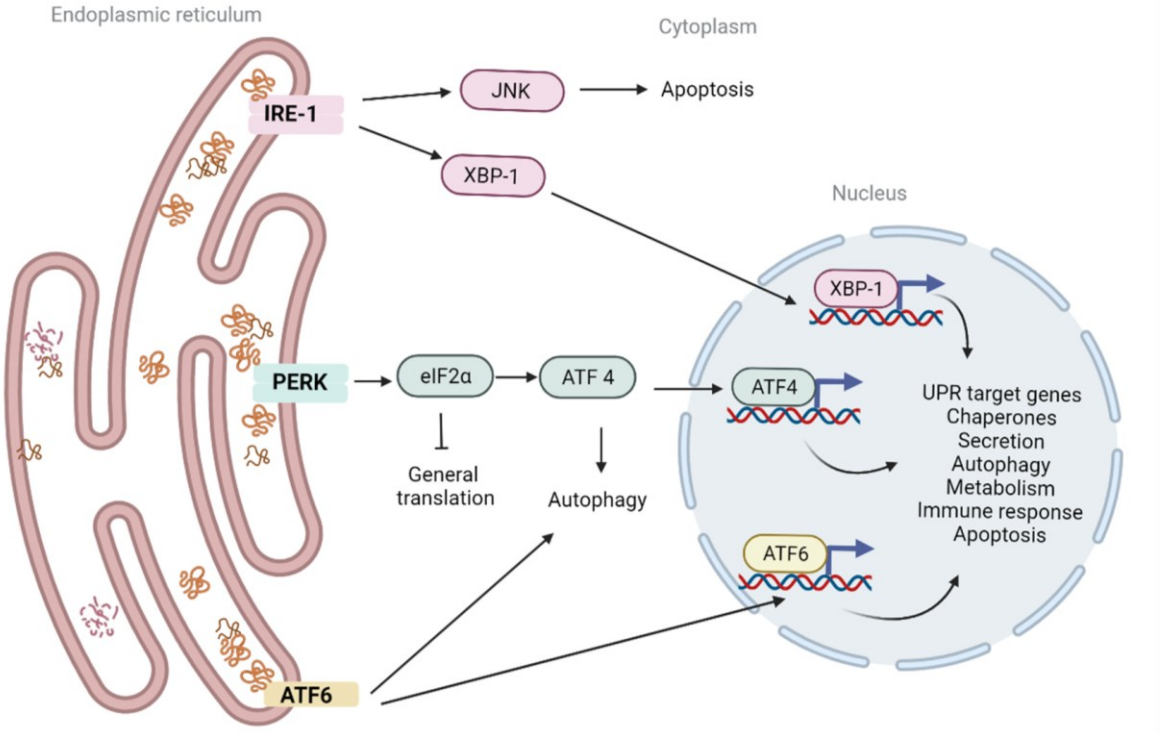

Fig. 2 Endoplasmic reticulum stress is initiated by the accumulation of misfolded proteins in the lumen of the endoplasmic reticulum (ER). Three major sensors of misfolded proteins activate a process called unfolded protein response (UPR), which helps the cell to deal with increased ER protein load. The first sensor, inositol-requiring enzyme 1 (IRE1) can activate c-Jun N-terminal kinase (JNK) pathway, which can lead to apoptosis. IRE1's major downstream effector is X-box-binding protein 1 (XBP1), a transcription factor, which is spliced and translated under IRE1 activation. Protein kinase RNA-activated-like ER kinase (PERK) an another sensor of misfolded proteins. Upon activation of PERK, eukaryotic translation initiation factor 2 α (eIF2α) is activated, which leads to inhibition of translation. eIF2α also activates transcription factor 4 (ATF4), which is translocated to the nucleus, or can directly lead to autophagy activation. The last branch of the UPR is initiated by activating transcription factor 6 (ATF6). ATF6 can lead to induction of autophagy or is translocated to the nucleus. All three branches of the UPR lead to the transcription of numerous genes that help to alleviate ER stress. If the UPR is not able to deal with the amount of ER stress, it can lead to apoptosis (Illustration created using BioRender.com).

PERK, similarly to IRE1 is a transmembrane serine/threonine kinase with a sensor for misfolded proteins located in the ER lumen. When PERK is activated, it phosphorylates eukaryotic translation initiation factor 2 α (eIF2α), which leads to a reduction of translation and consequently lessens the load of proteins in the ER (Harding et al., 1999). Additionally, phosphorylated eIF2α leads to upregulation activation transcription factor 4 (ATF4) (Vattem and Wek, 2004), which was shown to induce autophagy proteins Beclin1, LC3, ATG5, ATG7 and ATG12, mediates the induction of a protective process called the integrated stress response, assembly of stress granules, resistance to oxidative stress, and other mechanisms (Kedersha et al., 1999; Harding et al., 2003; B'chir et al., 2013). Although PERK activates survival signaling, under prolonged ER stress it induces proapoptotic cascade through ATF4 and its downstream effectors, growth arrest and DNA damage-inducible 34 (GADD34), and CAAT/enhancer-binding protein homologous protein (CHOP) (Li et al., 2020). It has been shown, that PERK also plays a role in immune response, as it promotes inflammatory cytokine production (Jiao et al., 2011). This also takes part in the brain, as it was previously shown that PERK accelerates brain inflammation by inducing IL-6 expression in astrocytes through Janus kinase 1 (JAK1)/ signal transducer and activator of transcription 3 (STAT3) signaling pathway (Meares et al., 2014).

ATF6, the last main sensor of misfolded proteins in the ER is an ER transmembrane transcription factor. The sensor function of the ATF6 is mediated through ER chaperone named immunoglobulin-binding protein (BiP), which dissociates from ATF6 in response to the accumulation of misfolded proteins (Shen et al., 2005). ATF6 then dislocates from the ER membrane and is transferred to the Golgi, where it is cleaved and its basic leucine zipper protein domain is released, which is transported to the nucleus and acts as a transcription factor (Haze et al., 1999, 6). Target genes that are activated by ATF6 include BiP, CHOP, and Grp94 (Yoshida et al., 2000, 6). ATF6 has been shown to lead to the induction of autophagy by activating Beclin1 (Gade et al., 2014).

1.4. Spinal cord injury

Spinal cord injury (SCI) can be characterized as damage to the spinal cord that causes temporary or permanent changes in its structure or function. Traumatic SCI occurs when an acute external mechanical impact (resulting, for instance, from a fall, motor vehicle accident, violence) damages the spinal cord (Ahuja et al., 2017). The damage leaves SCI patients with devastating multisystem complications stemming from the loss of sensory, motor, and

autonomic system functions, resulting in sensory loss, paralysis, cardiorespiratory complications (Linn et al., 2000; Claydon et al., 2006), immune system deficiency (Brommer et al., 2016), dysfunction of the bladder, bowel and sexual function (Benevento and Sipski, 2002), neuropathic pain (Cardenas and Felix, 2009) and further symptoms (Eckert and Martin, 2017). SCI patients are not only affected physically, their quality of life and role in society is changed, which results in mental afflictions. Care for these patients presents a high economic and psychological burden on their families as well as on society. As SCI cannot be prevented, the development of effective treatments is crucial.

Pathophysiology of traumatic SCI (Fig. 3) has two phases- primary and secondary injury. Primary injury is a consequence of the initial traumatic event, produced by disruption of the spinal cord tissue due to external mechanical force. In this phase, the damage causes cell death, interruption of the vasculature, compromises the blood-spinal cord barrier, but rarely fully transects anatomical continuity of the spinal cord (Rowland et al., 2008). Events of the primary phase simultaneously initiate a cascade that leads to secondary injury and further damages the spinal cord, often to a greater extent compared to what occurred during the primary injury (Ahuja et al., 2017). Inflammation, edema and hemorrhage develop within the tissue, which leads to necrosis and ischemia (Venkatesh et al., 2019). In minutes and following weeks after the initial injury, at the so-called sub-acute phase of secondary injury, new mechanisms are initiated that contribute to the injury. These include disruption of ionic homeostasis, glutamate excitotoxicity, production of reactive oxygen species (ROS), lipid peroxidation, disruption in autophagy flux, accumulation of nitrous oxide, glial scar initiation, and energy failure. In months and years following the trauma, the sub-acute phase converts into a chronic injury. Chronic injury is characterized by continued apoptosis, central cavitation, glial scar formation, alteration in ion channels and receptors, and numerous other mechanisms. Oligodendrocytes, one of the most vulnerable cell types of the CNS, undergo apoptosis, leading to demyelination and damage of surviving axons (Beattie et al., 2002). The chronic phase brings about some regenerative processes as well, including axon sprouting (Oyinbo, 2011). These scarce endogenous regenerative efforts are impeded by the non-permissive environment that is formed in the extracellular matrix during the sub-acute and chronic phase of the injury. The cystic cavity containing extracellular fluid, bands of connective tissue, and macrophages was found to be a formidable barrier for axon regrowth and cell migration (Milhorat et al., 1995). The glial scar is formed by reactive astrocytes around cystic cavities to prevent damage to the adjacent tissue. The mesh-like array containing axonal processes and extracellular matrix proteins such as chondroitin sulfate

proteoglycans, tenascin, and NG2 proteoglycan restrict axon regeneration and plasticity (McKeon et al., 1991). Even in the non-lesioned tissue, the extracellular matrix of the CNS is not permissive for neural regrowth. Degenerating oligodendrocytes and axons release myelin proteins such as neurite outgrowth inhibitor A, oligodendrocyte-myelin glycoprotein, and myelin-associated glycoprotein into the environment, which were also shown to inhibit regeneration (Geoffroy and Zheng, 2014).

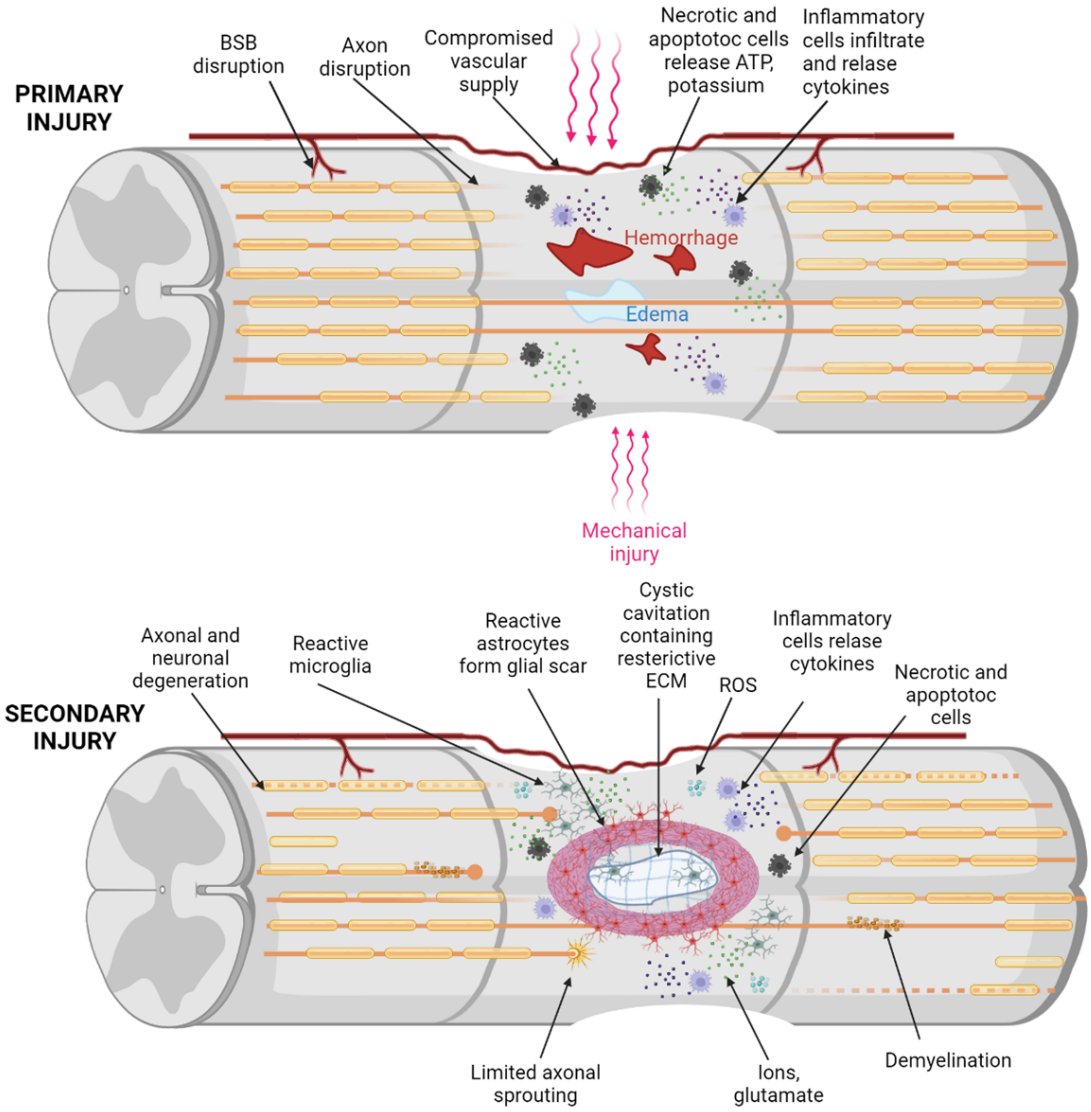

Fig. 3 Pathophysiology of spinal cord injury. Primary injury is a consequence of the initial external impact. The damage of mechanical injury causes cell death, transects axons, compromises the vasculature, and disrupts the blood-spinal cord barrier (BSB). Hemorrhage and edema develop at the injury site and first inflammatory cells start to infiltrate it, releasing cytokines, which lead to further activation of the inflammatory cascade. Dead cells release ATP and ions into the environment. Secondary injury can last from minutes to months and years after the primary injury. Axonal and neuronal degeneration occurs, along with demyelination. Some limited axonal sprouting occurs as well, but the regeneration effort is obstructed by the inhibitory extracellular matrix (ECM) environment formed at the lesion site. Astrocytes are activated and form a glial scar, secluding the injury and cystic cavitation. Microglia are also activated and release cytokines and perpetuating the inflammation together with other cells of the immune system. Reactive oxygen species (ROS), ions

and glutamate are released at the injury site as well, further contributing to the chronic injury. (Illustration created using BioRender.com).

The pathology of SCI is complex and multifaceted. Recovery and regenerative strategies are therefore usually challenging and limited. It is considered that the prevention of tissue damage in the acute and sub-acute phases of secondary injury is of critical importance (Venkatesh et al., 2019). In the following two chapters, the involvement of inflammation and autophagy in secondary SCI will be explored further, as these mechanisms were the focus of research in this thesis.

1.4.1. **SCI and inflammation**

The secondary degeneration after SCI is generated primarily by factors produced directly by the damaged tissue, including ROS, chemokines and cytokines, and other molecules released because of ischemia, hemorrhage, excitotoxicity, and ionic imbalance. Many of these molecules initiate different facets of the inflammatory response. Inflammation is therefore considered to contribute significantly to secondary damage after SCI (David and Kroner, 2015). However, inflammation is not exclusively detrimental, it was shown that it can be also beneficial, as it is crucial for clearance of cellular debris, controlling infections, and restoring homeostasis of the tissue. Even so, it is crucial that the inflammation remains controlled, induced at the right time point after SCI and that the right activation state of immune cells is achieved (Miron and Franklin, 2014).

There are several cell types involved in the inflammatory response following injury. In the first phase of the inflammation, microglia, and astrocytes are activated and converge to the injury site along with blood-borne neutrophils (Jones et al., 2005). Astrocytes respond acutely to CNS injury by increasing the production of cytokines and chemokines, which induce recruitment of neutrophils and pro-inflammatory macrophages (Pineau et al., 2010; Cekanaviciute and Buckwalter, 2016). Microglia respond very quickly to injury and are likely the first cell type to react within minutes. First, they extend their processes toward the injury site which appears to have a role in controlling the lesion size (Hines et al., 2009). Soon after, microglia retract their processes, take on amoeboid shape and phagocytize cellular debris. After activation, microglia cannot be distinguished from macrophages, which originate from monocytes infiltrating the injury site (David and Kroner, 2011). Proteolytic and oxidative enzymes produced by neutrophils are the first line of bodies' defense against

pathogens, but their role in SCI is not fully understood (David and Kroner, 2015). It was proposed that neutrophils sterilize the damaged area and prepare it for following 'repair', but their numbers are so overwhelming, that they create 'bystander' tissue damage (Taoka et al., 1998). Approximately three days after injury, macrophages, B- and T-lymphocytes are recruited to the injury site (Beck et al., 2010). Acute damage to the blood-spinal cord barrier allows monocytes to infiltrate the spinal cord tissue, where they transform into macrophages (Zhou et al., 2014). Together with resident microglia that transformed into macrophages, these cells help in wound healing after SCI through the production of growth-promoting factors such as neurotrophin-3 (NT-3), nerve growth factor (NGF) (Elkabes et al., 1996), and through to their capacity for phagocytosis and scavenging of injured cells and myelin debris (Zhou et al., 2014). However, macrophages can also have a detrimental effect on SCI, as was shown that they can shift into pro-inflammatory phenotype through the influence of tumor necrosis factor (TNF)-α after SCI (Kroner et al., 2014). These pro-inflammatory macrophages express MHCII, present antigens to T cells, and influence the activation and regulation of further immune response (David et al., 2015). Like other immune cells, lymphocytes' response to SCI is complex (Walsh et al., 2014). It was reported, that after SCI, the autoimmune activity of T and B lymphocytes are formed and potentially exacerbate injury to axons and induce demyelination, leading to functional loss (Popovich and Jones, 2003; Ankeny et al., 2006). On the other hand, some argue that this autoimmunity stemming from CD4+CD25+ regulatory T cells is neuroprotective (Kipnis et al., 2002).

Although cellular components of the inflammatory response are the major effectors in secondary injury after SCI, it is important to bear in mind that their actions are orchestrated by signaling proteins- cytokines, growth factors, and related molecules. Cytokines are a large family of small proteins participating in communication between cells that are usually related to the modulation of the immune response, but also have multiple other effects that affect the physiology of health and disease. These peptides, proteins, or glycoproteins, are produced by many cells and can be categorized into a pro-inflammatory or anti-inflammatory group based on the net balance of their effects (Ramesh et al., 2013; Garcia et al., 2016). Although these signaling molecules have complex effects on SCI and subsequent recovery, cytokines with generally anti-inflammatory effects are interleukin (IL)-4, IL-10, IL-12, IL-33, interferon (IFN)-β, and IFN-γ, while pro-inflammatory are IL-1β, IL-6, IL-17, TNF-α, macrophage inflammatory protein (MIP)-1α (Garcia et al., 2016; Ren et al., 2018).

1.4.2. **SCI and autophagy**

In the past few years, autophagy has been extensively studied in the connection with secondary damage after SCI. It was confirmed by numerous studies that there is upregulation of autophagic markers at the SCI lesion (Kanno et al., 2011; Chen et al., 2012; Tang et al., 2014; Yan et al., 2017; Li et al., 2019a). The studies suggest that the accumulation of APs occurs very early, during the initial stages of secondary injury, even within hours after impact, and remain upregulated for weeks after the injury. However, the role of autophagy in SCI, whether it is beneficial or detrimental has long been controversial (Wu and Lipinski, 2019). Even a recent meta-analysis study suggests, that both induction and repression of autophagy leads to neuroprotection after SCI. The discrepancies between the results of the studies can be caused by differences in SCI models, type of therapy, it's timing and duration. For example, upregulation of autophagy was found to be more beneficial in compression-type injury, compared to contusion (Zhang et al., 2020). Therefore, the role of autophagy after SCI may depend on the cell type that was damaged, the severity of the injury, and other parameters. It was previously confirmed that motor neurons (MNs) are more vulnerable to disruption of autophagy (Muñoz-Galdeano et al., 2018) and that this is leading to ER stress and apoptosis (Liu et al., 2015). Although AP accumulation doesn't occur just in neuronal somas, also in injured axons (Ribas et al., 2015), it is currently unknown whether it contributes to axonal damage. Apart from neurons, glia are also influenced by autophagy after neurotrauma. Upregulation of autophagy markers was observed in oligodendrocytes, astrocytes, and microglia after SCI, but further studies are needed to determine how it affects their survival and function (Wu and Lipinski, 2019).

What studies tend to agree on, is that upregulation of autophagic markers after SCI is not due to upregulation of autophagy itself, but due to inhibition of autophagic flux. This was confirmed by upregulation of both of LC3-II and p62/SQSTM1 proteins at the lesion site (Tanabe et al., 2011; Liu et al., 2015; Muñoz-Galdeano et al., 2018). One of the possible mechanisms in which trauma contributes to disruption of autophagy is through excessive production of ROS and reactive nitrogen species (RNS). High levels of ROS and RNS can modulate autophagy through the S-nitrosylation of proteins in the mammalian target of rapamycin (mTOR) and c-Jun N-terminal kinase pathways, which are key regulators of autophagy (Filomeni et al., 2015). ROS can also inflict damage to lysosomal membranes and therefore disrupt the autophagy flux. On the other hand, stimulation of autophagy by ROS has also been reported. Injury-mediated oxidative damage probably influences autophagy depending on the severity and mechanism of the injury (Wu and Lipinski, 2019).

There is also the possibility, that autophagy is mediating the inflammatory response after SCI, but the cross-talk between inflammation and autophagy remains to be poorly understood (Qian et al., 2017b).

1.4.3. **SCI treatment**

There are currently no approved pharmacologic treatments for improving outcomes after SCI. Even the management of SCI patients continues to be controversial. The absence of consensus in treatment strategies has halted the standardization of care for patients with SCI. The most effective clinical treatment currently is early surgical decompression and stabilization (Torregrossa et al., 2020). High-dose treatment of glucocorticoid methylprednisolone was previously been recommended in acute SCI, but recent studies showed it does not contribute to neurologic recovery and could lead to adverse effects (Liu et al., 2019). Despite the lack of effective therapies in use, numerous treatment and management strategies are in various stages of preclinical research and clinical trials. These include cell-based therapies, biomaterial implantation, hypothermia induction, cerebrospinal fluid drainage, spinal cord or brain stimulation, and pharmaceuticals with neuroprotective or neuroregenerative properties. Pharmaceutical approaches target many different mechanisms, such as promotion of neuronal regeneration with antibody against Nogo, Rho-ROCK inhibitor, Catherin or GM-1 ganglioside, reducing glutamate excitotoxicity with basic fibroblast growth factor and riluzole, while a great portion of them are targeting inflammation (Ashammakhi et al., 2019; Shah et al., 2020; Torregrossa et al., 2020).

Due to the dual role of inflammation after SCI injury, global immunosuppressive therapies such as methylprednisolone and minocycline administration may not be contributing to recovery. More complex and immunomodulatory approaches have been proposed as potentially more beneficial (Chio et al., 2021). Extensively studied immunomodulatory therapies with promising results include administrations of human immunoglobulin G (Brennan et al., 2016), monoclonal antibodies against CD11d/CD18 (Bao et al., 2004; Gris et al., 2004), granulocyte colony-stimulating factor (Guo et al., 2015; Park et al., 2020), natural compounds such as curcumin (Machova Urdzikova et al., 2015) or green tea polyphenol epigallocatechin gallate (Machova Urdzikova et al., 2017) and rapamycin (RAPA) (Chen et al., 2013).

RAPA is a natural anti-fungal agent that acts as an allosteric inhibitor of the mTOR. The mTOR pathway (Fig. 4) is a key metabolic pathway, which is deeply involved in multiple vital cellular mechanisms, including regulation of cell death and survival, metabolism, and proliferation through the control of many physiological processes such as transcription and translation, ribosomal biogenesis, cytoskeletal organization, vesicular trafficking and autophagy (Wullschleger et al., 2006). This pathway is extensively studied for its involvement in mechanisms of trauma and various diseases of the CNS. Its actions are mediated through two mTOR complexes mTORC1 and mTORC2, their downstream effectors, ribosomal protein S6 kinase (S6K) and eukaryotic translation initiation factor 4E -binding protein (4E-BP) and Akt, which is phosphorylated by mTORC2, but is upstream of mTORC1 (Laplante and Sabatini, 2012; Jhanwar-Uniyal et al., 2017).

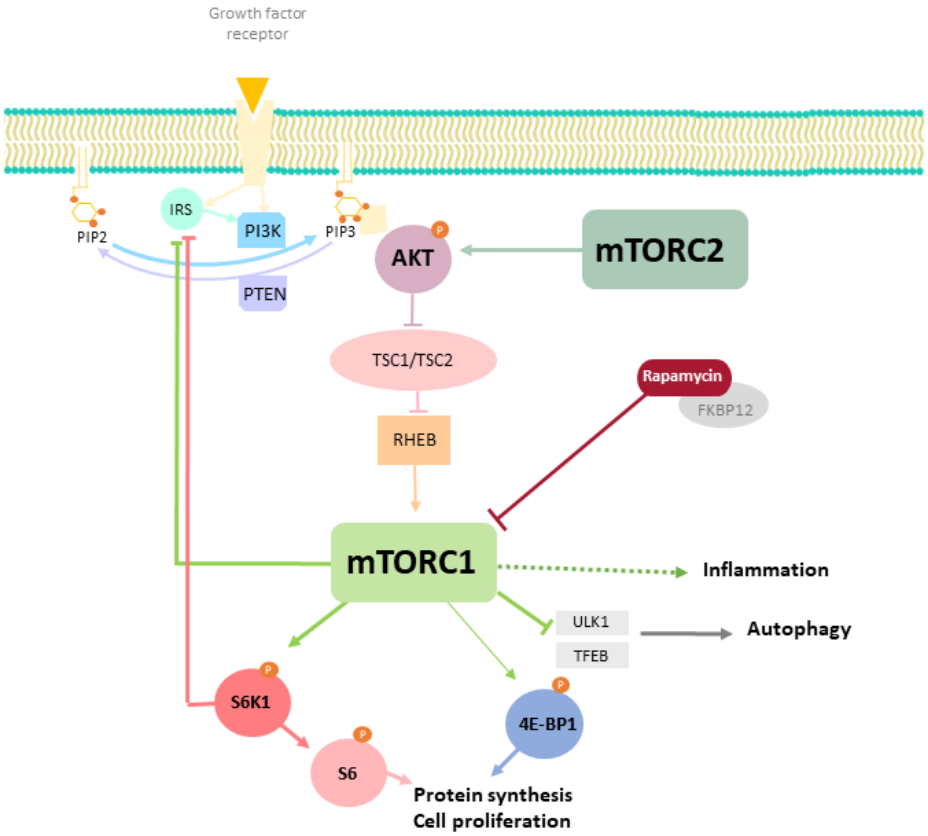

Fig. 4 The mTOR pathway and its repression by rapamycin (RAPA). Insulin receptor substrate-1 (IRS) or other factors lead to activation of Akt, through phosphatidylinositol 4,5-bisphosphate (PIP2) transition to phosphatidylinositol (3,4,5)-trisphosphate (PIP3) by phosphoinositide 3-kinase (PI3K). Akt suppresses tuberous sclerosis complex (TSC), which causes disinhibition of the small GTPase RHEB (Ras homolog–mTORC1 binding) and RHEB and its subsequent activation inhibits mTOR complex 1 (mTORC1). Akt can be furthermore activated by mTOR complex 2 (mTORC2). Active mTORC1 leads to phosphorylation of ribosomal protein S6 kinase 1 (S6K1) and translation initiation factor 4E-binding protein 1 (4E-BP1). The substrate of S6K, S6 and 4E-BP1 lead to protein synthesis and cell proliferation. Furthermore, mTORC1 suppresses autophagy through Unc-51 like autophagy activating kinase (ULK1) and transcription factor EB (TFEB) inhibition and indirectly can induce

inflammation. RAPA, attached with FKBP12 inhibits mTORC1. Phosphatase and tensin homolog (PTEN). Adapted from Vargova et al., 2021.

RAPA, a selective mTORC1 inhibitor has been previously used as a treatment in neurodegenerative disorders (Spilman et al., 2010; Tsvetkov et al., 2010), including SCI (Sekiguchi et al., 2012; Tang et al., 2014; Li et al., 2019a) and was shown to lead to neuroprotection. Neuroprotective effects of mTOR inhibition are thought to be mediated through induction of autophagy and immunomodulation. mTOR is recognized as a master regulator of autophagy since its inhibition is required for multiple steps of autophagy (Fig. 1) (Dossou and Basu, 2019). RAPA and its derivates are potent immunosuppressant drugs, used following organ transplantation (Baroja-Mazo et al., 2016). Importantly, it has been previously shown to reduce neuroinflammation and neuron death (Xie et al., 2014; Srivastava et al., 2016).

1.4.4. **Models of SCI**

In the pursuit of a remedy and knowledge of the pathophysiology of the SCI, researchers have used various animal models. An accurate animal model should be anatomically and pathologically similar to human SCI, be inexpensive, replicable, and require minimal training. Rat models are the most frequently used in SCI studies as they fulfill most of the desired requirements. Based on the injury type, SCI rat models can be classified into contusion, compression, and transection models. In the contusion model, transient force such as weight-drop, electromagnetic or air-pressure impact is applied to displace and damage the spinal cord. In compression models, the spinal cord is compressed for a prolonged period with devices such as compression clips, inflatable. balloon, or others. Transection is characterized by the complete or partial severing of the spinal cord (Cheriyan et al., 2014; Ahuja et al., 2017). These *in vivo* models have been essential for the preclinical evaluation of behavioral and systemic outcomes of drug treatments and will remain an indispensable element of preclinical drug development.

Nevertheless, in SCI research scientists often need to take a step back and try to understand what is taking place at the cellular level. One of the biggest obstacles in SCI treatment currently is the inability of mature CNS neurons to regenerate after injury. We still don’t fully understand the mechanisms that prevent regeneration, but many factors seem to be contributing to this phenomenon, including malfunction of proper transcriptional,

translational and epigenetic programs at appropriate subcellular locations in the CNS neurons (van Niekerk et al., 2016; Petrova et al., 2021), deviations in vesicular transport and decreased signaling of some pathways in axons. The proper function of these processes collectively provides intrinsic regeneration ability in immature neurons, they malfunction abruptly with neuronal maturation (Nicholls and Saunders, 1996; Koseki et al., 2017; Petrova and Eva, 2018). Development and aging in the CNS involve many complex pathways, so it is demanding to investigate their influence on the regeneration capacity of neurons *in vivo*. On the other hand, *in vitro* models can provide wide-ranging tools and approaches to examine distinct neuronal subtypes, to manipulate and characterize neuronal behavior, and to discover mechanisms connecting the development and regeneration of CNS neurons (Abu-Rub et al., 2010; Franssen et al., 2015). Hence, characterizing axon growth inhibition *in vitro* is a useful approach that could bring further understanding of the CNS regeneration limitations. Numerous *in vitro* culture models have been used previously to investigate CNS axon regeneration. Primary neuronal cultures were established by dissociating neural tissue from rodents at various ages (Donaldson and Höke, 2014). The tissues most commonly utilized for the cell cultures are dorsal root ganglia (DRGs) (Cheah et al., 2016), hippocampus (Kaech and Banker, 2006; Moore et al., 2009), and cortex. Primary spinal cord cultures were also developed previously (Thomson et al., 2008; Eldeiry et al., 2017), but their characterization is limited and were not deemed to be suitable for axon regeneration studies. The study of the regenerative ability of spinal interneurons (SpINs) is of exceptional interest, as it was revealed, that mild, structurally incomplete SCI can lead to partial recovery due to spontaneous reorganization of neural circuits (Bareyre et al., 2004; Martinez et al., 2012). Also, the growth of SpIN neurites across mouse SCI can be incited by treatments to boost neuronal regenerative ability, axonal chemoattraction, and glial scar permissiveness (Anderson et al., 2016). Crucial elements of neuroplasticity in these incomplete SCIs are SpINs because they create substitute paths to transmit information between cells below and above the lesion (Courtine et al., 2008; May et al., 2017). The establishment and characterization of culture containing spinal cord neurons is therefore necessary and valuable.

1.5. Amyotrophic lateral sclerosis

ALS is a late-onset neurodegenerative disease characterized by degeneration of upper and lower MNs, causing progressive and fatal paralysis. The median age of ALS onset is 64

years and is usually diagnosed by the early symptoms of limb muscle weakness, twitching, and cramping. The aggressive advancement of the disease usually leads to the development of dyspnea and dysphagia and eventually death by respiratory failure after about 3 years after the disease onset. In 90-95% of cases, ALS occurs sporadically, without any clear genetic cause, while 5-10% of the cases are familial, inherited in an autosomal dominant fashion. These observations indicate that ALS develops under influence of both genetic and environmental factors. (Boillée et al., 2006; Zarei et al., 2015; Hardiman et al., 2017; Masrori and Van Damme, 2020). Mutations in genes encoding TAR DNA-binding protein 43 (TDP-43), C9orf72, superoxide dismutase 1 (SOD1) and encoding RNA binding protein FUS (FUS) are responsible for the majority of familial cases of ALS (Chiò et al., 2014). Reported environmental risk factors include smoking, exposure to certain chemicals, and radiation (Zarei et al., 2015).

Although the pathophysiology of ALS is not well understood, gross pathological characteristics of ALS include atrophy of the skeletal muscles and the motor cortex due to degeneration of MNs. Axonal loss and astrogliosis lead to discoloration and sclerosis of the pyramidal tracts (the corticospinal and the corticobulbar tract) accompanied by the thinning of the hypoglossal nerves and ventral roots of the spinal cord (Hardiman et al., 2017). The pathological hallmark of the disease is an accumulation of ubiquitylated protein aggregates in MNs, leading to neuronal injury and death. In 95% of the cases, TDP-43 is the main component of the protein inclusions (Van Deerlin et al., 2008). TDP-43 is an RNA- and DNA-binding protein engaged in numerous processes including transcription, splicing, RNA transport, and formation of stress granules. TDP-43 is mainly a nuclear protein, but it can be shuttled into the cytoplasm. Accumulation of cytoplasmic TDP-43 and depletion of its nuclear fraction is common in ALS (Mackenzie et al., 2010). Apart from TDP-43, SOD1 and p62/SQSTM1 positive protein inclusions are also observed in ALS patients. SOD1 is an important antioxidant enzyme, catalyzing the production of O_2 and H_2O_2 from superoxide species generated during cellular respiration. It operates as a particularly stable dimer, but in ALS it undergoes conformational and functional modifications and causes toxicity through interactions with various proteins and mechanisms (Mejzini et al., 2019). The progression of the disease is mediated through a prion-like mechanism, where the pathological protein complexes spread to healthy cells through cell-to-cell transmission (Polymenidou and Cleveland, 2011). Among cellular processes implicated in the disease mechanisms are disturbances in RNA metabolism, nucleocytoplasmic transport defects, compromised DNA repair, impaired protein homeostasis, excitotoxicity, oxidative stress, mitochondrial

dysfunction, disruption of axonal transport, neuroinflammation, vesicular transport defects, and other (Fig. 5) (Taylor et al., 2016).

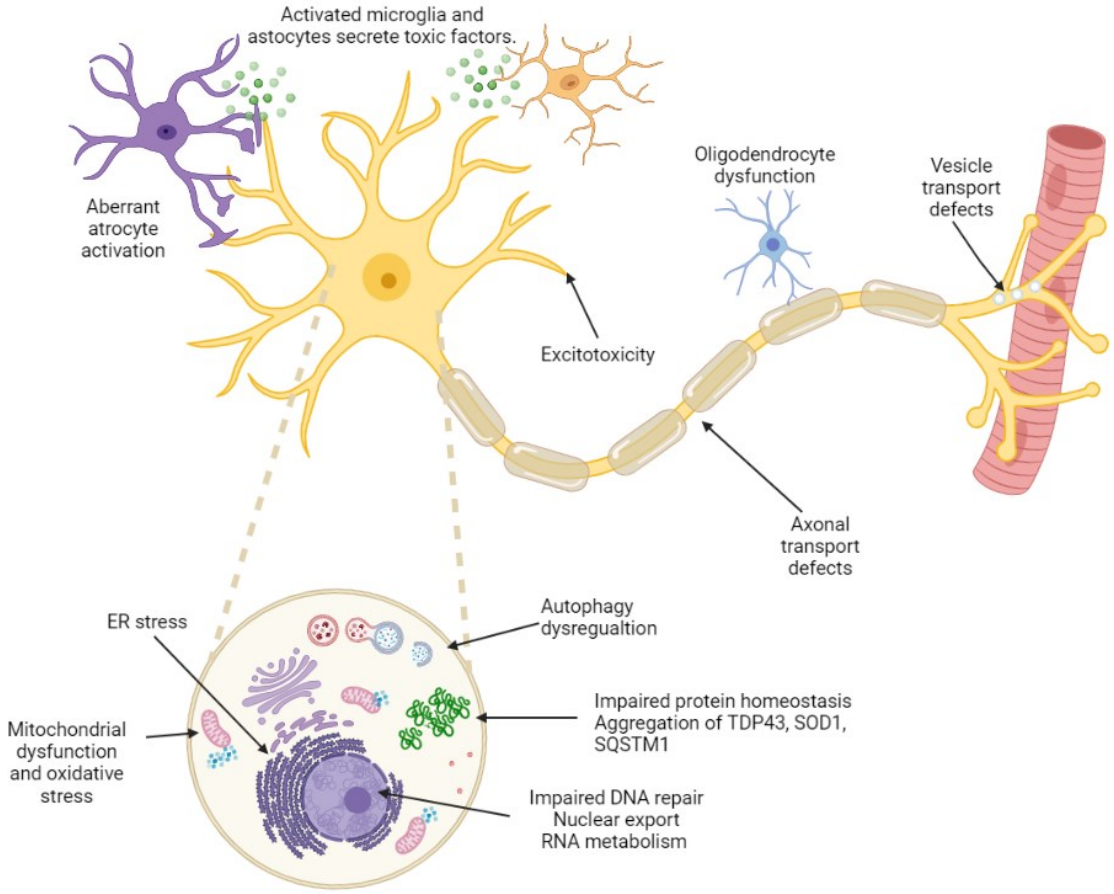

Fig. 5 Proposed mechanisms contributing to pathology of amyotrophic lateral sclerosis. Endoplasmic reticulum (ER); TAR DNA-binding protein 43 (TDP-43); superoxide dismutase 1 (SOD1); sequestosome 1 (SQSTM1) (Illustration created using BioRender.com).

The fate of MNs in ALS can be heavily influenced by the extracellular environment, especially due to the influence of glia. It was shown that ALS can be induced by overexpression of mutant SOD1 in nonneuronal cells (Clement et al., 2003). Additionally, ALS astrocytes were found to release toxic factors that cause the death of wild-type (WT) MNs (Fritz et al., 2013; Qian et al., 2017a). While multiple types of glia were linked with ALS onset and progression (Filipi et al., 2020), particular interest in the role of astrocytes arose in recent years. In ALS, similarly to other neurodegenerative disorders, astrocytes change morphology and assume reactive phenotype. Gene transcriptome analyses revealed that there are at least two types of reactive astrocytes. A1 reactive astrocytes are characterized as harmful, as they upregulate many genes that are known to be destructive to synapses, while A2 phenotype reactive astrocytes upregulate numerous neurotrophic factors,

that promote neuronal survival and growth and synapse repair (Zamanian et al., 2012; Liddelow and Barres, 2017). Induction of particular reactive astrocyte phenotype seems to be dependent on activation of one out of two important transcription factors. A1 toxic phenotype is induced by nuclear factor kappa-light-chain-enhancer of activated B cells (NF-κB) signaling (Lian et al., 2015), while helpful A2 reactive astrocytes are dependent on signal transducer and activator of transcription 3 (STAT3) activation (Anderson et al., 2016).

Despite growing knowledge of the disease mechanisms implicated in ALS, pathological events that initiate neurodegeneration remain unclear. It is likely a cumulative result of multiple distinct interacting mechanisms, rather than a result of a single initiating event. Remarkably, many of the genes linked with ALS were found to cluster in a few key pathways: RNA metabolism, protein quality control and degradation, and cytoskeletal and axonal transport (Masrori and Van Damme, 2020). Curiously, the ER is a common link between these mechanisms, which is why it is believed that ER dysfunction, ER stress and closely connected pathway of autophagy are central and early processes present in the pathology ALS (Cai et al., 2016).

1.5.1. **ALS and ER stress**

Strong indication that ER stress is involved in ALS was determined by analysis of human postmortem spinal cord tissue and the tissue of transgenic animal models of ALS. Multiple studies reported activation of all three pathways of UPR, elevated ER chaperones and cell death signals connected to ER stress in ALS tissues (Ilieva et al., 2007; Ito et al., 2009; Sasaki, 2010; Farg et al., 2012). Alterations of patients' ER morphology were also observed previously (Oyanagi et al., 2008), as well as the presence of TDP-43 protein inclusions in the ER of MNs of patients with both familial and sporadic ALS (Johnson et al., 2010; Sasaki et al., 2010). TDP-43 overexpression leads to ER stress induction through upregulation of ATF6 and XBP1. ER stress, in turn, modulates TDP-43 sub-cellular distribution, accumulates it in the cytoplasm, which further potentiates the TDP-43 pathology. The vicious cycle leads to uncontrolled ER stress, formation of stress granules through p-eIF2α, formation of protein inclusions and eventually cell death. Whether the ER stress is the consequence or the initiator of TDP-43 pathology, or in other words, which culprit starts the vicious cycle in ALS is still not clear (Walker et al., 2013; de Mena et al.,

2021). A very similar complex relationship was observed between SOD1 and ER stress (Medinas et al., 2018, 2019).

Aberrant astrocyte reactivity has been recently indicated as a potential contributor to ALS pathology. STAT3 activation in astrocytes was found to be required for recovery of injured MNs (Tyzack et al., 2014). Injured MNs initiate STAT3 signaling in astrocytes by upregulation of Ephrin type-B receptor 1 (EphB1), which is a ligand of ephrin-B1 receptor, located on astrocytic membrane (Fig. 6A). Interestingly, STAT3 activation by injured neurons seems to be impaired in $SOD1^{G93A}$ ALS mice and human $SOD1^{D90A}$ ALS patient-derived iPSC-astrocytes. Gene expression data of human $SOD1^{D90A}$ iPSC-astrocytes revealed strong upregulation of one particular gene of interest in these cells, encoding pleckstrin homology like domain family A member 3 (PHLDA3) protein (Tyzack et al., 2017). PHLDA3 is a recently described repressor of Akt. It binds to phosphatidylinositol phosphates (PIPs) on the cell membrane and disables binding and phosphorylation of Akt, which in turn inhibits the mTOR pathway (Takikawa and Ohki, 2017) (Fig. 6B). It was also reported that PHLDA3 overexpression causes ER stress and leads to cell death of hepatocytes (Han et al., 2016). Furthermore, ER stress was shown to lead to brain inflammation by inducing IL-6 expression in astrocytes (Meares et al., 2014). Given the strong involvement of ER stress in ALS pathology, it is of great value to investigate the role of this novel molecule in astrocytes.

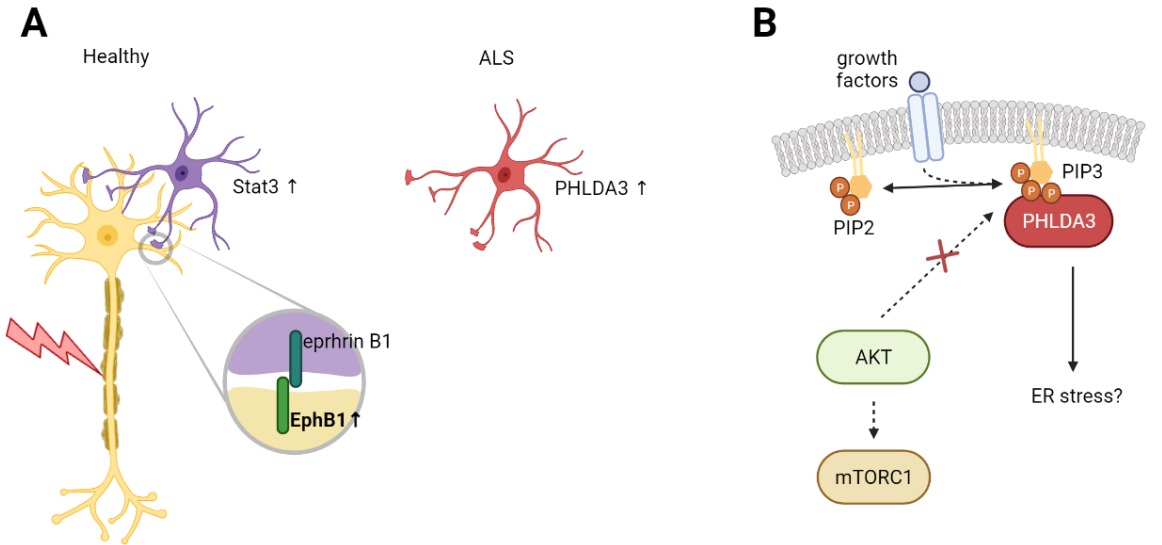

Fig. 6 Aberrant astrocyte activation in amyotrophic lateral sclerosis (ALS) (A). Injured motor neurons upregulate ephrin type-B receptor 1 (EphB1) which leads to activation of ephrin B1 on astrocytic membrane and activation of signal transducer and activator of transcription 3 (Stat3) signaling in healthy astrocytes. ALS astrocytes fail to activate Stat3 but are activated into a harmful

phenotype and upregulate expression of pleckstrin homology like domain family A member 3 (PHLDA3). PHLDA3 is a newly described protein, found to inhibit Akt and subsequently mTOR complex 1 (mTORC1) (B). PHLDA3 preferentially binds to phosphatidylinositol-3, 4, 5-triphosphate (PIP3), prohibiting Akt recruitment to the cytoplasmic membrane. Phosphatidylinositol-4, 5-bisphosphate (PIP2) is a precursor of PIP3 (Illustration created using BioRender.com).

1.5.2. **ALS and autophagy**

Studies have shown that in ALS, similarly to other neurodegenerative diseases, autophagy is highly upregulated (Wong and Holzbaur, 2015). Autophagy proteins LC3, Beclin-1, p62 and Atf5-Atg12 were found to be elevated in MNs of ALS patients, as well as in animal models (Morimoto et al., 2007; Li et al., 2008; Hetz et al., 2009). Upregulation of autophagy in astrocytes and microglia was also reported in mSOD1-Tg mice, particularly at late symptomatic stages (Tian et al., 2011). Moreover, mutations in genes coding core autophagy proteins such as p62/SQSTM1 or Optineurin were linked with ALS. Other ALS-related mutations were found in genes that have an indirect functional role in autophagy, such as *ALS2, C9orf72, CHMP2B, DCTN, FIG4, FUS, PFN1, TDP-43, TUBA4A, UBQLN2, VAPB,* and *VCP* (Amin et al., 2020).

The role of autophagy in ALS is still not entirely clear. It was postulated, that the dysfunction of autophagy-regulated degradation can lead to accumulation of protein aggregates in ALS (Ramesh and Pandey, 2017; Vicencio et al., 2020). The close connection of autophagy and ALS-associated genes also indicates that these mutations can cause dysfunction of different stages of autophagy and lead to ALS pathology (Yao, 2021). On the other hand, increasing evidence suggest that the role of autophagy in ALS is not so straightforward. It is very likely that extensive crosstalk between other pathways and autophagy may, directly and indirectly, influence autophagy and vice versa. Activation of autophagy by other processes such as damaged DNA, oxidative and ER stress can overwhelm the autophagy pathway or impair the autophagic flux (Fujikake et al., 2018). Overactivation of autophagy has been previously been proposed to be an uncommon death pathway in neurons (Nixon and Yang, 2012). Furthermore, autophagy inhibition was shown to be neuroprotective in certain neurodegenerative conditions (Lee and Gao, 2009). Similarly, inhibition of autophagy by n-butylidenephthalide seems to be beneficial in $SOD1^{G93A}$ mouse model of ALS, as it leads to a prolonged lifespan of the mice and decreased MN loss (Hsueh et al., 2016; Zhou et al., 2017). In contrast, induction of mTOR-independent autophagy by trehalose (Castillo et al., 2013), carbamazepine (Zhang et al., 2018) and verapamil (Zhang et al., 2019) was shown to prolong the lifespan of $SOD1^{G86R}$ mice.

Tamoxifen treatment, which induces autophagy in mTOR dependent manner (Wu et al., 2016) showed a modest effect in slowing progression of ALS in patients (Chen et al., 2020), further proving the complexity of ALS and autophagy relationship.

1.5.3. **ALS treatment**

ALS management mostly relies on multidisciplinary care and symptomatic treatment using pharmacological or non-pharmacological interventions (Masrori and Van Damme, 2020). Therapies influencing disease progression are limited. Currently, there are only two disease-modifying drugs used for ALS treatment named riluzole and edaravone and even those provide only limited clinical benefits (Jack J. Chen, 2020). Riluzole is a glutamate antagonist, which inhibits glutamate release from MNs by multiple possible mechanisms, leading to reduction of excitotoxicity which has a potent role in ALS pathology (Jaiswal, 2016). Riluzole treatment offers modest prolonged survival benefits ranging from 6 to 21 months (Hinchcliffe and Smith, 2017). Edaravone is a scavenger of free radicals and an antioxidant, causing a reduction of oxidative stress and cell death. Clinical trials of edaravone treatment in ALS report mixed outcomes. While some studies report that edaravone treatment may delay motor function deterioration (Yoshino and Kimura, 2006; Tanaka et al., 2016), other saw no beneficial outcomes (Abe et al., 2014). Because of the mixed results, edaravone has not yet been approved for ALS treatment in the European Union.

In recent years, novel therapeutic strategies targeting multiple proposed disease mechanisms or targeting mutated genes directly have been extensively tested in ALS patients or animal models, showing significant potential for clinical use in the future (Xu et al., 2021).

Gene therapies, especially in familial ALS have shown great promise in animal studies and their safety was confirmed in clinical studies. In these studies suppression of ALS related genes *SOD1, TDP43*, *C9orf72* is achieved through multiple strategies, including anti-sense oligonucleotides (Miller et al., 2013, 2020; Becker et al., 2017), RNA interference (Stoica et al., 2016; Martier et al., 2019; Mueller et al., 2020) and CRISPR-Cas9 genome editing system (Gaj et al., 2017).

Cellular mechanisms involved in ALS pathology are usually targeted pharmacologically. Mito Q has been shown to mitigate oxidative stress and prolong the life span of $SOD1^{G93A}$ mice (Miquel et al., 2014). Glutamate excitotoxicity alleviation by a high-

dose of methylcobalamin was shown to increase survival of mouse model of ALS (Ikeda et al., 2015) and showed possible benefits in ALS patients if administered at an early stage of the disease (Kaji et al., 2019). Mitigation of ER stress and bioenergetic dysfunction by combining sodium phenylbutyrate and taurursodiol treatment led to slower functional decline in ALS patients (Paganoni et al., 2020). Autophagy regulation has also been extensively studied as a potential therapeutic strategy as discussed previously. Due to the complexity of ALS pathology and autophagy cross-talk, it is still not clear which part of the autophagy pathway should be targeted to achieve effective and robust treatment.

Increasing evidence has reinforced the notion that stem cell transplantation could become a prospective therapy for ALS. The original concept of replacing degraded MNs with neural progenitors or stem cells was found to be too challenging, but the attempts revealed considerable benefits of transplantation treatment either way (Boulis et al., 2011). To date, various types of stem cells, including mesenchymal stem cells (MSCs) (Forostyak et al., 2011), neural stem cells (NSCs) (Zalfa et al., 2019), and hematopoietic stem cells (HSCs) (Appel et al., 2008) have been applied in ALS preclinical and clinical trials. MSCs can be derived from fat tissue, bone marrow, umbilical cord and peripheral blood. Compared to the other stem cell types, MSCs are easily obtained from the patients and possess lesser rejection risk and fewer ethical issues, which is why they are the preferred cell type used in regenerative studies (Xu et al., 2021). The therapeutic effect of transplanted MSCs is broad and needs further exploration, but it is reported, that the main mechanism of action is mediated through paracrine signaling. Factors such as brain-derived neurotrophic factor (BDNF), glial cell-derived neurotrophic factor (GDNF), insulin-like growth factor-1 and vascular endothelial growth factor (VEGF) are secreted by the MSCs and provide neurotrophic support to MNs and slow their degeneration (Forostyak et al., 2013). Aside from the paracrine mechanism, the application of MSCs in ALS rat modes led to reduction of apoptosis and inflammation and increased survival of MNs (Forostyak et al., 2014). Human MSCs (hMSC) transplantation in a mouse model of ALS was shown to improve motor function, extend survival and reduce neuroinflammation (Vercelli et al., 2008). Phase I clinical trials already confirmed the safety of MSC application in ALS patients (Nabavi et al., 2019). A recent meta-analysis of stem cell therapy in ALS clinical trials concluded that therapy with MSCs has a transient positive outcome on the progression of the disease (Morata-Tarifa et al., 2021). The same analysis importantly pointed out that intravenous delivery of MSCs is ineffective, indicating the significance of favoring intrathecal and intramuscular application in future trials.

2. AIMS AND HYPOTHESES

The main aim of the thesis was to study intracellular degeneration mechanisms occurring during the pathology and mechanisms of regeneration that are induced by therapy of SCI and ALS. The PI3K-AKT-mTOR signaling is one of the most important, central intracellular pathways, that plays a significant role during neural development as well as neural degeneration and repair. The mTOR signaling is fundamentally involved in the regulation of autophagy, a cellular degradation mechanism whose role in SCI and ALS was explored in the first two experiments of the thesis (Experiment 1 and Experiment 2). Another possible connection of this pathway in ALS pathology is through a recently discovered molecule PHLDA3 that was found to be elevated in ALS astrocytes. This issue was addressed in Experiment 3. Since intracellular mechanisms can be studied more efficiently in *in vitro* settings, Experiment 4 of the thesis was focused on establishing a novel model of spinal cord culture that could be utilized for further exploration of the mentioned pathways.

2.1. Experiment 1: Treatment of acute SCI with mTOR pathway inhibitors rapamycin or pp242

RAPA, a mTORC1 inhibitor was explored as a possible treatment for acute SCI in previous studies with success. The exact mechanism of RAPA treatment after SCI, however, needs to be explored further. Additionally, mTORC2 is not inhibited by this molecule, which leaves parts of the mTOR pathway active. Dual inhibition of both mTOR complexes can be achieved by administration of pp242.

2.1.1. **Hypotheses of experiment 1**

Hypothesis 1: Treatment of acute SCI with mTOR pathway inhibitors rapamycin or pp242 will lead to recovery through induction of autophagy and alteration of inflammatory response.

Hypothesis 2: Treatment of acute SCI with dual mTOR pathway inhibitor pp242 will cause a more pronounced effect on SCI outcomes, compared to RAPA treatment.

2.1.2. Specific aims of experiment 1

1) Comparison of the effect that RAPA vs. pp242 treatment has on mTOR pathway after SCI, by studying levels of downstream proteins in the spinal cord tissue.
2) Evaluation of autophagy and inflammation levels after mTOR pathway inhibition during acute SCI of the rat spinal cord.
3) Assessment of structural and functional recovery of rats after SCI treated by mTOR inhibitors RAPA and pp242.

2.2. Experiment 2: Treatment of ALS in SOD1^{G93A} rats with a repeated intrathecal and intramuscular application of MSCs

MSCs have been used successfully for the treatment of ALS in animal models and some clinical trials. The mechanism of action in which MSCs lead to decreased progression and improved motor function in ALS animal models and patients is still not clear.

2.2.1. Hypothesis of experiment 2

Treatment of ALS in SOD1^{G93A} rats with repeated application of human MSCs leads to neuroprotection and extended lifespan partly through alteration of autophagy mechanism.

2.2.2. Specific aims of experiment 2

1) Evaluation of autophagy pathway after treatment of ALS with hMSC in SOD1^{G93A} rats.
2) Studying the life-span and structural integrity of MNs in SOD1^{G93A} rat model of ALS after transplantation of hMSC.

2.3. Experiment 3: Studying the effect of PHLDA3 overexpression in astrocytes

Upregulation of PHLDA3 was found in SOD1^{D90A} ALS patient-derived iPSC-astrocytes. This molecule is a recently discovered Akt inhibitor and was reported to be involved in ER stress. Its role in astrocytes or ALS is not known.

2.3.1. Hypotheses of experiment 3

Hypothesis 1: PHLDA3 overexpression induces ER stress in WT astrocytes.

Hypothesis 2: PHLDA3 overexpressing astrocytes can influence the survival of MNs.

2.3.2. Specific aims of experiment 3

1) Investigation of the effect that PHLDA3 transfection has on WT astrocytes *in vitro,* by analyzing ER stress markers and cytotoxicity assays.
2) Studying the effect of PHLDA3 transfected astrocytes on MN survival by treating MN cultures by conditioned medium.

2.4. Experiment 4: Establishing a robust *in vitro* model of spinal cord interneurons

In order to study processes of neurodegeneration and neuroregeneration of spinal cord neurons, a reliable culture model is required. The majority of established primary neuronal culture systems are either made from cortical tissue, or dorsal root ganglia, which do not fully represent the biology of spinal neurons. Viability of murine embryonic CNS tissue is far greater compared to adults', which is why conventional models of cortical neurons are isolated from embryonic or early postnatal mice or rats. However, the regenerative ability of embryonic CNS neurons is far greater compared to mature neurons. Due to mentioned reasons, a new culture of spinal cord neurons was established, isolated from embryonic spinal cords and left to mature *in vitro*, during long-term cultivation.

2.4.1. Hypothesis of experiment 4

Spinal cord neurons isolated from mouse embryo mature *in vitro*.

2.4.2. Specific aims of experiment 4

1) Establishing a robust, long-term culture of spinal cord neurons.
2) Studying the composition of a newly established culture of spinal cord neurons.
3) Assessing maturation state of neurons in the culture

3. METHODS

3.1. Animals

Male Wistar rats, with mean weight of 300–330 g, were used in Experiment 1- SCI treatment. Transgenic (Tg) Sprague Dawley rats overexpressing human SOD1 with Gly-93-Ala mutation were used as a model of ALS. Rat experimental groups and treatments are specified in the following paragraphs. For primary astrocyte and neuronal cultures, C57BL/6J WT mice were used. C57BL/6-Tg(CAG-RFP/EGFP/Map1lc3b)1Hill/J reporter mice (common name: CAG-RFP-EGFP-LC3) were used for visualization of autophagy in neuronal cultures. The animals were kept at 21-23°C in on a 12-h light/12-h dark cycle, provided with water and food *ad libitum.* Experiments were conducted according to the European Communities Council Directive of 22 September 2010 (210/63/EU) and authorized by the Ethics Committee of the Institute of Experimental Medicine CAS and the Ethics Committee of the Czech Academy of Sciences.

3.1.1. **SCI and treatment**

SCI was induced in rats using a previously described balloon-compression model surgery (Vanický et al., 2001). In brief, dorsal laminectomy at the T10 level was conducted on rats anesthetized with isoflurane 2.5-3 vol.% (Arrane) and buprenorphine 0.05– 0.1 mg/kg (Reckitt Benckiser). A Fogarty® catheter (Edwards Lifesciences) was placed into epidural cavity, positioning the balloon at the level of the T8 vertebra. 15 μL of saline solution was applied to inflate the balloon, compressing, and injuring the spinal cord for 5min. Next, the balloon was removed, and the injury site was closed. Ampicillin (60mg/kg) was administered during recovery, every day for 5 days. Buprenorphine (0.05–0.1 mg/kg) was administered for pain relief as required. Caretakers helped the animals with feeding and manual urinary excretion. The animals were randomly separated into four experimental groups and treated postoperatively with: 5 mg/kg RAPA (Chem Science), 5 mg/kg pp242 (APExBIO), vehicle- SCI control group (2% DMSO, 5% triton, saline), and a no-lesion and no-treatment control group, as summarized in Tab. 1. The intraperitoneal treatment was administered once a day, starting from the second day, until the sixth day after the SCI (five repeated treatments). Animals were sacrificed on the seventh day after surgery, when spinal cord tissue and blood were collected for analysis.

3.1.2. **ALS animal treatment**

The onset of the ALS disease in Tg SOD1^{G93A} rats was assessed by monitoring animals' body weight once a week. Weight loss ranging from 5% to 8% of the previously recorded body weight in two consecutive weeks was considered to be the disease onset. This symptom usually appeared during 18th week postnatally. After the onset of the disease, the first batches of experimental cell therapies were administered, separating the animals into six groups (Tab. 1). hMSC cell suspension was injected either intrathecally (5x10^5 cells, total volume 50µl) into spinal canal at the level of the L3-L5 vertebrae (SC group), or intramuscularly (2x10^5 cells, total volume 100µl) into the *quadriceps femoris* of both hind limbs (M group), or into both locations (SC+M group). CondM group received intrathecal injection of conditioned medium (total volume 100µl), in which hMSC were cultivated. Control group (group PBS) received intrathecal (50µl) and intramuscular (2x100µl) injection of phosphate-buffered saline (PBS). Sprague Dawley littermates without SOD1^{G93A} mutation were WT controls. The treatments were repeated two more times, with 14 days apart. The cell therapy was administered to animals sedated with isofurane (Abbott Laboratoties). Immunosuppressive treatment consisting of cyklosporin A, (10 mg/kg; Novartis Pharama), azathioprin (4 mg/kg; GlaxoSmithKline) and metylprednisolon (2 mg/kg; Pfizer) was applied to all animals prior to any procedure. After the procedure, the rats were observed during following days for motor damage, such as tremors or paralysis of the hind limbs. Animals were kept alive until the end-stage of the disease. The end stage was diagnosed if two of following criteria were present: failure of the rat to adjust its position for 30s when placed on its side, onset of paralysis in two or more limbs, or a 30% decline in body weight, 75% decline in motor activity and a decline in grip strength by 75%.

Tab. 1 Animal experimental groups summary

Rat species	**Experimental group**	**Pathology**	**Treatment**	**n**
Wistar	RAPA	SCI	Rapamycin	17
	pp242	SCI	pp242	17
	Vehicle control	SCI	Vehicle	18
	No lesion control	/	/	4
Sprague Dawley	SC+M	Tg SOD1^{G93A}	Intramuscular and intrathecal hMSC	12
	SC	Tg SOD1^{G93A}	Intrathecal hMSC	9
	M	Tg SOD1^{G93A}	Intramuscular hMSC	8
	CondM	Tg SOD1^{G93A}	Intrathecal conditioned media	8
	PBS	Tg SOD1^{G93A}	Intramuscular and intrathecal PBS	12
	WT	/	/	10

3.1.3. **Behavioral testing**

To assess functional recovery after SCI and treatment, Basso, Beattie, and Bresnahan (BBB) open-field locomotor test was used as described (Basso et al., 1995). Rats' locomotor abilities in an open-field area were evaluated by two independent examiners for four minutes. A score ranging from 0 to 21 was given to each animal based on their capability to perform actions such as bodyweight support, forelimb–hindlimb coordination, hindlimb joint or tail movement.

3.2. Cell cultures

3.2.1. **hMSC culture**

The hMSCs isolated from bone marrow were supplied by Bioinova Ltd. The cells were isolated and cultivated as defined previously (Forostyak et al., 2014; Machova Urdzikova et al., 2014; Ruzicka et al., 2017). After the first passage, the hMSCs were cryopreserved until further application. After thawing, cells were expanded in MEM Alpha media containing 10% fetal bovine serum (FBS), 1% glucose and 5% Primocin (Biogene). After third passage, the cells were examined for MSC surface markers as described previously (Turnovcova et al., 2009) and used for the cell therapy. Conditioned medium was prepared using the same batch of hMSC by plating the cells at a density of 4000 cells/cm^2 and allowed to grow in the same medium for three days.

3.2.2. **Astrocyte culture**

Primary astrocytes were isolated from cerebral cortices of P0-3 C57BL/6 WT mice. The mice were decapitated, and the cerebral cortex was dissected in Hibernate E (Gibco, Thermo Fisher) on ice. Next, the tissue was washed in HBSS (Gibco, Thermo Fisher) and dissolved using 10µl 0.05% trypsin (Gibco, Thermo Fisher) in 2ml HBSS for 10min at 37°C. Tissue was moved into a solution containing Hibernate E, 0.4% bovine serum albumin (BSA) (Sigma) and 100µg/ml DNase (Sigma). The tissue was disrupted by trituration using P1000 pipette. Residual tissue was triturated in second solution containing Hibernate E, 0.4% BSA and 20µg/ml DNase. Cell suspension was spun for 10min at 775 RPM. Pellet with the cells was resuspended in culture media comprising of DMEM with glutamax (Gibco, Thermo Fisher), 10%FBS (Gibco, Thermo Fisher) and 1% penicillin/streptomysin

(Gibco, Thermo Fisher). Cells were seeded on a culture flask and maintained in a culture incubator on 37°C and 5% CO_2. Cultivation media was changed twice a week until confluency of the culture was reached, which happened approximately after a week after seeding. Next, the cells were shaken overnight at 260 RPM and 37°C. Medium contained non-astrocytic cells and was removed, while adherent astrocytes were passaged using 0.05% trypsin. The shaking was repeated once confluency of the culture was reached once again. The astrocytes seeded after the second shaking were used for experiments. The experiments were conducted on cells transfected with PHLDA3- green fluorescent protein (GFP) construct, CMV-empty or GFP-only plasmid controls and non-transfected controls. Transfections were done using Lipofectamine 2000 (Thermo Fisher) according to the manufacturer's instructions.

3.2.2.1. Transfection survival assay

Astrocytes plated onto glass coverslips coated with poly-L-ornithine (Sigma) were transfected using Lipofectamine 2000 (Thermo Fisher) according to manufacturer's instructions. To evaluate the toxicity of the transfection, several ratios of lipofectamine and plasmid DNA were tested. Lipofectamine volumes that were tested were 0.5µl, 1µl, 2µl and 3µl, whereas the analyzed amounts of PHLDA3-GFP and empty GFP plasmids were 0.5µg and 1µg per well in a 24 well plate. The plasmid DNA and lipofectamine mixtures were added to astrocyte cultures and incubated overnight. 48h after transfection, the cells were fixed using 4% paraformaldehyde (PFA) in 0.1M PBS (pH 7.4). Transfected astrocytes were analyzed using immunocytochemistry. DAPI stained nuclei of the surviving cells were counted using Cell Counter plugin in Fiji (Schindelin et al., 2012).

3.2.2.2. LDH-Cytotoxicity Assay

To assess the cytotoxicity of PHLDA3 overexpression in WT astrocytes, lactate dehydrogenase (LDH) activity was measured in transfected cells using LDH-Cytotoxicity Assay Kit II (Abcam). LDH is present in all eukaryotic cells and is released upon cytoplasmic membrane disruption, which is why its activity is widely used as a marker of cytotoxicity. Astrocytes plated on a 96 well plate transfected with PHLDA3 or CMV controls were incubated for 24h with culture medium, after which LDH activity present in the media was measured according to manufacturer's instructions.

3.2.2.3. H_2O_2 assay

To evaluate oxidative stress in astrocytes overexpressing PHLDA3, H_2O_2 concentration was measured in culture medium using ROS-Glo™ H2 O2 Assay kit (Promega). H_2O_2 is a convenient compound to analyze, as it's the most stable. type of ROS. H_2O_2 levels were measured in astrocyte culture medium according to manufacturer's protocol. Additionally, to PHLDA3 and CMV transfected astrocytes, positive controls of both groups were investigated. Positive controls were treated with 400nM thapsigargin (Sigma) for 5h prior H_2O_2 measurement.

3.2.3. **MN culture**

The protocol was based on previously published protocol by (Graber and Harris, 2013). Spinal cords of E13.5-E14.5 embryonic C57BL/6J WT mice were dissected in Hibernate-E medium (Gibco, Thermo Fisher) on ice. The tissue was rinsed with 1ml of HBSS (Gibco, Thermo Fisher) twice and digested in Neuron Isolation Enzyme (Thermo Scientific™ Pierce). Enzyme was removed and the tissue was disrupted by trituration in 700µl Hibernate E, 100µl FBS, 100µl 4% BSA (Sigma), 100µl DNase (Sigma) and then again in 900µl Hibernate E, 100µl BSA and 20µl DNase. The cell suspension was centrifugated at 1700rpm for 15min at 4°C on top of 1ml of 20% Percoll (Sigma), diluted in L-15 medium (Gibco, Thermo Fisher). The pellet containing enriched population of MNs was resuspended in 1ml Hibernate E and centrifugated again at 1400rpm for 5 min at 4°C. The pellet was resuspended in cultivation medium containing 1x N21 (R&D Systems), 1x SATO (Sigma), 5ug/ml insulin (Sigma),1mM sodium pyruvate (Gibco, Thermo Fisher), 2mM Glutamax (Gibco, Thermo Fisher), 40ng/ml T3 (Sigma), 1ug/ml laminin (Gibco, Thermo Fisher), 2.2ug/ml 3-isobutyl-1-methylxanthine (Sigma), 417ng/ml forskolin (Sigma), 5ug/ml N-Acetyl-L-cysteine (Sigma), 1% Penicillin-Streptomycin (Gibco, Thermo Fisher), 10ng/ml BDNF (Sigma), 10ng/ml Ciliary Neurotrophic Factor (Peprotech) and 10ng/ml GDNF (Peprotech). Cells were counted and plated on poly-L-ornithine (Sigma) and laminin (Sigma) coated glass coverslips in a density of 150 000 cells per well of the 24-well plate.

The cultures were treated with neuronal culture medium conditioned in astrocyte cultures. The conditioned medium was added to the culture of MNs after third day *in vitro* (DIV). Cultures were treated again at DIV6 with fresh conditioned medium. Cultures at

DIV3, DIV6 and DIV9 were fixed using 4%PFA, stained and analyzed. Three replicate cultures were treated with the conditioned medium.

3.2.4. **Culture of spinal cord neurons**

The method for producing mature spinal cord neurons was created based on previously described spinal cord culture methods (Thomson et al., 2008), cortical and hippocampal neurons (Barbati et al., 2013; Koseki et al., 2017; Petrova et al., 2020), with adjustments. Spinal cords of E13.5-E14.5 embryonic C57BL/6J WT mice were dissected in Hibernate-E medium (Gibco, Thermo Fisher) on ice. The tissue was rinsed with 1ml of HBSS (Gibco, Thermo Fisher) twice and digested in Neuron Isolation Enzyme (Thermo Scientific™ Pierce). 30µl of enzyme was added per 1 spinal cord and incubated for 9min at 37°C. After incubation, enzyme was removed, and tissue was transferred to disruption medium 1 (DM1) (Tab. 2). Tissue was disrupted in this solution by trituration with P1000 tip. The suspension was removed and remaining tissue was triturated again in disruption medium 2 (DM2) (Tab. 2). Tissue suspension was pressed through polished Pasteur pipette onto a 40µm cell strainer. Plating medium (PM) (Tab. 2) was added to the strained cell suspension in 1:1 ratio. The solution was centrifuged 5min at 90g at 37°C. Pellet was resuspended in in 2ml of PM. Cells were counted and plated on glass coverslips 100ug/ml poly-D-lysine (Thermo Fisher) prepared with pH 8.6 borate buffer. To visualize autophagic flux in axons, cells from autophagy reporter mice were mixed with their WT littermates in 1/100 ratio. The cells were placed either in a 24-well plate on 12mm borosilicate glass coverslips (Karl Hecht), or 10-well CELLview™ Cell Culture Slides with glass-bottom (Greiner). The ideal plating density of dissociated cells in the culture was approximately 93,000 cells/cm^2. 1h after plating, cultivation medium (CM) was added to the PM in 1:1 proportion. Culture was maintained by replacing ½ of old media for fresh CM. In order to limit glia proliferation, ITS+ supplement was omitted in CM after first 7 DIV.

Tab. 2 Media used for preparation and maintenance of culture of spinal cord neurons.

Medium	Composition
Disruption medium 1 (DM1)	Hibernate-E (Gibco, Thermo Fisher), 0.8% BSA (Sigma-Aldrich) 100µg/ml DNase (Sigma-Aldrich)
Disruption medium 2 (DM2)	Hibernate-E, 0.4% BSA 20 µg/ml DNase
Plating medium (PM)	50% DMEM, low glucose (Gibco, Thermo Fisher) 25% Horse serum (Gibco, Thermo Fisher) 25% HBSS without Ca^{2+} or Mg^{2+} (Gibco, Thermo Fisher) 1% Penicillin-Streptomycin (10,000 U/mL) (Gibco, Thermo Fisher)
Cultivation medium (CM)	MACS Neuro Medium (Miltenyi Biotech) 2% NeuroBrew 21 (Miltenyi Biotech) 1% Glutamax (Thermo Fisher) 1% ITS+ (Sigma-Aldrich) 1% Penicillin-Streptomycin

3.2.4.1. Transfection of spinal cord neuron culture

The cells were transfected using NeuroMag magnetofection (OZ Biosciences) at DIV3 with CAG-GFP plasmid. The CM was aspirated, stored, and substituted with 80% of regular cultivation volume of unsupplemented MACS Neuro Medium (Miltenyi Biotech). A suitable. amount of DNA plasmid was combined with magnetic beads in OptiMEM medium (Gibco, Thermo Fisher) and incubated for 15min at room temperature (RT). The amount of reagents used varied based on the cultivation volume of the specific plate used in experiment. The ratios were calculated according to an optimized 24-well plate protocol, where 0.2µg of DNA, 0.8µl of magnetic beads, and 100µl of OptiMEM were added per well. OptiMEM volume correspond to 20% of the regular cultivation volume. Following the incubation, the mixture was added carefully into wells with cells and unsupplemented medium. Next, the cultures were incubated on top of a strong magnet which came with NeuroMag Starting Kit (OZ Biosciences), for 20min at 37°C. The magnet was removed, and culture was incubated for another 40min, after which original CM was put back to the wells. GFP expression was visible 24h after transfection. The protocol of transfection was optimized to achieve low-efficacy transfection so that only a small number of the cells in the culture expressed GFP This way, the morphology of individual neurons could be observed.

3.2.4.2. Electrophysiological recordings

The whole-cell patch-clamp technique was implemented to assess the electrical properties of neurons. Borosilicate glass micropipettes with approximate 10 MΩ tip resistance were made using a P-97 Flaming/Brown micropipette puller (Sutter Instruments). Pipettes were filled with intracellular solution (130mM KCl, 0.5mM $CaCl_2$, 5mM EGTA, 2mM $MgCl_2$, 3mM ATP and 10mM HEPES with pH 7.2). Cells grown on glass coverslips were placed on the recording chamber, under Axioskop microscope (Zeiss), equipped with a high-resolution AxioCam HR digital camera (Zeiss) and electronic micromanipulators (Luigs & Neumann). Electrophysiological recordings were performed on cells perfused with artificial cerebrospinal fluid (135mM NaCl, 1mM $MgCl_2$, 2.7mM KCl, 10mM glucose, 2.5mM $CaCl_2$, 1mM Na_2HPO_4 and 10mM HEPES with pH 7.4 and osmolality 312.5 ± 2.5 mOsmol/kg). The recordings were performed with a 10 kHz sample frequency and amplified with an EPC9 amplifier, operated by the PatchMaster software (HEKA Elektronik), and filtered using a Bessel filter. Resting membrane potential (E_m) was measured by switching the EPC9 amplifier to the current-clamp mode. Raw recordings were analyzed with the FitMaster software (HEKA Elektronik). Membrane capacitance (C_m) was measured by applying Lock-in protocol in the PatchMaster software. Input resistance (IR) was measured from the current charge at 40ms after the onset of the 50ms depolarizing pulse from the holding potential of -70mV to -60mV. To determine the sodium currents (I_{Na+}), neurons were depolarized, while the current amplitude was recorded at a voltage step with the maximal current activation. The Na^+ component was isolated by subtracting the time- and voltage-independent currents, while the peak value was deemed to be the I_{Na+}. Action potentials were recorded in the current-clamp mode. The current ranged from 50pA to 1nA, in 50pA increments; the pulse interval was 300ms. Cells that emitted at least one AP were considered capable of generating AP.

3.3. Western blot

Four types of protein samples in three different experiments were analyzed using western blot method:

- Experiment 1: Rats after SCI and treatment were sacrificed; spinal cords were rapidly dissected and stored at −80 ◦C until protein isolation. Spinal cord portions (~1 cm) around the lesion were cut and disrupted in RIPA buffer (50 mM Tris (pH 8), 1% Triton X-100, 150 mM NaCl, 1 mM EDTA, sodium dodecyl sulfate, 0.5% sodium deoxycholate, 0.1%,

a protease inhibitor (PhosphoSTOP™ EASYpack, Roche, Sigma), and phosphatase inhibitor (cOmplete™ Protease Inhibitor Cocktail, Roche, Sigma). Homogenates were incubated on ice for 30 min and vortexed every 5 min. Next, samples were sonicated in three pulses for 10s and vortexed once more and centrifuged at 14,000× g at 4 ◦C for 15 min. Supernatant contained the protein suspension and was used for further analysis.

- Experiment 2: Tg SOD1^{G93A} rats were sacrificed after end-stage of the disease was exhibited. Spinal cords (L1-L6) and muscles (*quadriceps femoris*) were rapidly dissected and stored at −80 ◦C until protein isolation. Spinal cord proteins were isolated using AllPrep DNA/RNA/Protein Mini Kit (Hilde) following the manufacturer's instructions. Muscle proteins were homogenized in RIPA buffer with handheld rotor-stator homogenizer. Next, homogenates were handled following the same procedure as described in experiment 1.
- Experiment 3: Cultured astrocytes 48h after transfection, were treated with RIPA buffer and scraped from the plate surface using cell scraper. The lysates were collected, centrifuged at 12 000RPM at 4°C, after which pellets were discarded.

Concentration of proteins in samples obtained using described methods were measured using BCA assay (Pierce). 30µg of proteins were separated by electrophoresis on a 4–15% Mini-PROTEAN® TGX™ Precast Protein Gels, or Stain-free gels (Bio-Rad). After electrophoresis, if stain-free gel was used, it was put under 302 nm UV lamp to activate fluorescence of proteins in the gel and to capture an image of total protein content using Azure Biosystems c400. Then, proteins from gel were transferred to a PVDF membrane (Life Technologies) following standard protocols for wet transfer. Membranes containing fluorescent proteins from Stain-free gels were imaged to capture total protein contents. Next, membranes were incubated in either 5% dried milk (Cell Signaling), or 5% BSA (Sigma) in Tris-buffered saline/Tween-20 (TBST), overnight, based on antibody requirements. Then, primary antibodies were incubated with the membranes in the same blocking solution overnight 4°C with light shaking. Membranes were washed three times in TBST for 5min, after which 2h incubation with secondary antibody in TBST followed. Dilutions and other information about used antibodies are listed in Tab. 3. Secondary antibodies were discarded by washing the membranes three times in TBST for 5min. Horseradish peroxidase (HRP) conjugated secondary antibodies were visualized by activating chemiluminescence using ClarifyTM Western ECL Substrate (Bio-Rad) and imaged using Azure Biosystems c400. Signal quantification was performed using Fiji software.

Tab. 3 Antibody specifications used for western blot analysis

Primary antibodies			
Immunogen	**Cat. #**	**Dilution**	**Manufacturer**
Beclin-1	ab207612	1/2000	Abcam
eIF2α	9722	1/1000	Cell signaling
p- eIF2α	9721	1/1000	Cell signaling
p- Akt	4060	1/2000	Cell signaling
PHLDA3	LS-C385473	1/500	LSBio
β-actin	A2228	1/1000	Sigma
Akt	9272	1/1000	Cell signaling
Akt	4691S	1/1000	Cell signaling
4E-BP1	9644	1/1000	Cell Signaling
p-4E-BP1	2855	1/1000	Cell Signaling
LC3b	ab192890	1/2000	Abcam
LC3b	2775	1/1000	Cell Signaling
NAR	ab10096	1/1000	Abcam
Synaptophysin	ab32127	1/1000	Abcam
p62	ab56416	1/1000	Abcam
ChAT	AB144P	1/1000	Milipore
Secondary antibodies			
Immunogen	**Cat. #**	**Dilution**	**Manufacturer**
Mouse IgG (H+L)	115-035-003	1/10000	J.ImmunoResearch
Rabbit IgG (H+L)	111-035-003	1/10000	J.ImmunoResearch
Goat IgG (H+L)	31402	1/20000	Thermo Scientific

3.4. Cytokine measurement

Inflammatory and anti-inflammatory cytokine production was assessed in spinal cord tissue and blood of rats after SCI and subsequent treatment as defined previously (Machová Urdzíková et al., 2014). A customized Milliplex inflammatory cytokine immunoassay kit (Millipore, Burlington, MA, USA) was used according to the manufacturer's instructions. Custom kit contained beads coated with primary antibodies against interleukin (IL)-10, IL-6, IL-1β, IL-2, IL-4, VEGF, IL-12p 70, regulated on activation, normal T cell expressed and secreted (RANTES), TNF-α, and MIP-1α. The assay is based on the attachment of beaded primary antibodies to the sample, washing off unbound antibodies and adding another batch of biotinylated primary antibodies. Streptavidin-R-Phycoerythrin (Life Technologies) is then used to attach to biotin and produce fluorescent signal, which is measured on Luminex 200™ System (Luminex) and analyzed with Magpix instrumentation software.

3.5. Immunohistochemistry

Animals were euthanized using transcardial perfusion with 4% PFA in PBS. Spinal column was extracted and incubated in 4% PFA overnight for fixation and then in a sucrose gradient (10-30% in 0.2M PBS) or embedded in paraffin.

For experiment 1, the spinal cords tissue 1 cm rostrally and caudally from the injury site were sectioned. Tissue was embedded in paraffin and sliced into 5 µm thick transversal sections. Paraffin sections from the lesion core 1mm apart from each other were processed using standard immunohistochemistry (IHC) protocols and stained with primary antibodies, which were detected with secondary antibodies, specified in Tab. 4. Detection of biotinylated antibodies was performed using a VECTASTAIN® ABC Kit (Vector Laboratories). Hematoxylin staining was used to stain and visualize the nuclei.

For experiment 2, frozen spinal cord (L1-L6) and muscles (*quadriceps femoris*) tissue was sliced transversally into 20µm sections. Blocking of the sections was performed in 3% goat serum and 3% bovine serum albumin in TBST buffer for 2h. After the sections were incubated with primary antibodies at 4°C overnight, followed by 2h incubation with secondary antibodies and DAPI for 5-10 min at room temperature. Antibody specifications are listed in Tab. 4. To identify apoptotic cells, terminal deoxynucleotidyltransferase (TdT)-mediated dUTP biotin nick-end labeling (TUNEL) assay (ApopTag® Red In Situ Apoptosis Detection Kit, Millipore) was performed according to the manufacturer's recommendations.

Tab. 4 Antibody specifications used in immunohistochemistry experiments

Primary antibodies				
Immunogen	**Cat. #**	**Dilution**	**Manufacturer**	
GAP43	sc-7457,	1/500	Santa Cruz	
ChAT	AB144P	1/100	Millipore	
LC3b	2775	1/100	Cell signaling	
NeuN	MAB377	1/100	Millipore	
p-S6	4858	1/150	Cell signaling	
α-Bungarotoxin*	B13423	1/500	Thermo Fisher	
Secondary antibodies				
Immunogen	**Cat. #**	**Conjugation**	**Dilution**	**Manufacturer**
Goat IgG (H+L)	A-11055	Alexa Fluor 488	1/200	Thermo Fisher
Goat IgG (H+L)	A-11058	Alexa Fluor 594	1/200	Thermo Fisher
Mouse IgG (H+L)	A-11029	Alexa Fluor 488	1/200	Thermo Fisher
Rabbit IgG (H+L)	BA-1000	biotin	1/400	Thermo Fisher

* not an immunogen for a primary antibody, it's a peptide extracted from *Bungarus multicinctus* venom, conjugated with Alexa Fluor 594

3.6. Immunocytochemistry

Fixation of the cultured cells was performed by 15min incubation in 4% PFA in PBS at room temperature, washed two times, and kept in PBS at 4°C. Permeabilization and blocking was done by incubating the fixed cells in 10% donkey or goat serum (depending on type of secondary antibodies used) and 0.4% Triton-X in PBS for 1h at room temperature with gentle shaking. Primary antibodies, diluted in 2% goat serum and 0.1% Triton-X in PBS were incubated with the cells overnight at 4°C with light shaking. Secondary antibodies were diluted in the same solution and incubated with washed cells for 1h at room temperature. Information about used antibodies is provided in Tab. 5. Next, nuclei were stained using DAPI diluted at 1/3,000 in PBS. Coverslips were mounted on microscope slides after washing.

Tab. 5 Antibody specifications used in immunocytochemistry experiments

Primary antibodies			
Immunogen	**Cat. #**	**Dilution**	**Manufacturer**
ChAT	AB144P	1/100	Millipore
Chx10	sc-365519	1/100	Santa Cruz
Doublecortin	sc-271390	1/200	Santa Cruz
GDNFR α1	ab8026	1/100	Abcam
Gephyrin	147 111	1/500	Synaptic systems
GFAP	ab4674	1/500	Abcam
GFP	A10262	1/1,000	Thermo Fisher
Homer 1	160 003	1/500	Synaptic systems
Lbx1		1/10,000	Prof. Dr. Carmen Birchmeier-Kohler lab
Lmx1b (guinea pig)		1/10,000	Prof. Dr. Carmen Birchmeier-Kohler lab
Lmx1b (rabbit)		1/10,000	Prof. Dr. Carmen Birchmeier-Kohler lab
Neurofilament 70 kDa	MAB1615	1/400	Sigma-Aldrich
Parvalbumin	195 002	1/500	Synaptic systems
PAX2	71-6000	1/200	Thermo Fisher
PHLDA3	LS-C385473	1/150	LSBio
PKC γ	sc-166385	1/100	Santa Cruz
p-S6	4858	1/150	Cell signaling
Tlx3 (guinea pig)		1/20,000	Prof. Dr. Carmen Birchmeier-Kohler lab
Tlx3 (rabbit)		1/10000	Prof. Dr. Carmen Birchmeier-Kohler lab
VGAT	131 008	1/500	Synaptic systems
VGLUT 1	135 011	1/500	Synaptic systems
WFA	L1516	1/500	Sigma-Aldrich
βIII tubulin	ab78078	1/1000	Abcam
βIII tubulin	ab68193	1/1200	Abcam
Secondary antibodies			
Immunogen	**Cat. #**	**Conjugation**	**Dilution** **Manufacturer**

Chicken IgY	A-11039	Alexa Fluor 488	1/200	Thermo Fisher
Guinea Pig IgG (H+L)	A-11074	Alexa Fluor 546	1/200	Thermo Fisher
Mouse IgG (H+L)	A-21052	Alexa Fluor 633	1/200	Thermo Fisher
Mouse IgG (H+L)	A-11032	Alexa Fluor 594	1/200	Thermo Fisher
Mouse IgG (H+L)	A-11001	Alexa Fluor 488	1/200	Thermo Fisher
Rabbit IgG (H+L)	A-11012	Alexa Fluor 594	1/200	Thermo Fisher
Rabbit IgG (H+L)	A-11035	Alexa Fluor 546	1/200	Thermo Fisher
Rabbit IgG (H+L)	A-11034	Alexa Fluor 488	1/200	Thermo Fisher
Rabbit IgG (H+L)	A-31556	Alexa Fluor 405	1/200	Thermo Fisher

3.7. Microscopy and image analysis

Whole spinal cord sections were imaged on a LEICA CTR 6500 microscope with FAXS 4.2.6245.1020 (TissueGnostics) software. Analysis of the number of p-S6- or LC3b-positive cells per mm2 and number TUNEL stained neurons (identified with NeuN) was performed using HistoQuest 4.0.4.0154 (TissueGnostics) software. Growth-associated protein 43 (GAP43) and lesion size analysis was performed using Fiji software.

Live cultures of spinal cord neurons were captured in brightfield mode on a Zeiss Axio Vert.A1 inverted microscope with AxioCam ERc 5s camera.

Fluorescence microscopy images of the cell cultures was performed on a LEICA CTR 6500 microscope. Analysis of spinal cord culture composition was performed by counting DAPI+ nuclei and βIII-tubulin (βIIIt) -positive cells using Fiji software. Analysis of doublecortin (DBC) and neurofilament 70kDa (NF70) expression was done by determining average gray value of captured signal in five random regions on the coverslip and subtracting the average value of background of every image in Fiji software. GFP-transfected neurons were used for morphology analysis using Fiji SNT plugin (Arshadi et al., 2020). Analyzed morphological properties were: number of branches, average length of branches, cable length, number of axonal branch points, axonal length, length of axonal branches, number of dendrites, cable length of dendrites and average dendrite length.

Confocal images were taken on a Zeiss LSM 880 Airyscan microscope. Confocal images were used for analysis of presynaptic and postsynaptic marker colocalization. Random regions of the coverslip were captured in a Z-stack mode with 0.5µm thickness. Z-stacks were processed in ZEN 3.1 (blue edition) (Carl Zeiss Microscopy GmbH). Maximum frontal projections were analyzed with Puncta Analyzer v2.0, a Fiji plugin written by Bary Wark (available at https://github.com/physion/puncta-analyzer), which automatically counted individual and colocalized synaptic puncta.

3.8. Laser axotomy

Cells cultivated on Greiner Bio-One CELLview™ Cell Culture Slides were transfected at DIV3 with GFP plasmid to visualize the morphology of individual cells. Axons were distinguished by morphologic standards established by Kaech and Banker (2006). Carl Zeiss AxioObserver.Z1 microscope with confocal module LSM 880 NLO and objective LD LCI Plan-Apochromat 25x/0.8 Imm Corr DIC M27 was used to image multiple cells before axotomy (axon cutting). Axotomy was performed by scanning a 3.4µm line transversally, in line-scan mode 100-200 times. Ti: Sapphire femtosecond laser Chameleon Ultra II (Coherent), set at 900nm and 80-100% laser power was used to cut the axons. Axons were cut approximately 250µm (253.8 +/- 75.160µm) from the cell body. After, an image every 30min for 14h following axotomy was recorded. Images and videos were analyzed using ZEN 3.1 (blue edition) and Fiji.

3.9. Autophagy flux tracing

To trace autophagic flux in axons, spinal cord culture with 1% LC3-RFP-GFP autophagy reporter cells was prepared. These reporter cells were isolated from CAG-RFP-EGFP-LC3 mouse embryos, which express LC3 protein tagged with red fluorescent protein (RFP) and GFP, resulting in yellow signal, if the AP is not merged with lysosome. After merging with lysosome, the pH of the vesicle drops, leading to quenching of GFP, leaving only RFP signal. Cells were plated Greiner Bio-One CELLview™ Cell Culture Slides and observed under Olympus SpinSR10 spinning disk confocal microscope. Individual axons of reporter neurons in different maturation states were recorded for 122s in 1s intervals. DIV22-23 cells were treated with 10ng/ml of RAPA (Chem-Science). Videos were analyzed in Fiji, using Multi Kymograph analysis. Static and moving red and green channel vesicles were counted manually in the kymographs.

3.10. Statistics

Statistical analyses were conducted on Sigmastat 3.1 (Systat Software Inc) or GraphPad 9 (Prism) software. Statistical differences between groups were determined using Mann Whitney test, one-way or two-way ANOVA, followed by Tukey's multiple comparisons or Newman-Keuls post hoc tests. Kaplan-Meier method was applied to measure the survival rate differences in ALS animals. Graphs were plotted using GraphPad 9 software

as means ± standard error of the mean (SEM). Statistically significant differences were marked as *p<0.05, **p<0.01, *** p<0.001.

4. RESULTS

4.1. Treatment of acute SCI with mTOR pathway inhibitors rapamycin or pp242

The main goal of this study was to compare the effects of RAPA and pp242 treatment in acute SCI. The inhibition of the mTOR pathway was evaluated by measuring the levels of the pathway effectors in the spinal cord tissue. To assess the mechanisms that mTOR inhibition affected after SCI, autophagy levels and inflammatory cytokine levels were analyzed. Finally, the effect of RAPA and pp242 treatment on structural and functional recovery was analyzed. The results from this section are included in a publication "Involvement of mTOR Pathways in Recovery from Spinal Cord Injury by Modulation of Autophagy and Immune Response" (Vargova et al., 2021). The results are summarized in Tab. 6.

Tab. 6 Summarization of Experiment 1 results. Arrows ↑ and ↓ mark upregulation or downregulation of measured responses in animals treated with rapamycin or pp242 compared to vehicle controls. Symbol ≈ marks no effect, ? marks unclear result.

		Rapamycin	pp242
Observed results in mTOR signaling	p-Akt	↑	≈
	p-4E-BP1	↑	↓
	p-s6	↓	↓
Physiological responses	Autophagy	↑	↑
	Inflammation	↓	↓↑?
	Structural recovery	↑↑	↑
	Functional recovery	↑	↑

4.1.1. Effect of RAPA and pp242 treatment of SCI on the mTOR Pathway

Phosphorylation levels of downstream effectors of mTORC1 and mTORC2 were assessed in injured spinal cords treated with RAPA and pp242 using western blot analysis (Fig. 7A-F). Relative band intensities of detected proteins were normalized to total protein content of stain-free gels. Normalized intensities of bands of phosphorylated and non-phosphorylated forms of Akt and 4E-BP1 were divided to evaluate the phosphorylation rate of these proteins. One-way ANOVA analysis, followed by Student-Newman–Keuls post hoc test revealed, that the highest phosphorylation of Akt (Ser473) was present in RAPA-treated

spinal cord tissue. Significantly lower phosphorylation of Akt was observed in animals treated with pp242 ($p = 0.031$) and vehicle ($p = 0.043$) (Fig. 7C). p-Akt expression was also lower in pp242 compared to vehicle control group, but this difference was not statistically significant. p-Akt levels in non-lesioned spinal cord tissue were lower compared to injured tissue ($p < 0.001$). Phosphorylation rate of 4E-BP1 was also the highest in RAPA-treated group compared to all other groups (Fig. 7F). p-4E-BP1 levels were lower in pp242 treated group compared to vehicle-treated controls ($p = 0.002$). Healthy spinal cord tissue had a lower phosphorylation rate of 4E-BP1compared to vehicle-treated group ($p = 0.001$).

Phosphorylation of protein S6 is commonly used to assess the activity of mTORC1, as it's a product of S6K1 activity, a kinase activated by mTORC1 (Jhanwar-Uniyal et al., 2017). IHC was chosen to examine p-S6 levels in injured spinal cords treated with mTOR inhibitors (Fig. 7G–J). The number of p-S6 positive cells per area was counted in five spinal cord sections from the center of the lesion. The highest number of p-S6+ cells was present in vehicle-treated controls, while no significant differences were found between RAPA and pp242-treated groups.

4.1.2. **Autophagy is enhanced by RAPA or pp242 inhibition of mTOR pathway in SCI**

Regulation of autophagy in spinal cord tissue after SCI and treatment was investigated using western blot and IHC analysis of LC3b levels (Fig. 8). Upregulation of LC3b-II after SCI in all groups compared to healthy controls was observed by western blot analysis and subsequent one-way ANOVA with Student-Newman–Keuls post hoc test ($p < 0.001$) (Fig. 8 A-C). RAPA and pp242 treatments caused significant decrease in LC3b-II compared to vehicle-treated rats ($p = 0.002$ and $p < 0.001$ respectively). No differences in LC3b-II levels between RAPA- and pp242-treated groups were observed ($p = 0.228$). IHC analysis of the spinal cord lesion core confirmed the results from western blot analysis (Fig. 8 D-G) The number of LC3b+ cells per tissue area was found to be lower in RAPA- or pp242-treated rats, compared to vehicle-treated controls ($p=0.0254$ and $p<0.001$ respectively). Although there was a trend of decrease of LC3b+ cells in pp242 group compared to RAPA group, this difference was not significant ($p = 0.0513$). Together these results indicate, that autophagy is upregulated after SCI and that RAPA and pp242 treatment cause further activation of this pathway, in a similar manner.

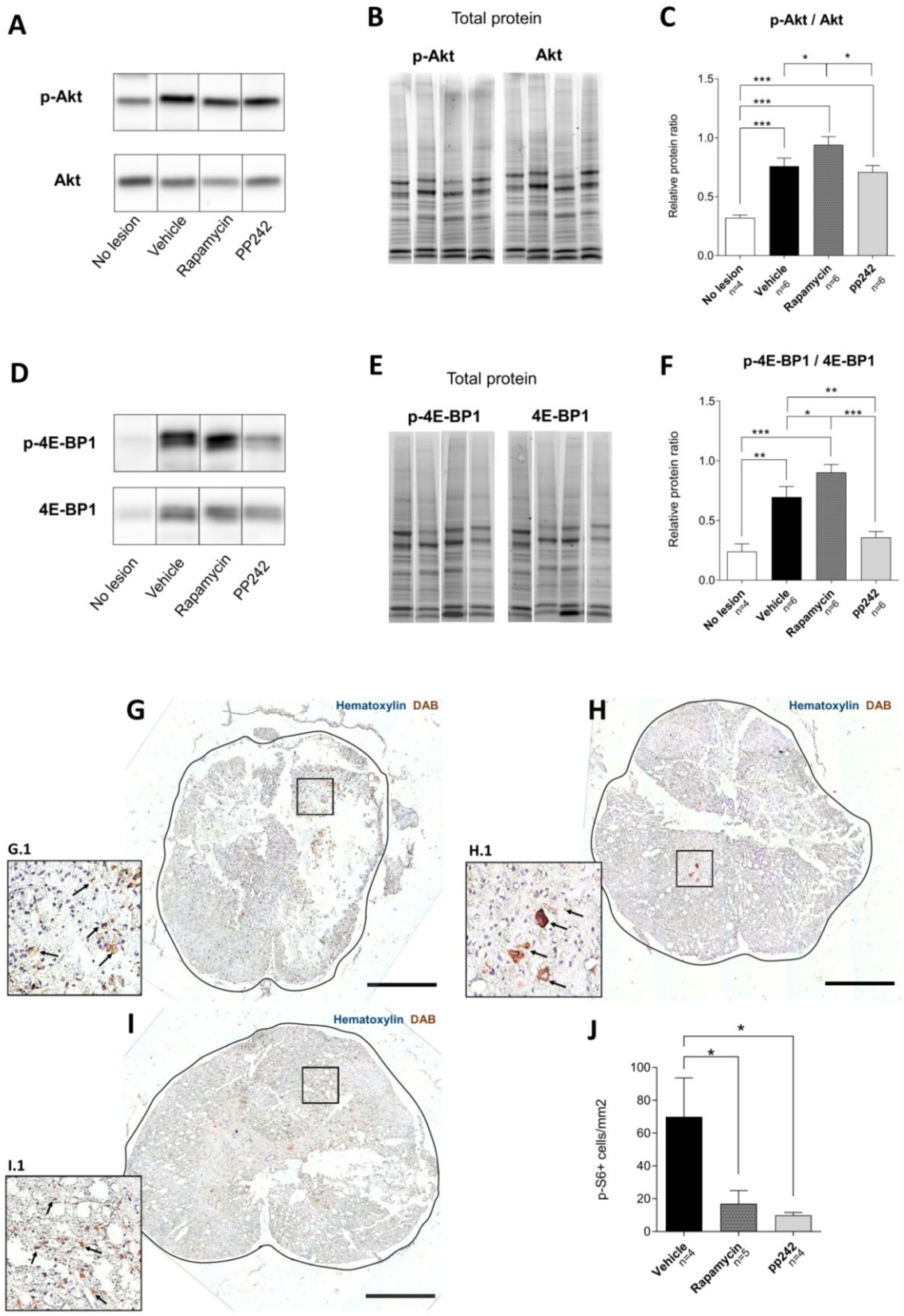

Fig. 7 RAPA or pp242 inhibition of mTOR pathway after SCI analyzed by western blot of proteins isolated near the lesion site (A–F). Immunoblots of treated and control groups are demonstrated for each evaluated protein (A, D). Total protein content was visualized using stain-free technology (B, E) and used as a control for uniform protein loading and normalization of relative band intensities during analysis. Presented total protein stains match the sample lanes in panels with representative blots of individual proteins. Normalized phosphorylated forms of protein band intensities were

divided by intensities of corresponding non-phosphorylated proteins to quantify the phosphorylation levels. The ratio of p-Akt/Akt was significantly higher in all groups after SCI compared to uninjured group (A-C). RAPA treatment led to increase in p-Akt/Akt ratio (C). Similarly, p-4E-BP1/4E-BP1 ratio was significantly higher in all groups after SCI compared to uninjured group (D-F). RAPA treatment initiated an increase, while pp242 led to decrease of 4E-BP1 phosphorylation (F). Activity of mTOR pathway was also investigated by immunocytochemistry, by analyzing the number of p-S6 positive cells in spinal cord sections in the proximity of the lesion (G-J). Both pp242- (I) and RAPA- (H) treated SCI caused a similar level of p-S6 decrease (J) compared to vehicle controls (G). Scale bars: 500µm; arrows are pointing to examples of DAB-stained pS6+ cells in G.1, H.1, and I.1 images, which are 1:4 magnifications of corresponding areas of the spinal cord sections. Data on graphs are displayed as means SEM; *p<0.05, ** p<0.01, ***p<0.001.

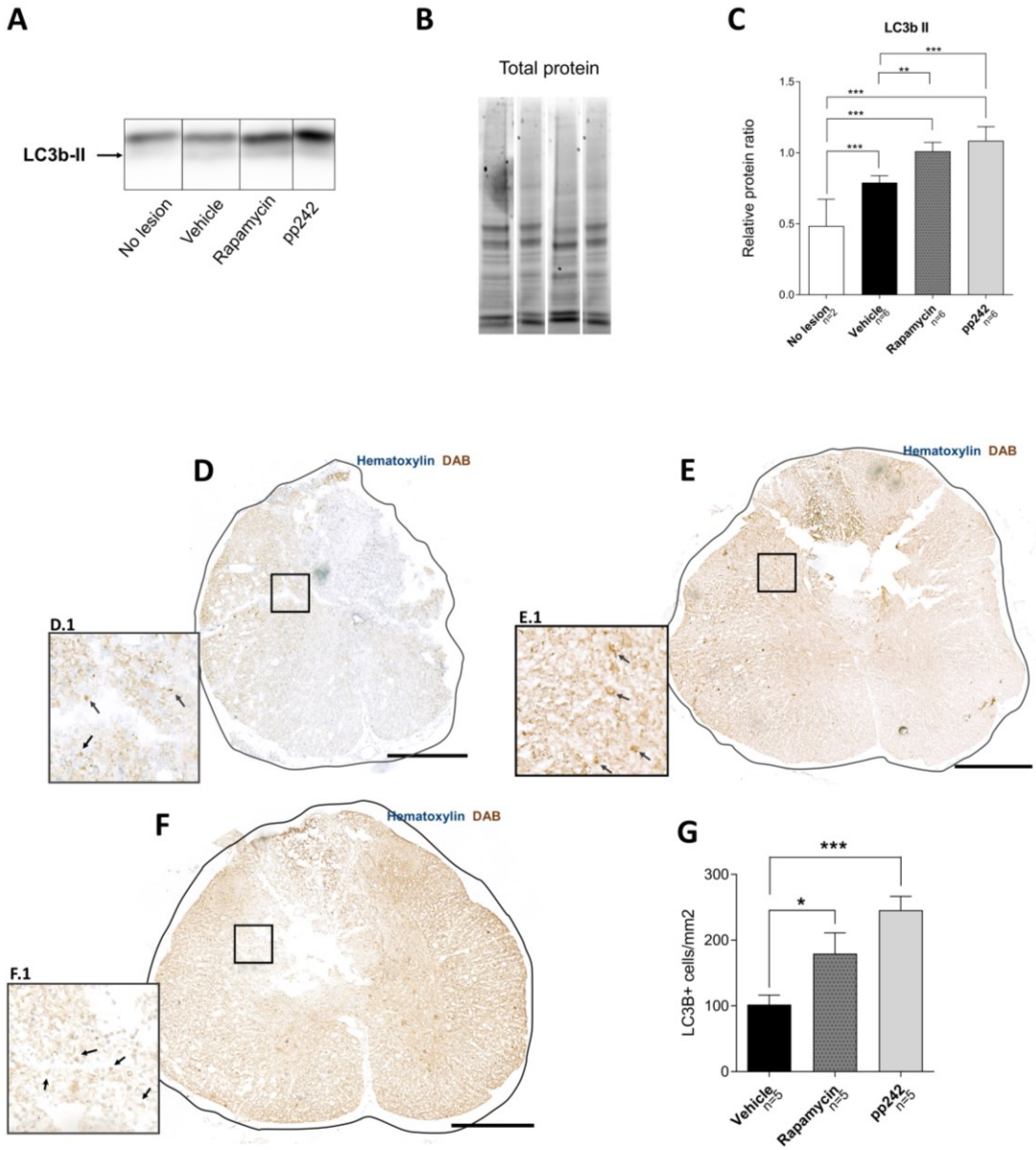

Fig. 8 Inhibition of mTOR pathway by RAPA and pp242 induces autophagy in SCI. Representative protein blots of LC3b-II are shown in panel A. Total protein contents, visualized by stain-free technology were used for blot normalization. Total protein lanes (B) are corresponding to the protein blots shown in A. Autophagy upregulation was confirmed in all injured spinal cords (C). Additionally, upregulation of autophagy in both RAPA and pp242 groups was observed, compared to vehicle controls. Immunohistochemical analysis of LC3b+ cells was performed in spinal cords treated with vehicle (D), RAPA (E) and pp242 (F). Similar to western blot results, image analysis

results have shown that RAPA and pp242 treatment cause activation on autophagy after SCI (G). Scale bars: 500μm; arrows are pointing to examples of DAB-stained LC3b+ cells in D.1, E.1, and F.1 images, which are 1:4 magnifications of corresponding areas of the spinal cord sections. Data on graphs are displayed as means SEM; *p<0.05, ** p<0.01, ***p<0.001.

4.1.3. Inhibition of mTOR Pathway by RAPA or pp242 modifies cytokine release in SCI

To analyze inflammatory response in rats treated after SCI, concentrations of multiple cytokines in serum and spinal cord tissue were measured. Custom Milliplex inflammatory cytokine immunoassay kit enabled detection of IL-1, IL-2, IL-4, IL-6, IL-10, IL-12 p70, VEGF, TNF-α, RANTES, and MIP-1α (Fig. 9). Differences between some levels of cytokines were found between RAPA-, pp242- and vehicle-treated groups in both spinal cord tissue (Fig. 9A) and serum (Fig. 9B) by analyzing the raw data using one-way ANOVA with Student-Newman–Keuls post hoc test. The RAPA-treated animals had lower content of IL-1 (p=0.026), IL-6 (p=0.027) and IL2 (p=0.002) in spinal cord tissue compared to pp242 group, whereas concentrations of MIP-1α (p<0.001) and IL-1 (p = 0.044) and were reduced compared to the controls. Spinal cord tissue of pp242-treated rats had significant upregulation of IL-2 (p=0.003) and downregulation of MIP-1 (p=0.003) compared to controls. Systematic cytokine levels were measured in serum, where it was discovered, that both RAPA and pp242 treatments caused significant reduction of IL-1 (p=0.019 and p=0.03), IL-10 (p=0.048 and p=0.02) and MIP-1α (p<0.001 and p<0.001), compared to vehicle-treated control group. These changes were different compared to spinal cord tissue changes. Additionally, IL-2 concentration in serum was higher in pp242-treated group, compared to vehicle-treated rats (p = 0.046).

4.1.4. Suppression of mTOR induces the structural and functional recovery in SCI

GAP43 staining was used to investigate axonal sprouting in spinal cord sections (Fig. 10). GAP43 signal was present in form of puncta, due to short interval of recovery after SCI. GAP43+ green puncta were visible against yellow background after the sections were captured in both red and green fluorescence filter to exclude autofluorescence. Both RAPA- and pp242-treated rats had significantly higher numbers of GAP43+ puncta per section area (p<0.001 and p=0.032) compared to the control group, assessed by one-way ANOVA with Student-Newman–Keuls post hoc test. Remarkably, significantly inferior axonal sprouting was detected in the pp242 group, in comparison to the RAPA group (p=0.016).

Another assessment of structural recovery of the spinal cord was performed by the analysis of the lesion size. Lesion size area was quantified in spinal cord slices and divided by the area of spared tissue (Fig. 10A). The lesion size was found to be larger in control group equally compared to RAPA- and pp242-treated animals ($p < 0.001$). These outcomes indicate that inhibition of the mTOR pathway by RAPA and pp242 alleviates the progress of secondary injury and, therefore, may induce recovery after SCI.

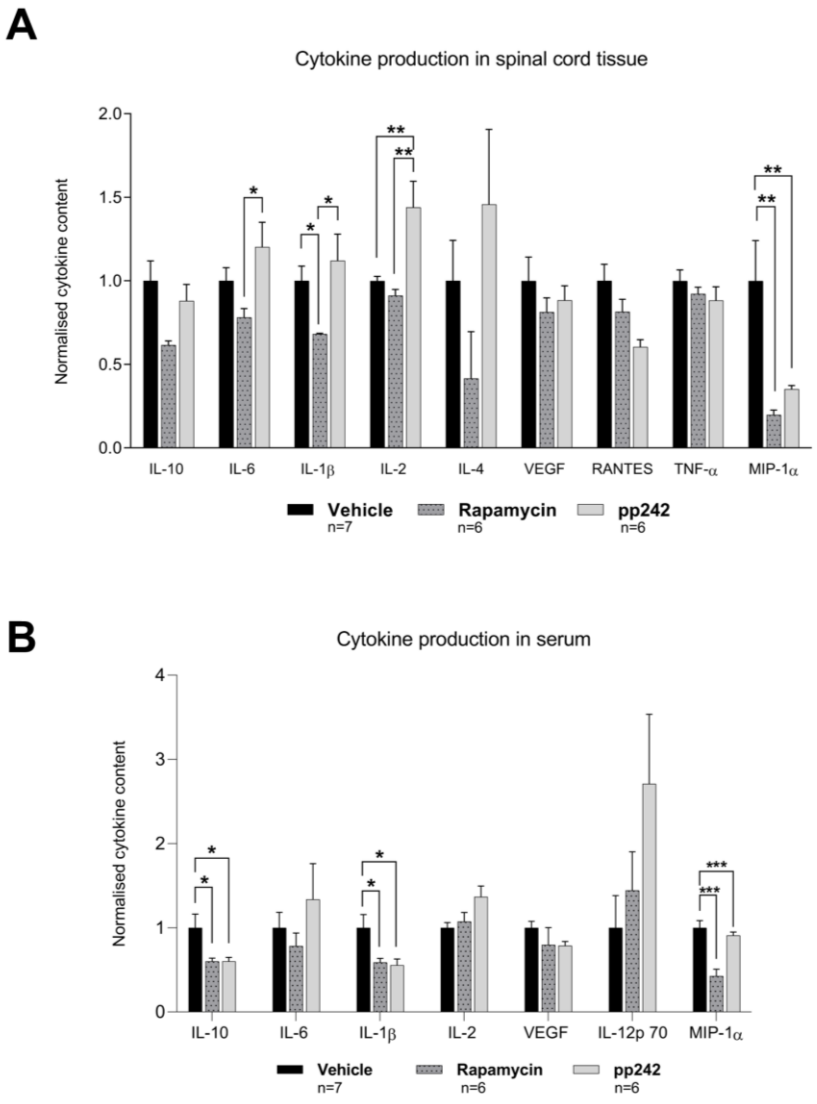

Fig. 9 Inhibition of the mTOR pathway by RAPA or pp242 modifies cytokine content in SCI. Investigation of cytokine concentrations in spinal cord tissue (A) and serum (B) after treatment of SCI. Measured data in treated groups were normalized to the mean concentration of the vehicle-treated control group for each cytokine. Data on graphs are displayed as means SEM; *p<0.05, ** p<0.01, ***p<0.001.

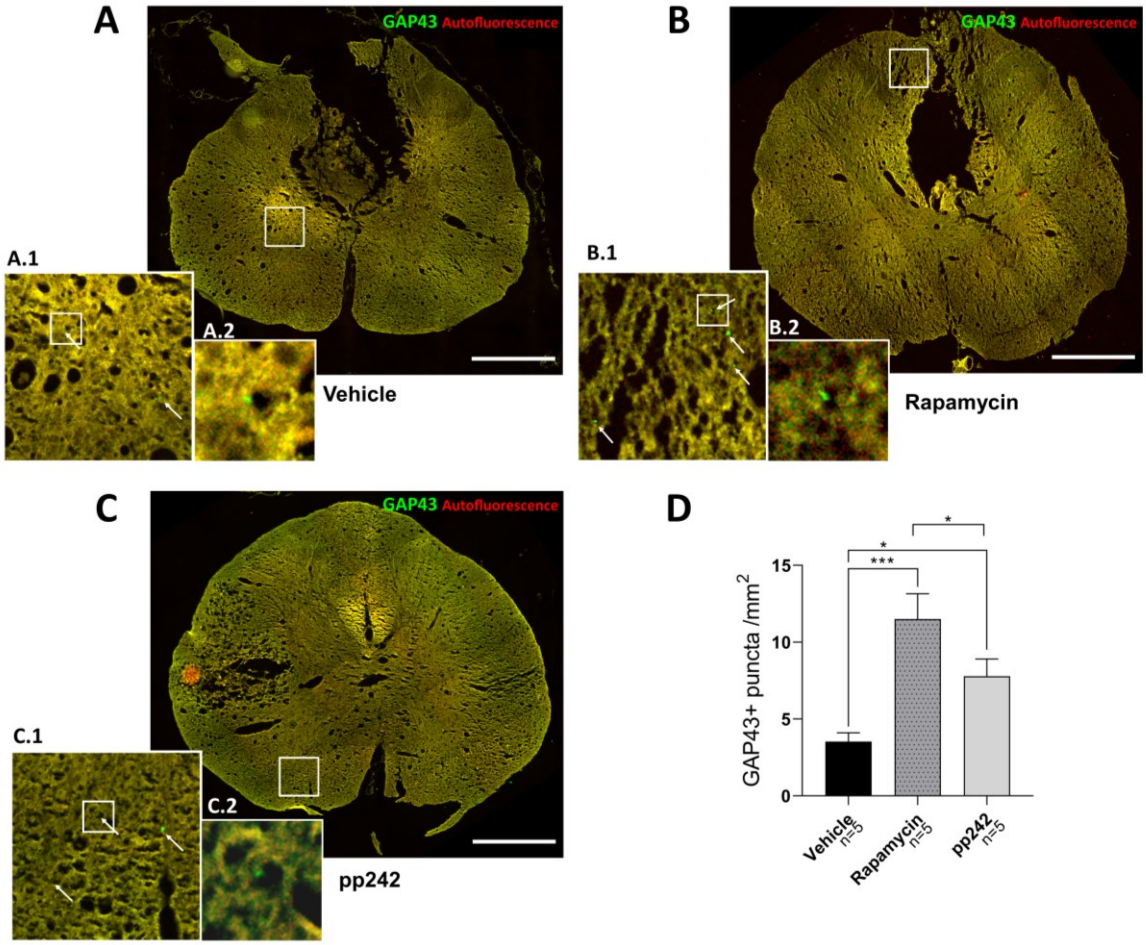

Fig. 10 Axonal sprouting analyzed by the number of GAP43+ puncta is enhanced after SCI treated with RAPA (B), compared to treatment with pp242 (C) and vehicle (A), as visualized in the graph (D). Scale bars: 500 μm; arrows are pointing to examples of GAP43+ puncta in A.2, B.2, and C.2 images, which are 1:4 magnifications of indicated areas of A.1, B.1, and C.1. A.1, B.1, and C.1 are 1:5 magnifications of areas indicated on corresponding spinal cord sections. Data on graph are displayed as means SEM; *p<0.05, ** p<0.01, ***p<0.001.

Locomotor recovery after SCI treatment was examined behaviorally, by the BBB open-field test (Fig. 11B). Improvement in BBB scores was observed in both RAPA and pp242 groups to a similar extent compared to controls ($p = 0.001$ and $p = 0.002$). The hindlimb movement was very limited to almost not existent in control group seven days after SCI, when the animals were scored on average 1.45 on 0-20 BBB scale. These scores are comparable to the scores of animals seven days after same type of injury that were reported in previous studies (Machova Urdzikova et al., 2015). On the other hand, partial to extensive movement in the hindlimbs was observed in RAPA- or pp242-treated rats, which received 3.5 and 3.6 average scores on the BBB scale, respectively.

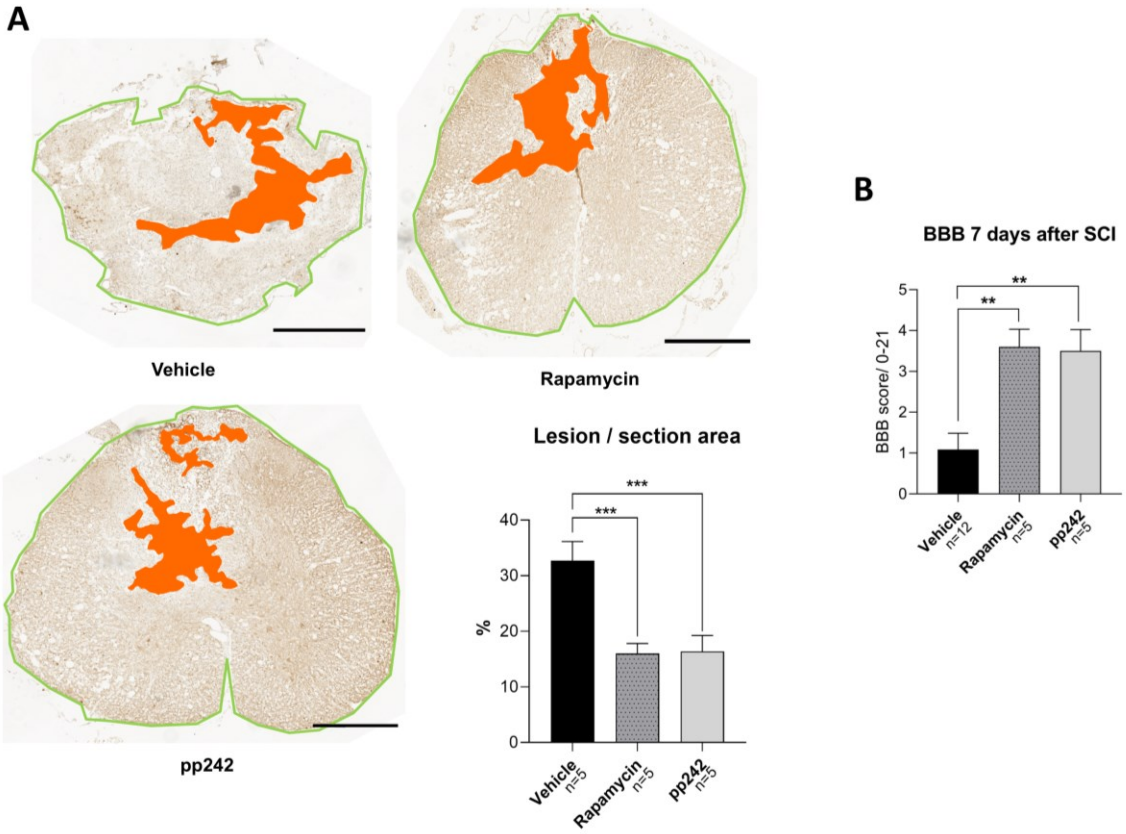

Fig. 11 Reduction of lesion size and increased locomotor recovery were instigated by mTOR inhibition in acute SCI. Smaller lesion size (A) was detected in the RAPA- and pp242- treated animals. Basso, Beattie, and Bresnahan (BBB) scores (B) were significantly higher after the SCI treatment with RAPA or pp242. Scale bars: 500µm. Data on graphs are displayed as means SEM; ** $p<0.01$, *** $p<0.001$.

4.2. Treatment of ALS in SOD1^{G93A} rats with a repeated intrathecal and intramuscular application of MSCs

This study aimed to investigate the effects of repeated application of hMSCs into various locations in rat model of ALS. Therapy was applied three times from the onset of the disease, 14 days apart to either spinal cord canal (SC), intramuscularly (M) into *quadriceps femoris* of both hind limbs, or both locations (SC+M). Whether medium conditioned with hMSCs is enough to induce therapeutic effect, intrathecal application of the medium (CondM) was tested. To investigate the mechanism through which hMSCs influence the course of the disease in ALS rats, autophagy markers were investigated in the spinal cord tissue. The therapeutic effect of individual hMSC treatments was evaluated in spinal cord tissue and *quadriceps femoris* and through observation of animals' survival. The results from this section are included in publication "A Combination of Intrathecal and Intramuscular Application of Human Mesenchymal Stem Cells Partly Reduces the Activation of Necroptosis in the Spinal Cord of SOD1^{G93A} Rats" (Řehořová et al., 2019).

4.2.1. Intramuscular and intrathecal application of hMSCs moderately alters autophagy pathway in SOD1^{G93A} rats

Concentrations of autophagy proteins Beclin-1, LC3b, and p62 were measured in spinal cord tissue (L1-L6) of the treated SOD1^{G93A} rats using western blot analysis (Fig. 12A–C). Relative intensity of band of housekeeping protein actin was used as loading control. In the Beclin-1 protein analysis (Fig. 12A), the only statistically significant difference, assessed by one-way ANOVA followed by Newman-Keuls post hoc test, was found in SC+M group, where a decrease was discovered, compared to WT controls ($p=0.028$). Other treatment groups and WT showed a trend of decrease of Beclin-1 compared to PBS control group, but this difference was not statistically significant. A significant increase of LC3b II/LC3b I ratio was found in M group, compared to WT ($p=0.023$). Other treatment groups demonstrated an increased ratio of this autophagy protein turnover compared to WT rats, but again, this difference was statistically significant only in PBS control group ($p=0.037$). No differences in p62 protein contents were found between any experimental groups (Fig. 12 C).

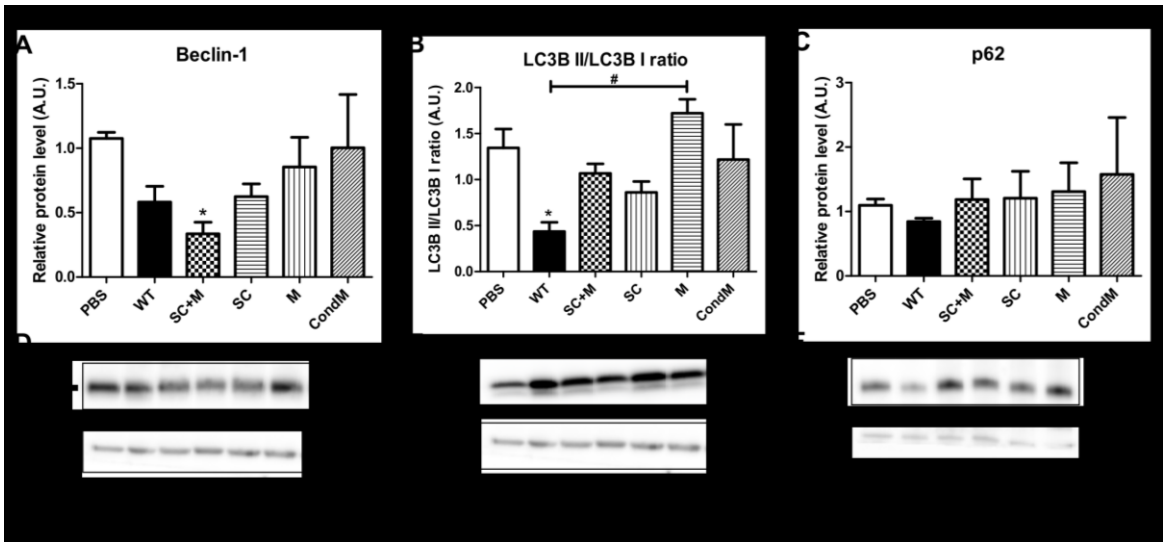

Fig. 12 Western blot analysis of autophagy pathway proteins was performed on spinal cord tissue of SOD1^{G93A} rats treated with human mesenchymal stem cells or conditioned medium (CondM). Beclin-1 expression (A,D) was upregulated in animals that received intrathecal and intramuscular therapy (SC+M), compared to wild-type controls. LC3BII/LC3BI ratio was greater in rats treated with intramuscular cell therapy (M), compared to WT controls (B,E). No significant differences between groups treated with phosphate buffer saline (PBS), WT, SC+M, intrathecal cell therapy (SC), M or CondM group was found in regards to p62 expression levels (C,F). Graphs are plotted as means + SEM; statistically significant differences of indicated bars compared to PBS group are marked with *$p<0.05$; #$p<0.05$.

4.2.2. **hMSCs cell therapy leads to prolonged survival, protection of MNs and neuromuscular junctions in SOD1^{G93A} rats**

To examine whether repeated hMSCs cell therapy impacts the course of ALS progression, the survival rate of SOD1^{G93A} rats was analyzed. All groups treated with hMSCs survived statistically longer compared to PBS control animals (Fig. 13A), The highest prolongation of lifespan was present in the SC+M group (217 ± 4 days, $p<0.001$), closely followed by the SC group (216 ± 8 days, $p=0.003$) and lastly in M group (206 ± 6 days, $p=0.027$), compared to PBS injected animals (198 ± 2 days). Rats injected with conditioned medium survived on average for 202 ± 11 days. The Kaplan–Meier plot (Fig. 13B) was used to visualize the probability of survival of the individual experimental groups.

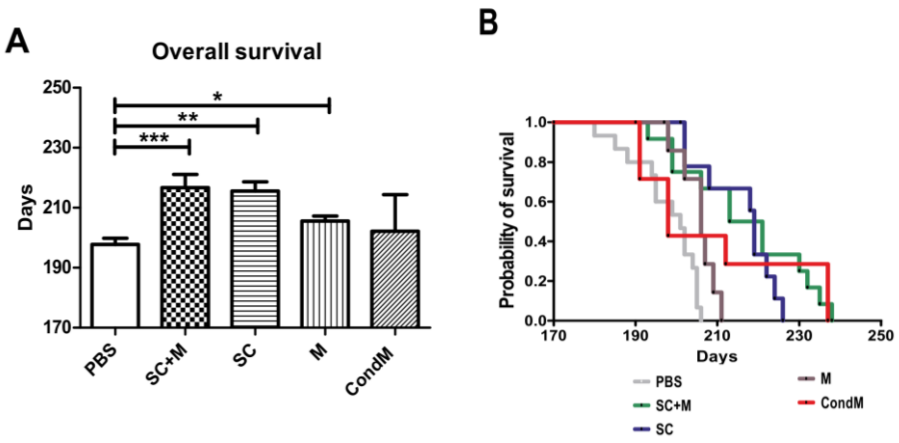

Fig. 13 The repeated treatment with human mesenchymal stem cells (hMSC) prolongs the lifespan of SOD1 transgenic rats (A). The longest survival was recorded in rats treated with intrathecal and intramuscular application of stem cells (SC+M), closely followed by intrathecally treated group (SC) and intramuscularly treated group (M), compared to the control group that received phosphate-buffered saline (PBS) injection. Animals that received an application of hMSC conditioned medium (CondM) did not survived longer compared to the controls. Probability of survival after different treatments was plotted using Kaplan–Meier graph (B). Graphs are plotted as means + SEM; *p<0.05, ** p<0.01, ***p<0.001.

To investigate whether hMSC could prevent the loss of MNs, choline acetyltransferase (ChAT), a marker of MNs was quantified in the lumbar spinal cord were quantified using IHC and western blot analysis. Significantly higher levels of ChAT were detected in WT animals and animals treated with the combination of intramuscular and intrathecal cell therapy, compared to PBS control group (Fig. 14A). Significantly higher ChAT levels were measured in WT spinal cords, compared to all types of therapy groups, except for SC+M group. The SC+M group also had significantly higher ChAT content compared to the M group. IHC analysis confirmed the ChAT western blot results (Fig. 14B, D). The number of ChAT+ cells was statistically higher in both WT and SC+M spinal

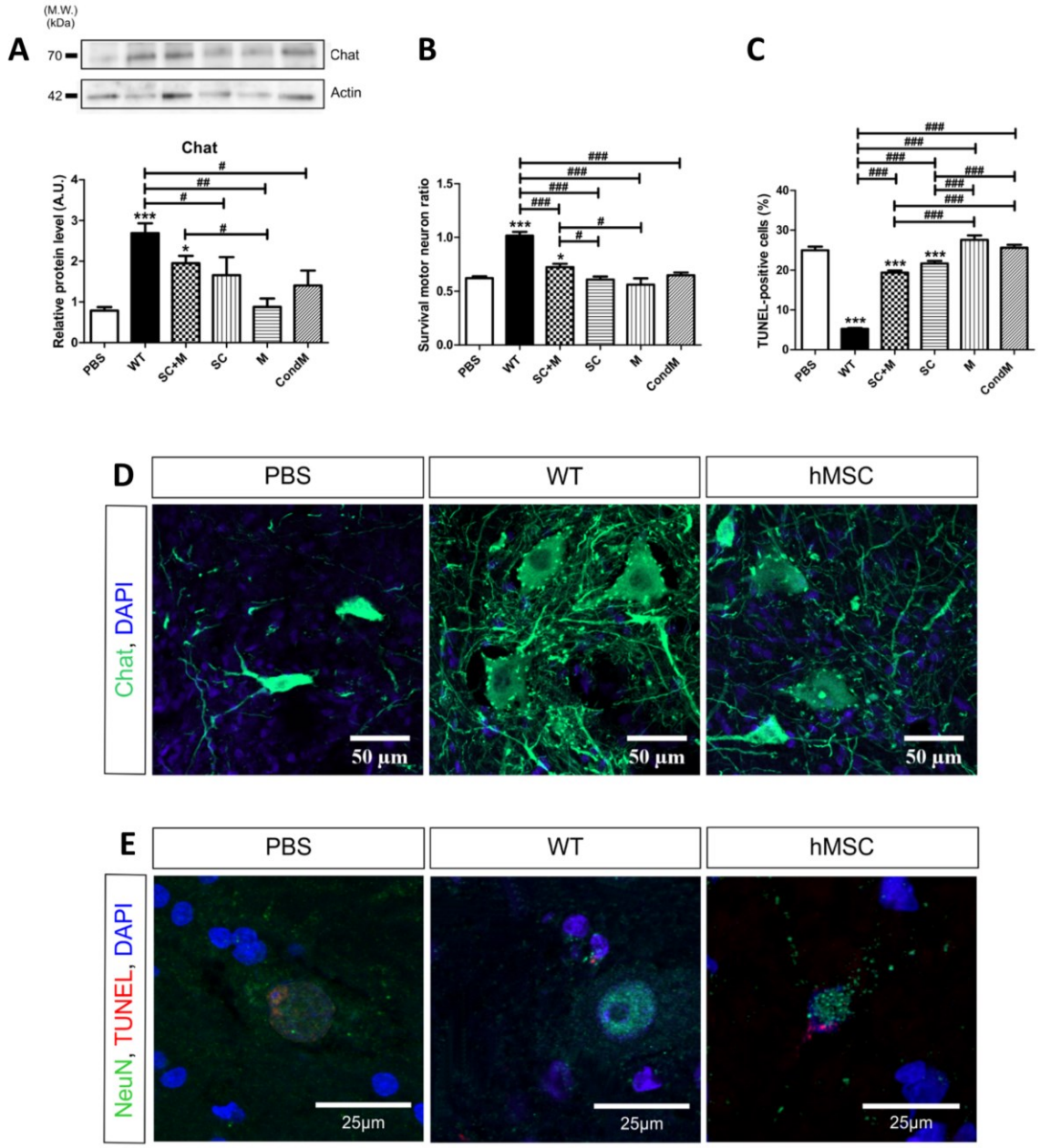

Fig. 14 Survival of motor neurons was evaluated in spinal cords of SOD1^{G93A} rats treated with human mesenchymal stem cells (hMSC). Choline acetyltransferase (Chat), a marker of motor neurons was evaluated in spinal cord tissue using western blot analysis (A). Wild-type (WT) rats had higher content of Chat, compared to rats treated with intrathecal (SC), intramuscular (M) cell therapy, as well as compared to rats treated with conditioned medium (CondM) or phosphate-buffered saline (PBS). Combination of intrahecal and intramuscular cell therapy (SC+M) led to higher preservation of Chat levels, compared to PBS controls and M group. Immunohistochemistry analysis of Chat (B, D) confirmed that SC+M group retained the highest number of motor neurons compared to other treatment groups. Apoptotic neurons in the ventral spinal cord were counted by NeuN and TUNEL colocalization (C, E). The lowest number of apoptotic neurons was observed in spinal cords of SC+M and SC treatment groups. Graphs are plotted as means + SEM; statistical comparisons of indicated bars compared to PBS group are marked as *p<0.05, ** p<0.01, ***p<0.001; other indicated comparisons indicate statistical significance as follows: # p<0.05, ## p<0.01, ### p<0.001.

cords, compared to PBS controls ($p<0.001$ and $p=0.029$ respectively). WT spinal cords had significantly more ChAT+ cells compared to all $SOD1^{G93A}$ spinal cords. SC+M experimental group retained significantly more ChAT+ cells in spinal cords compared to SC and M groups ($p=0.03$ and $p=0.015$, respectively). TUNEL assay was used to detect apoptotic cells in ventral horn neurons, stained by NeuN (Fig. 14C, E). Quantification of this staining revealed that WT rats had significantly lower apoptotic neurons in the ventral horns of the spinal cord, compared to all $SOD1^{G93A}$ rats. Application of hMSC intrathecally, or both intrathecally and intramuscularly led to a significant decrease of TUNEL positive number of neurons that were present in the ventral spinal cords of $SOD1^{G93A}$ rats, compared to controls treated with PBS ($p<0.001$ and $p<0.001$), or animals treated intramuscularly ($p<0.001$ and $p<0.001$), or with conditioned medium ($p=0.027$ and $p<0.001$).

Next, preservation of neuromuscular junction (NMJ) in *quadriceps femoris* was evaluated. Western blot analysis of the muscle tissue was performed, detecting contents of synaptophysin (Syn) (Fig. 15A-C), a presynaptic vesicle protein and nicotinic acetylcholine receptor α-7 (NAR) (Fig. 15D-F) a protein located on the membrane of skeletal muscle, that is vital for neurotransmission and muscle contraction. The proteins bands were normalized to total protein contents present on membranes, visualized by stain-free technology. The WT rats, as expected had significantly higher contents of both Syn and NAR compared to all $SOD1^{G93A}$ rats ($p<0.001$). The SC+M treatment group had significantly higher level of Syn protein, compared to PBS controls ($p=0.017$) and M group ($p=0.035$). Other treatments did not lead to preservation of Syn in the muscle. NAR expression was also highest in the SC+M treatment group, but the difference compared to the other experimental groups was not significant. NMJ were visualized by IHC, by staining the *quadriceps femoris* with α-Bungarotoxin, which attaches to α subunit of the NAR, and with an antibody against Syn (Fig. 15G). In the ALS rats treated with PBS only a very faint signal of Syn was detected. In the NMJ of SC + M treatment group, Syn signal was clearly visible, indicating that combination of intrathecal and intramuscular application of hMSCs partially protects against NMJ degeneration.

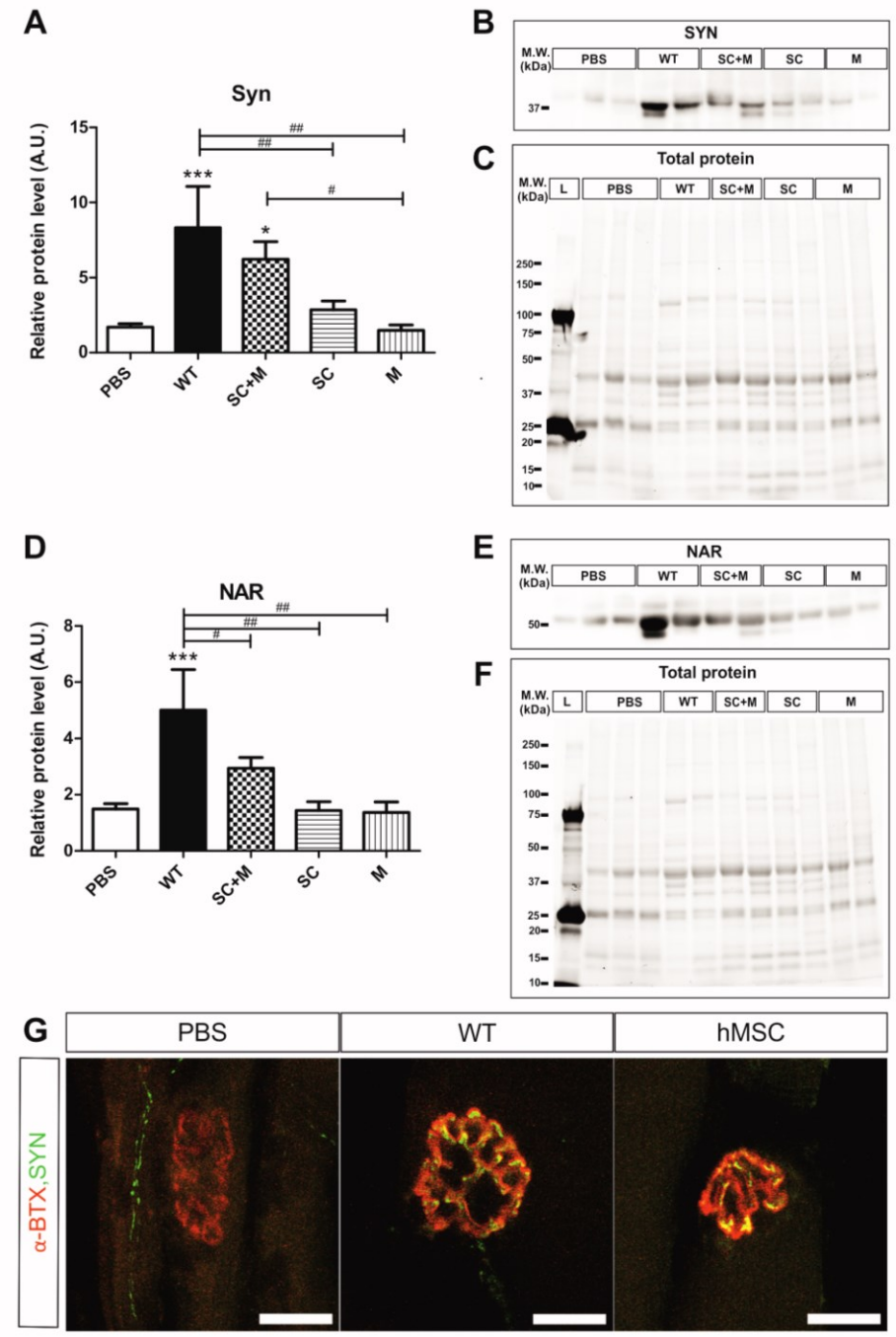

Fig. 15 Analysis of *quadriceps femoris* neuromuscular junction (NMJ) denervation was performed by using western blot and IHC analysis of the muscle tissue. The blots were used for detection of synaptophysin (Syn) (B) and nicotinic acetylcholine receptor α-7 (NAR) (E), after which relative band intensities were normalized to total protein contents visualized by stain-free technology (C and F respectively). Western blot revealed, that the NMJ denervation was slightly prevented in SOD1^{G93A} rats treated with intrathecal and intramuscular application (SC+M) of hMSC (A, D). Wild-type (WT) rats had significantly higher contents of both Syn and NAR proteins compared to all treatment groups and controls (PBS). Immunohistochemical staining using α-Bungarotoxin (α-BTX) and antibody against Syn (G) shows preservation of NMJ in SC+M group (hMSC), while PBS group almost lacked Syn signal. Scale bars: 20μm. Graphs are plotted as means + SEM; statistical comparisons of indicated bars compared to PBS group are marked as *p<0.05, ***p<0.001; other indicated comparisons indicate statistical significance as follows: # p<0.05, ## p<0.01, ### p<0.001.

4.3. Studying the effect of PHLDA3 overexpression in astrocytes

In this study, a role of a novel protein, PHLDA3 found to be upregulated in ALS astrocytes, was investigated in WT primary astrocyte cultures. After overexpressing the protein in WT astrocytes, their viability, presence of oxidative stress and ER stress was investigated. The effect of astrocytes overexpressing PHLDA3 on MNs was tested by treating cultures of MNs with astrocyte conditioned medium.

4.3.1. PHLDA3 overexpression in WT astrocytes is not cytotoxic, but leads to upregulation of ER stress

Transfection of WT astrocytes was optimized using multiple concentration ratios of lipofectamine and DNA. Transfection efficiency and the number of surviving cells was evaluated after transfecting the cells with a plasmid containing PHLDA3 tagged with GFP and compared to the cells transfected with a control-GFP plasmid (Fig. 16A). The transfection efficiencies and cell survival were comparable in both transfection groups. The best transfection rate with high cell survival was evaluated using 1µl of lipofectamine to 0.5µl of DNA per one well of the standard 24 well plate.

Successful overexpression of PHLDA3 in transfected cells was validated using western blot (Fig. 16B) and ICC (Fig. 16C) analysis. Significantly higher level of PHLDA3 protein was detected in cell suspension of the astrocytes transfected with PHLDA3-GFP construct, compared to non-transfected controls ($p=0.007$) and astrocytes transfected with CMV-empty plasmid ($p=0.014$), which had the same structure as the PHLDA3-GFP plasmid but did not contain any insert. In the ICC analysis, cultures were co-stained for astrocytic marker glial fibrillary acidic protein (GFAP) and PHLDA3 or GFP and PHLDA3 to validate the overexpression of PHLDA3 in transfected astrocytes (Fig. 16C). Strong signal of PHLDA3 or GFP was present only in the PHLDA3-GFP transfected astrocytes, indicating successful overexpression of the gene.

To investigate the effects of PHLDA3 overexpression in astrocytes, assays determining LDH activity and H_2O_2 contents were performed, as well as western blot analysis of its potential downstream effectors (Fig. 17). LDH activity and H_2O_2 levels (Fig. 17A) were not found to be different in cells expressing PHLDA3-GFP compared to cells transfected with control CMV-empty plasmid. This result indicates that PHLDA3 overexpression is not cytotoxic for WT astrocytes, does not induce production of ROS, or

interferes with their capacity to deal with oxidative stress. Interestingly, thapsigargin treatment did not induce higher production of H_2O_2 in either experimental group, indicating that ER stress induction in astrocytes does not lead to production of ROS.

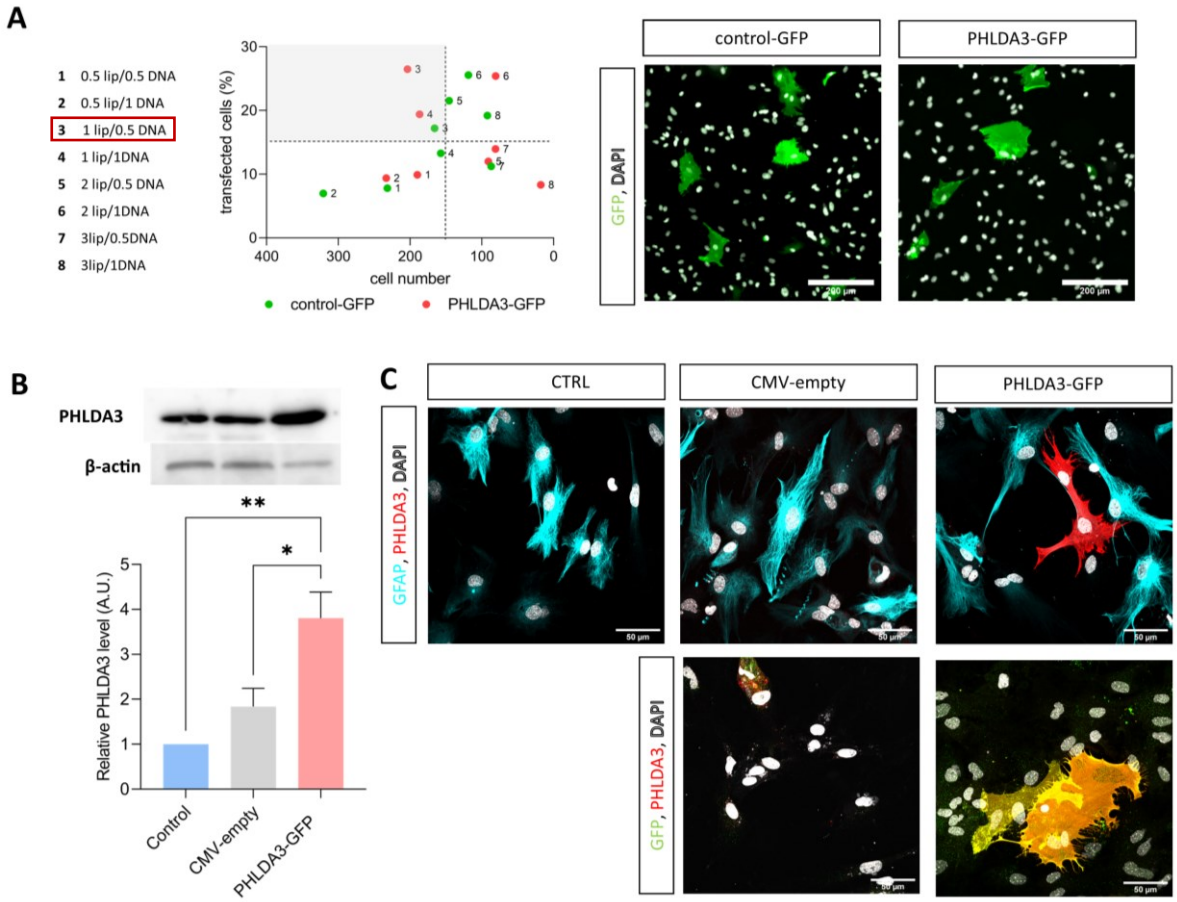

Fig. 16 Transfection optimization protocol (A) was performed by comparing surviving cells and transfection percentages of multiple concentration ratios of lipofectamine (lip) and DNA. Astrocytes transfected with control-GFP and PHLDA3-GFP plasmids had comparable survival rates and transfection efficiencies. The optimal transfection reagent ratio was deemed to be 1µl of lipofectamine to 0.5µl of DNA. Western blot analysis of cell lysates showed upregulation of pleckstrin homology like domain family A member 3 (PHLDA3) protein in cells transfected with PHLDA3-GFP construct, compared to non-transfected controls (Ctrl), or CMV-empty control construct (B). Immunocytochemistry of astrocytic marker, glial fibrillary acidic protein (GFAP) co-labeled with PHLDA3 demonstrates that PHLDA3 is overexpressed in astrocytes transfected with a PHLDA3-GFP, but it's absent in controls (C). Similarly, expression of green fluorescent protein (GFP) was present only in cells transfected with PHDLA3-GFP construct. Graphs are plotted as means + SEM; * $p<0.05$, ** $p<0.01$.

Phosphorylation levels of eIF2α and Akt were investigated using western blot analysis. Higher levels of p-eIF2α, an ER stress marker were found to be present in astrocytes overexpressing PHDLA3-GFP, compared to non-transfected and cells transfected with CMV-empty plasmid ($p=0.001$ and $p=0.005$) (Fig. 17B). Phosphorylation level of Akt was

not significantly decreased in PHLDA3 overexpressing astrocytes, compared to controls (Fig. 17C).

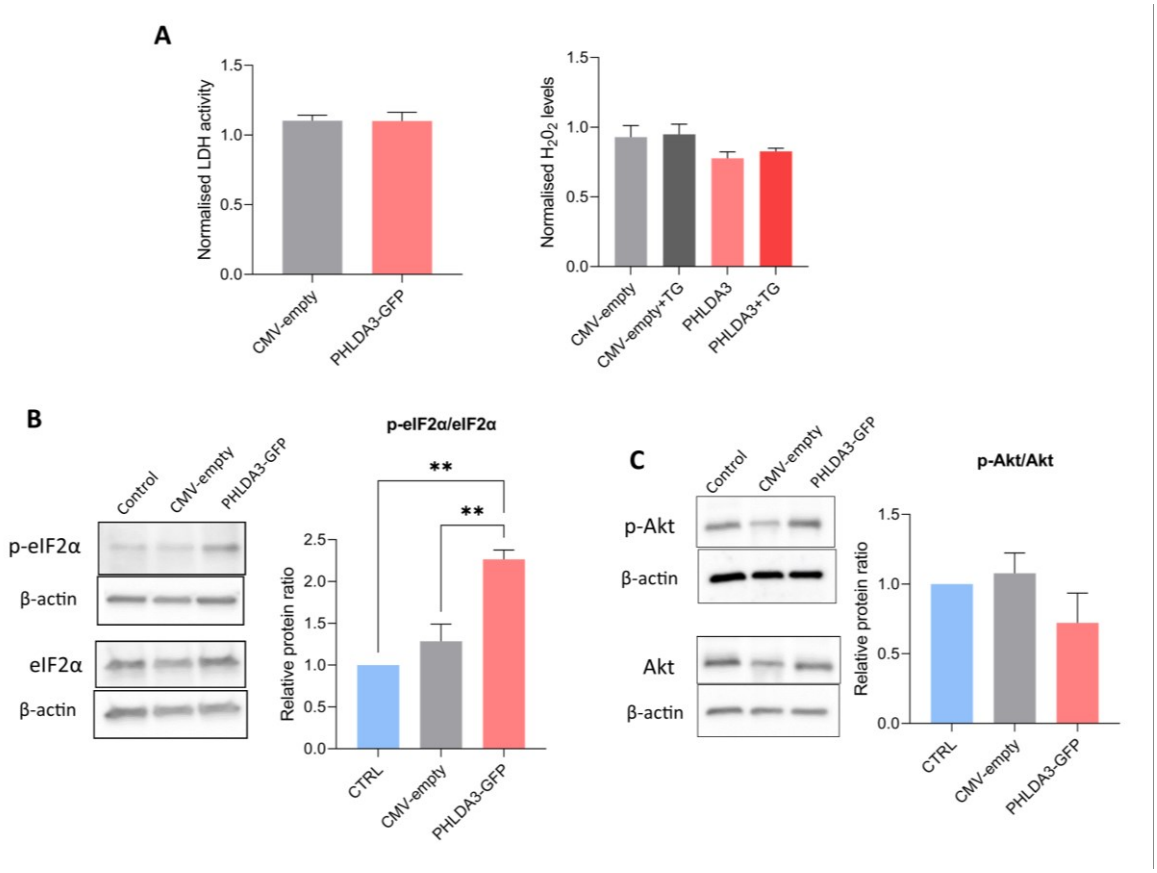

Fig. 17 Investigation of effects of pleckstrin homology like domain family A member 3 (PHLDA3) overexpression in astrocytes. Lactate dehydrogenase (LDH) activity and H_2O_2 contents were not affected by PHLDA3-GFP expression in astrocytes, compared to CMV-empty plasmid expression (A). Significantly higher phosphorylation level of eukaryotic translation initiation factor 2 α (eIF2α) was found to be present in PHLDA3-GFP transfected astrocytes compared to to non-transfected controls (Ctrl), or cells transfected with CMV-empty control construct (B). No differences in Akt phosphorylation levels were found between groups (C). Graphs are plotted as means + SEM; ** $p<0.01$.

4.3.2. **Conditioned medium from astrocytes overexpressing PHLDA3 decreases survival of MNs**

To investigate whether PHLDA3 overexpression in astrocytes leads to MN damage, cultures of MNs were treated with astrocyte conditioned medium. Astrocytes transfected with PHLDA3-GFP, CMV-empty control plasmid, or non-transfected controls were cultivated in fresh neuronal medium for 24h, producing PHLDA3 astrocyte conditioned medium (PACM), CMV astrocyte conditioned medium (CACM) and plain astrocyte conditioned medium (ACM), respectively. The conditioned media were added to MN

cultures on DIV3 and DIV6 to observe the long-term effect of the treatment. Cultures were stained for ChAT as a marker of MNs, βIII3-t as a general neuronal marker and DAPI (Fig. 18A). By counting the number of DAPI+ stained nuclei cells, an increase of cell number, normalized to the number of cells present at DIV3 was detected in all treatment groups, and between almost all time points, assessed by two-way ANOVA with Turkey's post hoc test (Fig. 18B). Slightly higher proliferation of cells was present in cultures treated with ACM, compared to CACM group at DIV9 ($p=0.025$). By counting the number of βIII3-t+ cells, no decrease in the number of neurons in any of the treatment groups was found (Fig. 18C). Interestingly, the relative number of ChAT+ cells decreased significantly at DIV9 in both PACM and CACM treated cultures, compared to ACM ($p<0.001$ and $p=0.001$ respectively) (Fig. 18D). PACM treated cultures also showed significantly lower survival of MNs, compared to CACM treated group ($p=0.0489$).

Together, these results indicate that transfected astrocytes release certain factors into their environment that decrease the proliferation of cells *in vitro* and decrease the survival rate of MNs specifically. Astrocytes overexpressing PHLDA3-GFP release factors that are more negatively affecting MN survival in culture, compared to astrocytes transfected with the control plasmid.

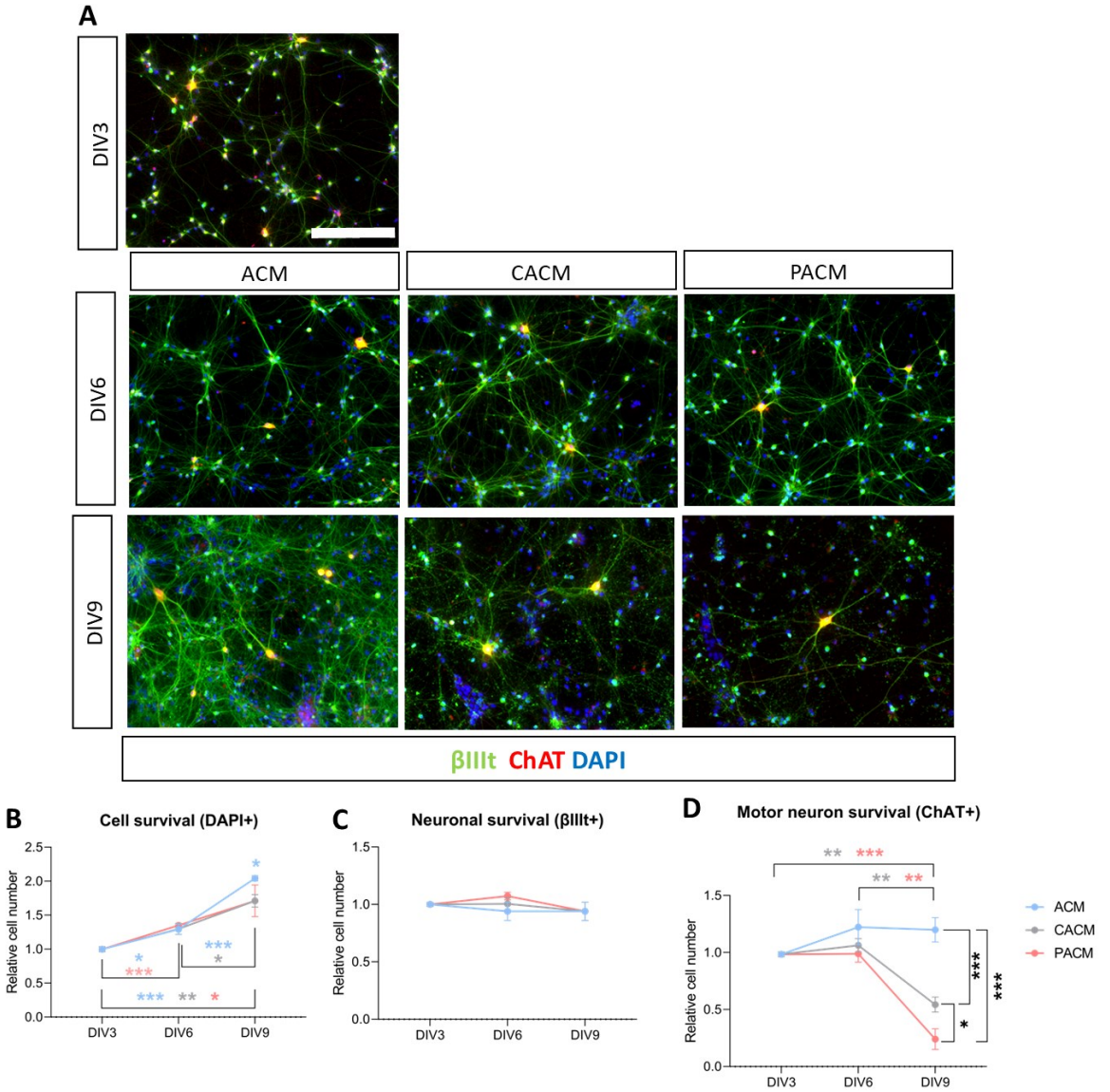

Fig. 18 Neuronal cultures with an enriched population of motor neurons were treated with medium conditioned in control astrocyte culture (ACM), CMV-empty transfected astrocyte culture (CACM) or PHDLA3-GFP transfected astrocyte culture (PACM). Immunocytochemical staining for choline acetyltransferase (ChAT), βIII-tubulin (βIIIt) and DAPI was performed on cultures cultivated until day *in vitro* (DIV) 3, DIV6 or DIV9 (A). Although cell proliferation was present in all groups, a slight increase of cell proliferation at DIV9 was found in ACM group (blue) (B). Neuronal populations in all groups remained stable. during the whole experiment (C). The number of ChAT+ cells marking motor neurons decreased in CACM (gray) and PACM (red) group at DIV9 (D), the decrease was more significant in PACM treated cultures. Scale bar: 200µm. Graphs are plotted as means ± SEM; * $p<0.05$, ** $p<0.01$, *** $p<0.001$.

4.4. Establishing a robust *in vitro* model of spinal cord interneurons

The main goal of this study was to establish a new culture of mature spinal cord interneurons, that could be used as a model for axon regeneration studies. After determining the culture conditions that enabled the embryonic neurons to remain in culture for at least four weeks, the properties of neurons were described. The results from this section are included in publication "Long-Term Cultures of Spinal Cord Interneurons" by Vargova et al., 2022.

4.4.1. Developmental changes through cultivation

At DIV1, cells adhered to the surface of the coated glass and began to grow processes (Fig. 19A). Cells developed processes at DIV1, that outspread visibly during DIV3 and DIV10 (Fig. 19B, C). Development of an intricate network of processes covering the entire culture surface was be seen by DIV17 (Fig. 19D), even more robustly in mature cultures at DIV41 (Fig. 19E) and DIV70 (Fig. 19F).

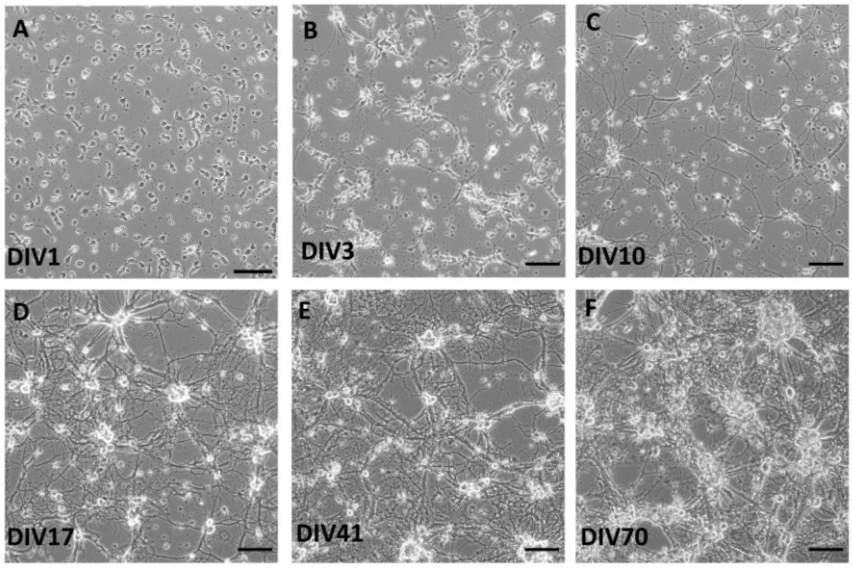

Fig. 19 Representative brightfield images of live culture isolated from embryonic spinal cords during cultivation day *in vitro* (DIV) 1 (A), DIV3 (B), DIV10 (C), DIV17 (D), DIV41 (E), and DIV70 (F). Extension of processes could be observed at DIV3 already, while more intricate network followed after longer cultivation period, after DIV17. Scale bars: 50μm.

The number of neurons in established culture was evaluated by counting βIII+ cells (Fig. 20). Even though the number of neurons was stable. (Fig. 20E), the number of all cells, evaluated by counting nuclei stained with DAPI, continued to rise through cultivation (Fig. 20F). Because of glia proliferation, the neuronal portion of the culture gradually, but

considerably, dropped from the mean of 60.6% at DIV3 to 29.5% at DIV20 (Fig. 20G). Regardless of the glial multiplication, long-term survival of neurons was accomplished, with the lengthiest continued culture being maintained past DIV72.

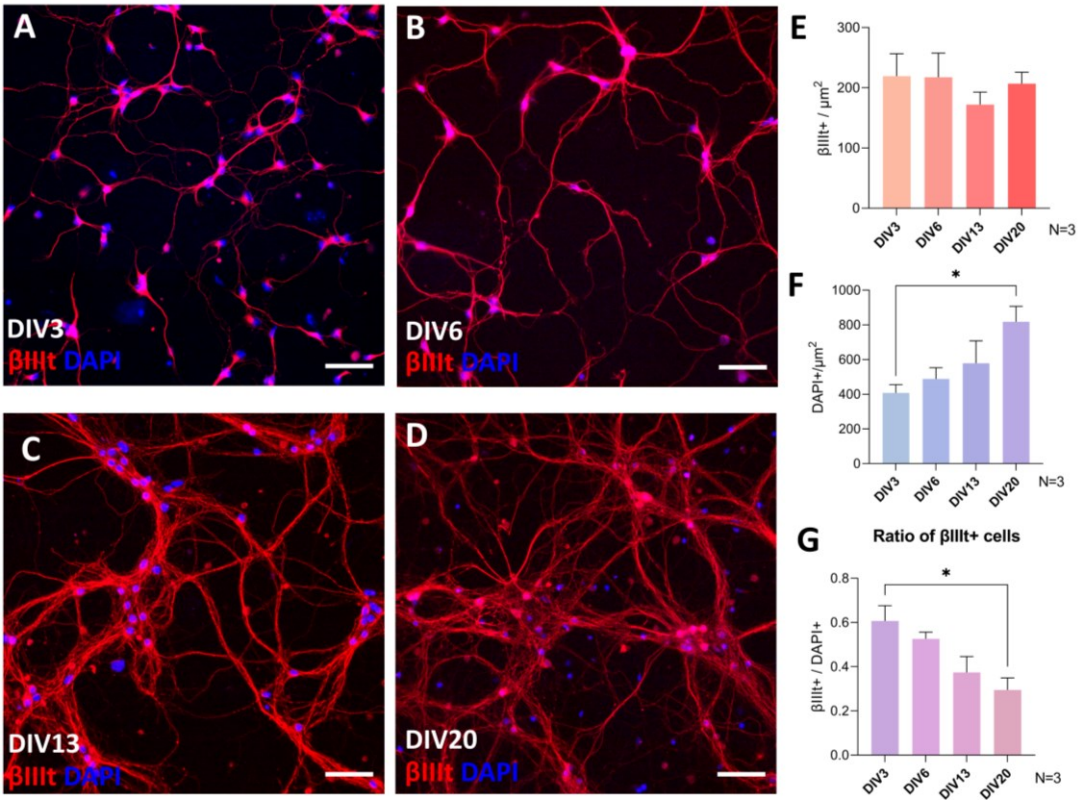

Fig. 20 Immunocytochemistry analysis of the spinal cord cultures at different days *in vitro* (DIV) 3 (A), DIV6 (B), DIV13 (C), and DIV20 (D). The total amount of neurons, established by counting βIII tubulin positive cells, was not fluctuating during cultivation (E), but the total number of cells evaluated using DAPI rose continuously (F), which caused a decrease in the fraction of neuronal population (G). N= number of separate cultures analyzed; Scale bars: 50µm; Graphs are shown as means + SEM, *p<0.05.

4.4.2. **Embryonic spinal cord cultures mature after approximately 15 days *in vitro***

Maturity of neurons isolated from E14 mice was investigated by studying their electrophysiological properties, expression of maturity markers, and formation of synapses. Together, the results indicate that the neurons mature after approximately DIV15.

4.4.2.1. Electrophysiological characterization of neurons in spinal cord culture

Electrophysiological properties of neurons in culture at multiple DIVs were recorded using whole-cell patch-clamp technique in order to characterize maturation of neurons from dissociated embryonic spinal cords.

The E_m is regarded as a universal characteristic of mature neurons (Sun et al., 2018). Mean E_m of neurons statistically declined from -55±12.2mV at DIV2 and -54.7±8.2mV at DIV9, to a value of -59.6±8.8mV at DIV16 ($p=0.01$ and $p=0.018$, respectively) and to -59.9±7.1mV at DIV24 ($p=0.006$ and $p=0.012$, respectively) (Fig. 21A), a value corresponding to mature interneurons. No additional significant alteration in E_m was detected between DIV16 and 24.

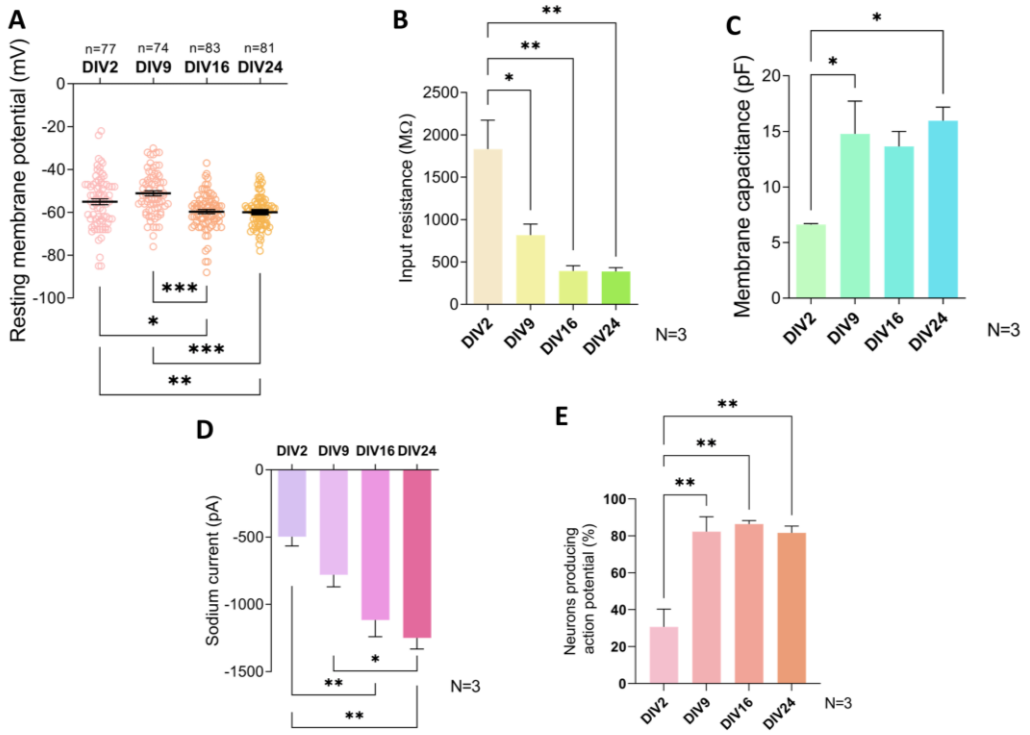

Fig. 21 Electrophysiological characteristics of neurons in new culture model. The measured resting membrane potentials (A) and sodium currents (D) did not alter significantly after day *in vitro* (DIV) 16. Stabilization of the values of input resistance (B), membrane capacitance (C) and the fraction of neurons producing action potentials (E) occurred after DIV9. N= number of separate cultures analyzed; n= number of cells analyzed; Graphs are plotted as means ± SEM; * $p<0.05$, ** $p<0.01$, *** $p<0.001$.

The number of ion channels corresponds to the cell size and is inversely proportional to the IR. A reduction in IR is used as an indicator of neuronal maturation (Takazawa et al., 2012; Kopach et al., 2020). The IR of measured neurons decreased significantly from DIV2 to DIV9 ($p=0.021$) (Fig. 21B). In older cultures, at DIV16 and DIV24, IR did not decrease further, compared to IR at DIV9.

The C_m is a parameter directly proportional to surface area of the membrane, which is increased during cell growth. Neurons grow their processes during development, which is why C_m was previously used to describe maturation of neurons (Golowasch et al., 2009).

Statistically significant increase of C_m transpired between DIV2 and DIV9, after which no further changes were observed (Fig. 21C). The average C_m at DIV2 was 6.63±0.13pF whereas at DIV9, it was 14.77±5.09pF (p=0.042).

Action potential amplitude is dependent on I_{Na+} and is changing during differentiation of neural cells, as reported previously (Song et al., 2013). Average I_{Na+} of -785.4±387.5pA was recorded at DIV9, which was statistically higher compared to DIV24 value -1248±684.3pA (p=0.031) (Fig. 21D).

Spontaneous activity of neurons in primary cultures was reported to be present in later stages of cultivation, corresponding to formation of synapses (Norris et al., 2006). The percentage of neurons producing action potential grew significantly between DIV2 and DIV9 (p=0.003) (Fig. 21E). Cultures after DIV9 did not have larger fraction of neurons producing AP.

4.4.2.2. Expression of maturity markers, NF70 and DBC in spinal cord culture

Maturity markers of cortical neurons NF70 and DBC were identified by Koseki et al., (2017) by RNA sequencing and corroborated by ICC. NF70 expression is increased, while DBC is decreased during maturation of the cortical cultures. To evaluate the maturation progression of spinal cord cultures, expression of mentioned markers was investigated using ICC (Fig. 22). Largest downregulation of DBC expression was observed between DIV6 and DIV13 (p=0.011) (Fig. 22A, C). Immunoreactivity of NF70 significantly increased at DIV20, compared to DIV6 (p=0.029) and DIV3 (p=0.025) (Fig. 22B, D).

4.4.2.3. Excitatory and inhibitory synapses formation in spinal cord culture

To study network development and neuronal connectivity in the culture, immunocytochemical colocalization of pre- and postsynaptic proteins of both inhibitory and excitatory synapse (Fig. 23). Presynaptic vesicular glutamate transporter 1 (VGLUT1) and postsynaptic density protein Homer1 were colocalized to detect the formation of excitatory synapses from DIV7 to DIV28 (Fig. 23A). The greatest change in colocalization of the excitatory synaptic markers was detected between DIV7 and DIV15 (p=0.003) (Fig. 23C). No further significant increase in colocalization was observed after DIV15. Colocalization of presynaptic marker gamma-aminobutyric acid transporter (VGAT) and gephyrin, a postsynaptic microtubule-associated protein responsible for anchoring inhibitory

neurotransmitter receptors, were analyzed to investigate formation of inhibitory synapses. (Fig. 23B). Correspondingly to excitatory synapses, inhibitory synapse formation rose significantly at DIV15, compared to DIV7 ($p=0.043$) (Fig. 23E). Additionally, significant growth of inhibitory synapses was observed between DIV15 and DIV28 ($p=0.029$).

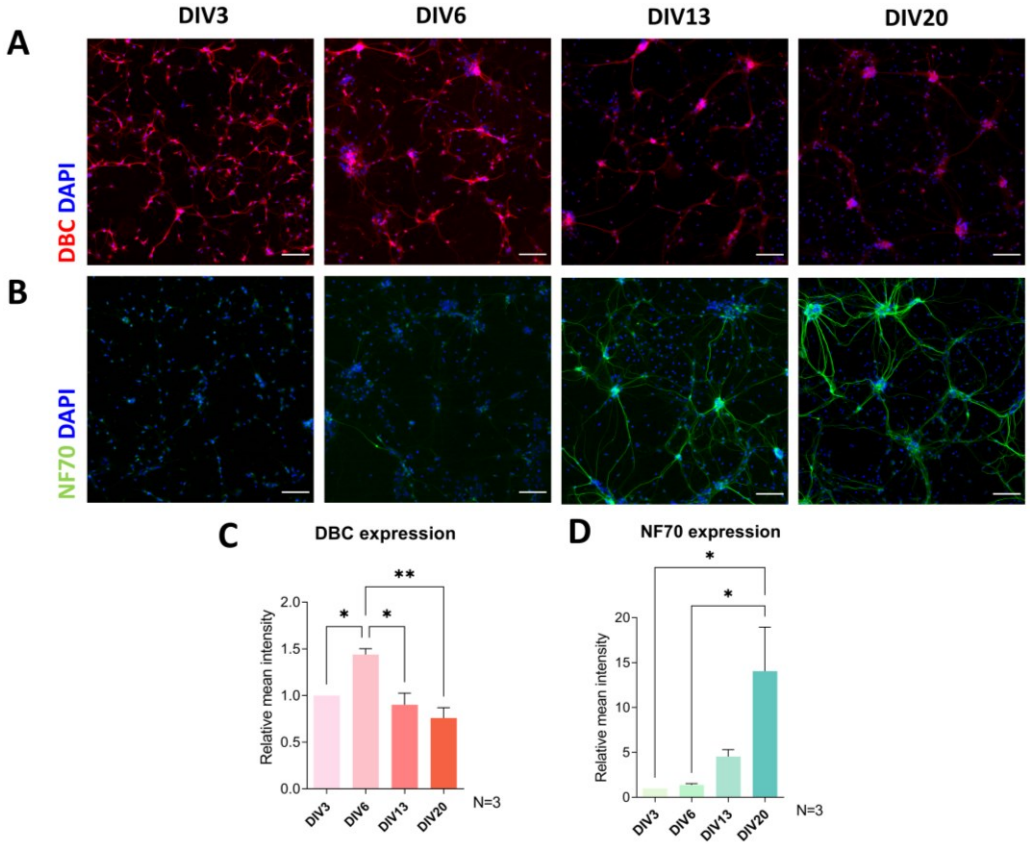

Fig. 22 Immunocytochemistry of maturity markers doublecortin (DBC) (A) and neurofilament 70kDa (NF70) (B) in various days *in vitro* (DIV) of the spinal cord culture. Doublecortin immunoreactivity decreased after DIV6 (C), while NF70 expression was upregulated at DIV20 (D). N= number of separate cultures analyzed; Graphs are plotted as means ± SEM; Scale bars: 100µm; * $p<0.05$, ** $p<0.01$.

To evaluate if the separate synaptic markers colocalize in different proportions during maturation, colocalized synaptic puncta were divided by total puncta (both synaptic and perisynaptic) counted for individual synaptic markers (Fig. 23D, F). It was found that portions of VGLUT1, Homer1, and VGAT that were synaptic (colocalized) were stable. in different DIVs. In contrast, the synaptic gephyrin fraction was not as constant (Fig. 23F). Synaptic gephyrin fraction significantly increased between DIV7 and DIV15 ($p=0.005$), indicating that gephyrin is participating in formation of inhibitory synapses more extensively in mature cultures.

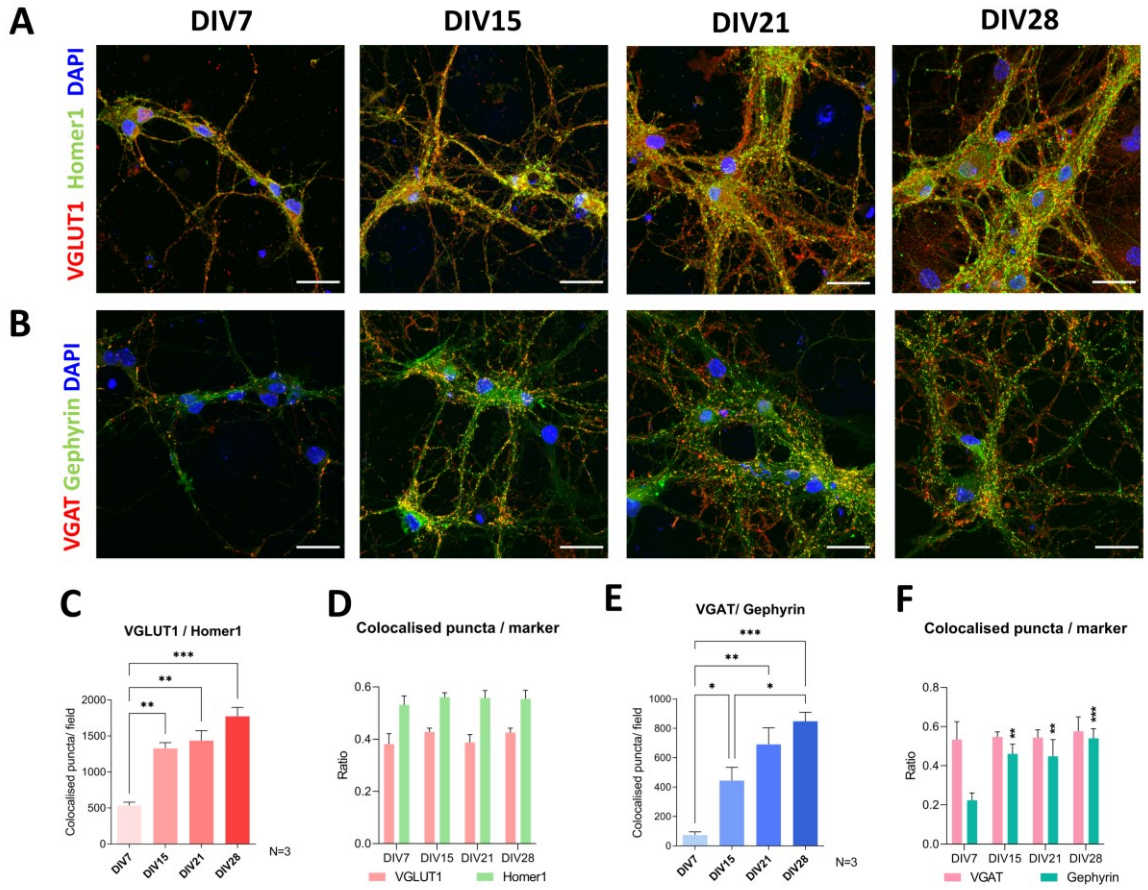

Fig. 23 Synapse formation during maturation of spinal cord culture was analyzed using immunocytochemical colocalization of presynaptic and postsynaptic markers. Presynaptic vesicular glutamate transporter 1 (VGLUT1), postsynaptic Homer1 (A, C, D), presynaptic vesicular gamma-aminobutyric acid transporter (VGAT) and postsynaptic Gephyrin (B, E, F) were used as markers of excitatory and inhibitory synapses, respectively. Formation of new synapses between *in vitro* (DIV) 7 and 15 was observed in both excitatory (C) and inhibitory (E) synapse analysis. The ratios of VGLUT1, Homer1 and VGAT colocalization remain unchanged during cultivation (D, F), whereas an increase of portion of Gephyrin marker colocalizing with VGAT was observed between DIV7 and DIV15 (F). N= number of separate cultures analyzed; Scale bars: 25µm; Graphs are plotted as means ± SEM; * $p<0.05$, ** $p<0.01$, *** $p<0.001$.

4.4.3. **Various neuronal markers are present in novel spinal cord culture**

Using immunocytochemistry, it was confirmed that neurons in spinal cord culture express transcription factors that are commonly used as markers of particular SpINs in developing spinal cord (Alaynick et al., 2011; Lu et al., 2015). Lbx1 (Fig. 24A), Lmbx1, Tlx3 (Fig. 24B), Chx10 (Fig. 24C), and Pax2 (Fig. 24I) were detected in varying amounts of neurons in the described *in vitro* model.

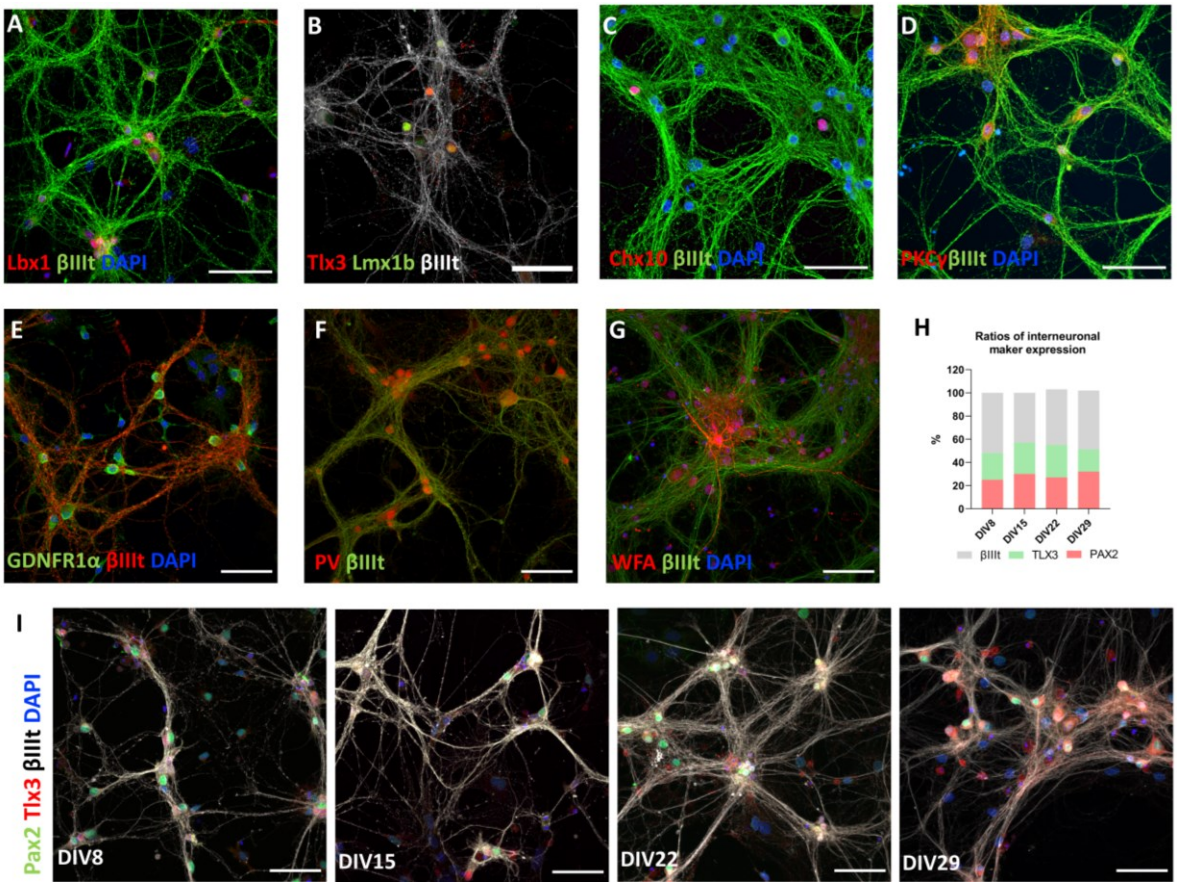

Fig. 24 Markers of spinal interneurons, transcription factors Lbx1 (A), Tlx3, Lmx1b (B), Chx10 (C), and Pax2 (I) are expressed by the neurons in primary spinal cord culture. Neurons were identified by βIII-tubulin (βIIIt), while nuclei were visualized using DAPI stain. Pax2+ and Tlx3+ neurons correspond to approximately half of neuronal population in all analyzed days *in vitro* (DIV) (H and I). Protein kinase C gamma (PKCγ) (D), GDNF family receptor alpha-1 (GDNFR1α) (E), parvalbumin (PV) (F), and *Wisteria floribunda* agglutinin (WFA) (G) were also expressed by the neurons in culture. Scale bars: 50µm.

The most common markers expressed by the neurons in the culture were Pax2 and Tlx3. Neurons identified by βIIIt were co-stained with Tlx3 and Pax2, after which the Tlx3+ and Pax2+ nuclei were counted. Pax2 was expressed by circa 28.5% of neurons, while 24.3% of neurons were Tlx3+ on average. The expression of these markers was stable. during cultivation (Fig. 24H). Almost no neurons were found that expressed both markers at the same time, confirming that the markers identify two different cell types. Similarly, estimation of expression of other markers was performed. 5.8% of neurons expressed Lbx1, while Lmx1b was expressed by 35.3% of neurons at DIV17. Majority of Lmx1b neurons were also positive for Tlx3. Chx10 was expressed sporadically by DIV20 neurons, averaging only around 30 cells per coverslip. ChAT expressing MNs were also present in the immature cultures (data not shown), but none survived through the long-term cultivation. Afterward,

protein kinase C gamma (PKCγ) (Fig. 24D), parvalbumin (PV) (Fig. 24F) expression was confirmed in subset of neurons at DIV20, and GDNF family receptor alpha-1 (GFRα1) at DIV 17 (Fig. 24E). The three proteins mentioned above were present in most cultured neurons. Perineuronal nets expressing neurons were identified by *Wisteria floribunda* agglutinin (WFA) staining only in exceptionally mature cultures (Fig. 24G). On average 23.5 WFA+ neurons were present at DIV72, per coverslip.

4.4.4. **Diverse morphologies of neurons in primary spinal cord culture**

Morphology of neurons could be analyzed on GFP-expressing neurons. Cultures at DIV3 were transfected using a low-efficiency protocol, after which only a few cells per coverslip were transfected and their processes could be successfully analyzed using the SNT plugin in Fiji. DIV7-8 neurons were classified into three groups based on the number of processes: simple, intermediate, and branched, (Tab. 7) (Fig. 25A). Effective grouping was validated by statistical differences of several morphological characteristics between the groups. Cable length (the summation of all lengths of processes) was recognized as a superior parameter for separating morphologies in mature cultures, at DIV14-15 (Fig. 25B), DIV21-22 (Fig. 25C), and DIV28-29 (Fig. 25D). At these time points, the morphology groups were named small, medium, and large. The groups and ranges of individual DIV timepoints are summarized in Tab. 7.

Tab. 7 Neuronal morphological groups of identified in spinal cord cultures; b- branches.

	Morphological group	**Range**	**N**	**N total**
DIV7-8	Simple	1-9 b	16	53
	Intermediate	10-19 b	23	
	Branched	20-58 b	14	
DIV15-16	Small	300-3000 µm	20	58
	Medium	3000-6000 µm	18	
	Large	6000-13000 µm	20	
DIV21-22	Small	900-3000 µm	13	44
	Medium	3000-7500 µm	22	
	Large	7500-14000 µm	9	
DIV28-29	Small	1700-4500 µm	12	38
	Medium	4500-8000 µm	18	
	Large	8000-20000 µm	8	

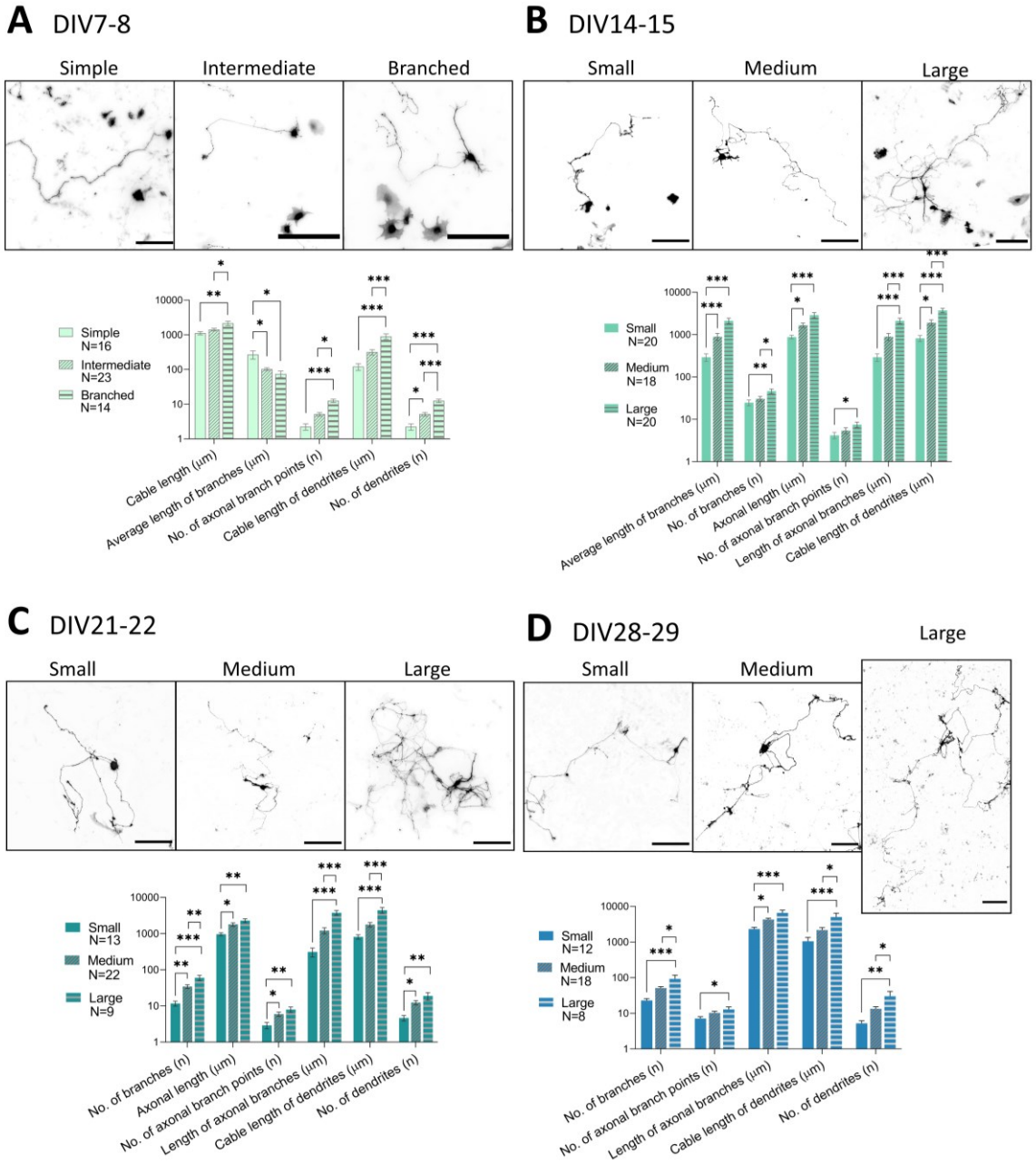

Fig. 25 Morphology analysis of neurons in spinal cord culture. Neurons transfected with green fluorescent protein (GFP) (black) were classified into simple, intermediate and branched groups at day in vitro (DIV) 7-8 (A) and into small, medium and large at DIV14-15 (B), DIV21-22 (C) and DIV28-29 (D). Scale bars: 200µm. The difference between morphological groups was verified by the analysis of morphological parameters using one-way ANOVA with Turkey's post hoc test. N= number of cells in a group; Scale bars: 200µm; Graphs are plotted as means ± SEM; * $p<0.05$, ** $p<0.01$, *** $p<0.001$.

Morphological parameters were compared between all neurons at different cultivation time points (Fig. 26). Significant change of the morphological parameters was observed between DIV7-8 and DIV14-15, after which the majority of the parameters did not change. The sum of all processes and the sum of axonal branches, however, continued to

increase in older cultures, indicating that in even mature cultures, processes continue to grow.

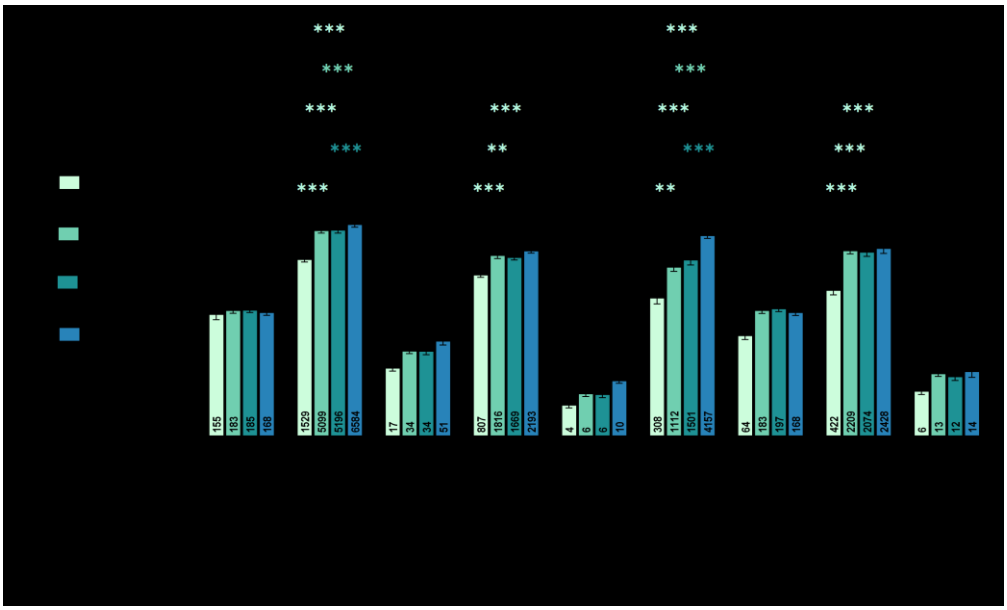

Fig. 26 Comparison of morphological parameters between different maturation stages – days *in vitro* (DIV). N= number cells analyzed; Graphs are plotted as means ± SEM; * $p<0.05$, ** $p<0.01$, *** $p<0.001$.

4.4.5. **Regenerative capacity of axons decreases with maturity**

The regenerative capacity of cultured spinal cord neurons was described by cutting their axons at DIV7, 16, and 23 using a 900nm laser and observing their response over 14h. Cultures were transfected with GFP plasmid in a low-efficiency protocol, to visualize individual cells and their separate processes. Two types of outcomes followed the axotomy: neurons either died or managed to seal off the damaged area. Across the experiments, the portion of neurons that died ranged from 6% to 25% and it did not correlate with neuronal age.

The cells that managed to close the injury site, formed a characteristic structure called a retraction bulb at the tip of the axon that was still attached to the cell body (Fig. 27A). The time that took the neurons to form the retraction bulb increased in older cultures (Fig. 27B). At DIV7 average bulb formation time was 1.7 ± 1.6h, while at DIV16 and DIV23 it was prolonged significantly to 3.8 ± 2.7h ($p=0.004$) and 4 ± 2.2h ($p=0.002$), respectively. Retraction bulb either formed right at the injury site, or further up the axon, closer to the cell body. Retraction distance was measured and compared between neurons at different DIV (Fig. 27C). At DIV7, average retraction distance was 31 ± 16.81 µm, which was shorter

compared to 40.6 ± 28.1 µm at DIV16 and statistically shorter comparted to 56.1 ± 43.5µm at DIV23 (p=0.02). Pearson's correlation analysis of retraction distance and retraction time across all cells at all maturity stages revealed a positive correlation between these two parameters (p<0.001) (Fig. 27D). This result indicates that if the cells respond slower to the injury, retraction of the axon tip will be longer.

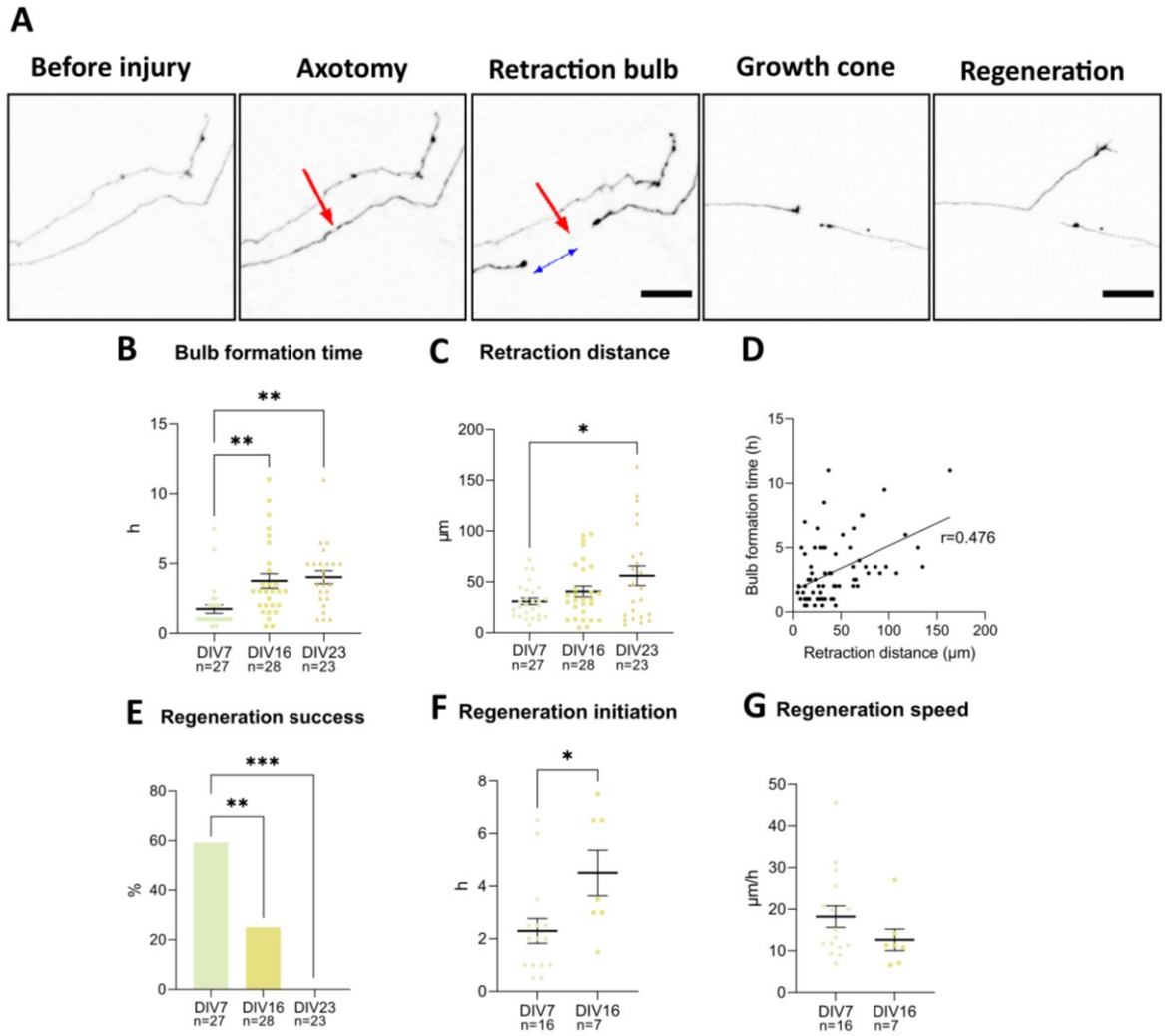

Fig. 27 Representative images of axotomy- axon cut performed on spinal cord neurons transfected the GFP (black), and events that followed (A). Axotomy location is indicated by red arrows. Characteristic retraction bulb formed at a certain distance from the injury, as indicated by the blue arrow. Retraction bulb formation time (B) and retraction distance (C) varied between neurons at different days *in vitro* (DIV). Positive correlation of the two analyzed parameters was found (D). Fraction of regenerating axons declined significantly with culture maturity (E). Regenerating axons managed to transform retraction bulb into a growth cone, but this initiation occurred faster in DIV7 cells compared to DIV6 neurons (F), whereas the speed of regeneration declined only slightly (G). Scale bars: 25µm; Graphs are plotted as means ± SEM of n number of cells; *p<0.05, **p<0.01, ***p<0.001.

Once the retraction bulb was successfully formed, two outcomes followed: axon regeneration, or regeneration failure (Fig. 27A). In regenerating axons, retraction bulb was transformed to a growth cone and synthesis of a new axon occurred. In axons failing to regenerate, retraction bulb usually showed a degree of mobility but failed to transform to a growth cone during 14h that it was observed for. Regenerating axons were present only in cells at DIV7 and DIV16, while no such axons were observed in cultures at DIV23 (Fig. 27E). At DIV7 59.3% of damaged neurons regenerated, while significantly lower percentage of 25% regenerated at DIV16 ($p=0.005$).

The speed of regeneration was also evaluated. Regeneration initiation – the time between successful retraction bulb formation and its transformation to a growth cone varied among cells (Fig. 27F). At DIV7 the initiation took on average 2.3 ± 1.8h, which was significantly shorter compared to 4.5± 2.3h at DIV16 ($p=0.013$). DIV7 cells also had higher regeneration speed – the length of new axon synthesized during 2h after initiation time, compared to DIV16 neurons, although this difference was not statistically significant (Fig. 27G).

4.4.6. **Intracellular mechanisms present in mature spinal cord neurons**

To study intracellular mechanisms of maturating spinal cord neurons and their axons, the cultures were stained for pS6 (Fig. 28). To identify axons of individual neurons, GFP transfected cultures were analyzed. Cells at DIV8 have different intracellular distribution of pS6 (Fig. 28A), compared to mature DIV22 cells (Fig. 28B). At DIV8, pS6 expression was evenly distributed in almost all neuronal somas (Fig. 28C) and was expressed distinctly in processes and axon tips. At mature DIV22 neurons, pS6 expression was concentrated mostly in soma, the signal in neurites was lower (Fig. 28D) and almost not existent at axon tips. Differential expression of pS6 in somas of the DIV22 neurons was also observed and the cells were divided to high and low according to pS6 signal intensity (Fig. 28C).

Autophagy in immature and mature axons was visualized using cells isolated from CAG-RFP-EGFP-LC3 mice, which express autophagy reporter LC3-RFP-GFP protein. In these cells, AP vesicles are both green and red, while in the fusion stage of autophagy flux, AL vesicles are red only (Fig. 29A). By tracing the vesicles along the axons of cells in different maturation stages using kymographs, difference between mobility and number of vesicles present in immature and mature axons was discovered (Fig. 29B). Immature axons

at DIV8 had significantly less AP and AL vesicles in their axons, as compared to DIV16-17 and DIV22-23 cells (Fig. 29C). On the other hand, the percentage of mobile vesicles was higher in immature axons, especially regarding AL. RAPA treatment induced mobility of AL in mature axons, indicating that inhibition of mTOR pathway influences axonal autophagy in spinal cord neurons. Mobile vesicles were predominantly moving retrogradely along the axons.

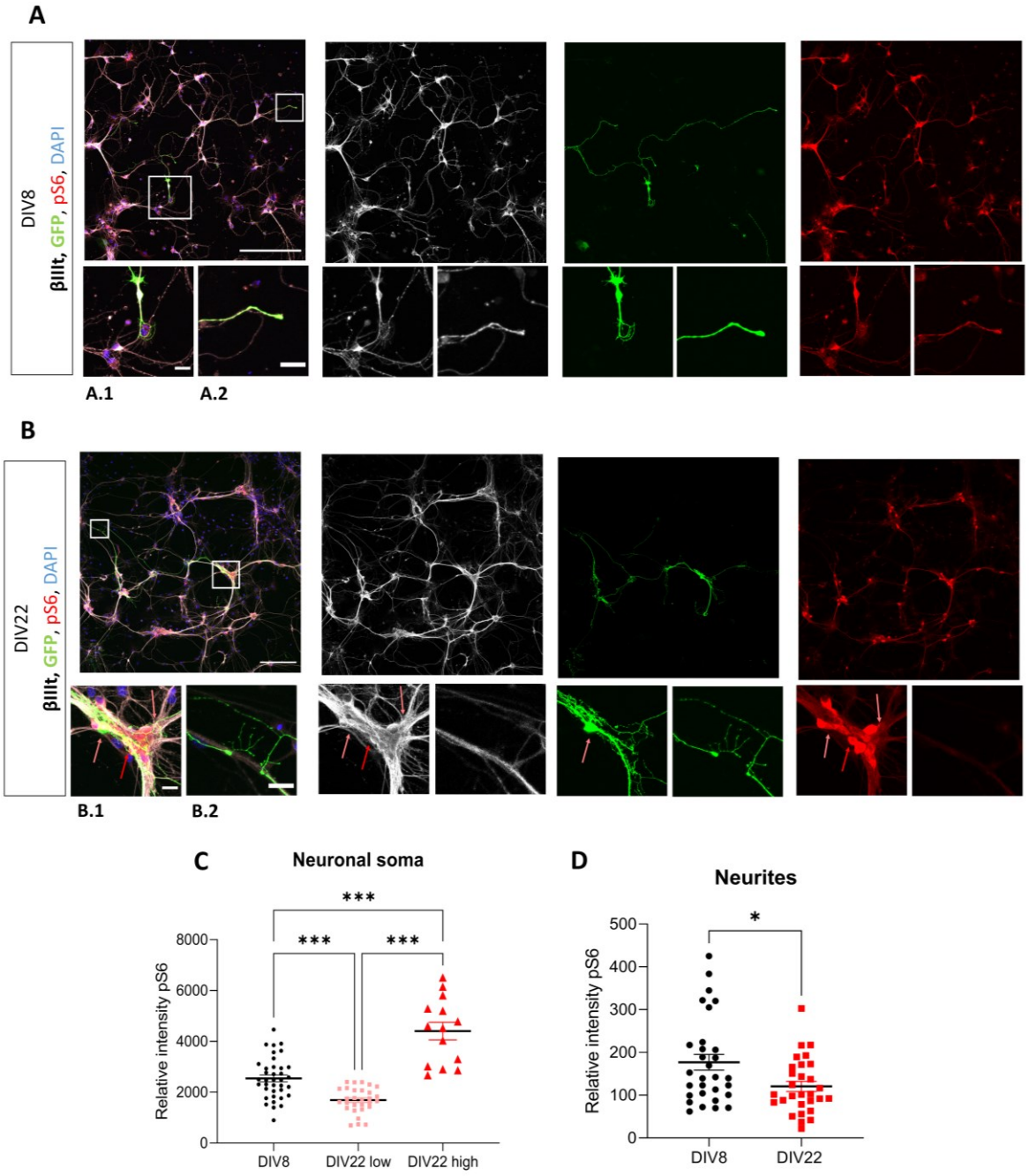

Fig. 28 Examination of intracellular distribution of pS6 protein (red) in immature day *in vitro* (DIV) 8 spinal cord neurons (A) and mature DIV22 neurons (B), transfected with green fluorescent protein (GFP) (green) and co-stained with βIII-tubulin (white) and DAPI (blue). Scale bars of A and B images are 200μm. A.1 and B.1 are showing details of somas, scale bars 20μm. A.2 and B.2 are

showing details of axon tips, scale bars 20µm. Red arrows are pointing to a cell with high pS6 expression, while pink arrows are pointing to cells with low pS6 expression. Graphs are plotted as means ± SEM; *p<0.05, ***p<0.001.

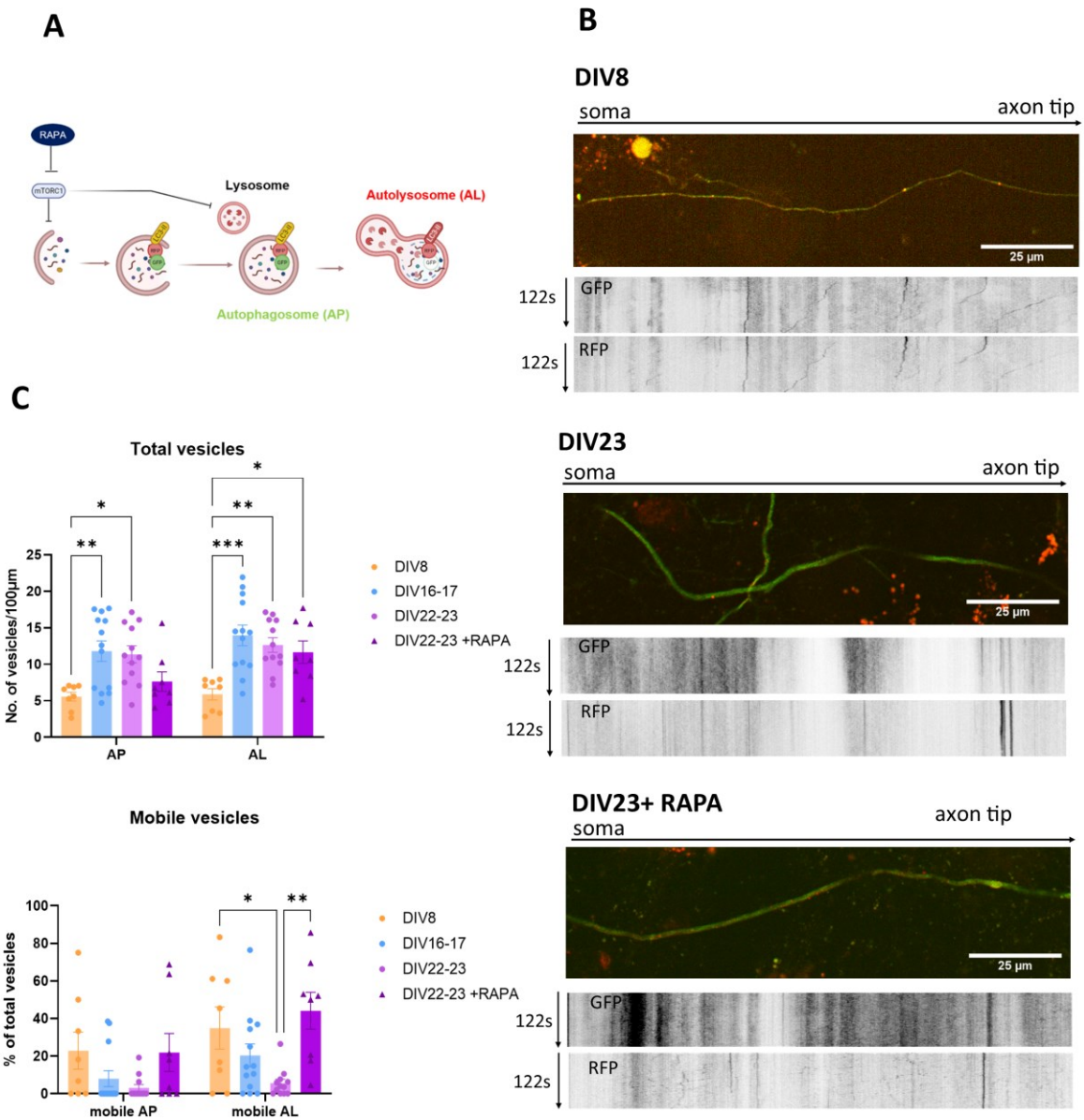

Fig. 29 Autophagy flux was traced in axons expressing LC3 protein tagged with RFP and GFP. Auophagosomes (AP) had both signals, while in autolysosomes (AL), due to lower pH, only RFP signal was visible (A). 122s videos of immature, mature axons and mature axons treated with rapamycin (RAPA), expressing LC3-RFP (red) and LC3-RFP-GFP (yellow) were analyzed using kymographs (B). Number of all vesicles and percentage of mobile vesicles were assessed (C). Graphs are plotted as means ± SEM; *p<0.05, **p<0.01, ***p<0.001.

5. DISCUSSION

5.1. Treatment of acute SCI with mTOR pathway inhibitors rapamycin or pp242

The mTOR pathway is in the center of many intracellular mechanisms and can influence processes such as cytoskeletal organization, transcription, translation, and autophagy (Wullschleger et al., 2006; Kanno et al., 2012). Its importance has been established in numerous CNS disorders, including SCI (Codeluppi et al., 2009; Chen et al., 2012, 2016; Sekiguchi et al., 2012; Wang et al., 2016; Li et al., 2019a). RAPA, a selective mTORC1 inhibitor, has been previously used in preclinical trials for SCI treatment to some success. It leads to neuroprotection through alteration of secondary injury (Sekiguchi et al., 2012; Chen et al., 2013; Du et al., 2017). RAPA alone, however, is not able to inhibit the mTOR pathway in total. Prolonged RAPA treatment has been shown to lead to activation of the PI3K/Akt through insulin receptor substrate-1 expression (IRS-1) (O'Reilly et al., 2006) (Fig. 4). This break in negative feedback loop causes mTORC1 activation through Akt. Akt is a direct effector of mTORC2 (Sarbassov, 2005), the second complex of the mTOR pathway, so by inhibiting mTORC2, Akt activity can be diminished. Inhibition of both complexes of mTOR can therefore lead to more effective deactivation of the pathway. Novel inhibitors targeting ATP-binding site, such as pp242, have the ability to act as dual inhibitors and successfully inhibit both mTORC1 and mTORC2, which was demonstrated in glioblastoma (Jhanwar-Uniyal et al., 2019).

Effect of mTOR pathway inhibition by RAPA or pp242 in spinal cord tissue after SCI were studied in experiment 1 (Tab. 6; Fig. 7). Successful inhibition of the mTOR pathway by both RAPA and pp242 was demonstrated by reduced p-S6 immunoreactivity in spinal cord sections of treated rats. Both inhibitors led to suppression of mTORC1, and its downstream effector S6K1, which resulted in reduction of p-S6 production (Brown et al., 1995). Protein 4E-BP1 is another mTORC1 substrate whose activity was analyzed in the spinal cord tissue. Injury on its own led to activation of this protein, which indicates that mTOR pathway is activated after SCI, which was reported previously (Wang et al., 2016). RAPA treatment further increased phosphorylation of 4E-BP1. Successful inhibition of p-4E-BP1 was achieved only by pp242 administration. Previous studies reported, that 4E-BP1 phosphorylation can be unaffected by RAPA treatment, while pp242 was shown to be more

effective (Feldman et al., 2009; Thoreen et al., 2009). Similar to 4E-BP1, Akt phosphorylation was upregulated in SCI spinal cords and the effect was enhanced by RAPA treatment. The upregulation of p-Akt after RAPA treatment of SCI was reported previously (Li et al., 2019a). P-Akt production was reduced by pp242 treatment compared to RAPA, but not significantly compared to vehicle controls. Unsuccessful inhibition of p-Akt by pp242 could have been caused by the acute SCI environment that sustained the increase in mTORC2 activity. Regardless, together these results point to differential inhibition of mTOR pathway between RAPA and pp242 treatment of acute SCI.

Previously reported possible mechanisms through which RAPA treatment can influence degenerative processes following SCI are autophagy and inflammation (Chen et al., 2013). Dual mTOR inhibitors, including pp242, were shown to induce autophagy even more effectively than RAPA (Gordeev et al., 2015). Its effect on autophagy after SCI, however, has not been yet investigated. Analysis of LC3b-II expression in spinal cord tissue revealed that this autophagy marker is upregulated after SCI (Fig. 8). RAPA treatment led to its further upregulation, and while dual inhibition by pp242 induced additional autophagic response, it was not significantly different compared to RAPA treatment. This result confirms the notion that mTORC1 inhibition induces autophagy, while mTORC2 role in autophagy is probably not substantial. This facet of mTROC2 activity is poorly understood, although it was suggested that mTORC2 suppresses autophagy indirectly, by activating mTORC1 (Kim and Guan, 2015). Upregulation of autophagy at the SCI lesion site has been confirmed by multiple studies (Kanno et al., 2011; Tang et al., 2014; Yan et al., 2017; Li et al., 2019a) and in performed experiment as well (Fig. 8). The role of autophagy in SCI is complex and controversial, as both inhibition and activation of this mechanism after SCI lead to neuroprotection (Zhang et al., 2020). The type of injury that is being treated and the timing of autophagy modulation after SCI seem to be important variables that need to be established in order to effectively use this mechanism for SCI therapy.

Immunosuppressive properties of RAPA have been long known, and it has been used to suppress inflammation in animal model of multiple sclerosis, experimental autoimmune encephalomyelitis (Li et al., 2019b). Suppression of inflammation after SCI was shown to reduce neuronal injury and lead to functional recovery (Machova Urdzikova et al., 2015, 2017). Inhibition of mTOR pathway has been explored in relation to inflammation after SCI previously. mTORC1 inhibition by RAPA administration after SCI leads to decrease of TNF-α expression (Chen et al., 2013), while dual inhibition of mTORC1 and mTORC2 was

shown to also reduce inflammatory cytokine levels, IL-1β and TNF-α after SCI (Cordaro et al., 2017). Our results demonstrate that RAPA-treatment leads to decrease in IL-1β and MIP-1α present in spinal cord tissue during acute SCI (Fig. 9). Both cytokines have been previously shown to contribute to inflammation and neuronal damage after SCI (Liu et al., 2008; Pelisch et al., 2020). pp242 treatment also led to decrease of MIP-1α, but levels of IL-6, IL-1β and IL-2 cytokines were higher compared to RAPA treated animals. Both IL-6 and IL-2 roles in SCI are not fully understood, but accumulating evidence suggests, that IL-6 neutralization can improve locomotor recovery after SCI (Okada et al., 2004; Mukaino et al., 2010). These results suggest that while both RAPA and pp242 lead to similar systemic immunosuppression, assessed by serum cytokine levels, RAPA treatment alone seems to lead to more favorable immunomodulation compared to pp242 administration after SCI.

Investigation of structural and functional recovery after SCI treated with RAPA or pp242 showed that these two treatments lead to similar lesion size reduction and BBB score improvement (Fig. 11). Previous studies using RAPA or dual mTOR inhibitors reported similar outcomes (Chen et al., 2013; Cordaro et al., 2017). On the other hand, axonal sprouting assessed by GAP43 IHC demonstrated that RAPA treatment leads to improved axonal recovery compared to pp242 treatment (Fig. 10).

Together these results prove that the first hypothesis of this experiment is true- the treatment of acute SCI with mTOR pathway inhibitors rapamycin or pp242 did lead to structural and functional recovery through induction of autophagy and alteration of inflammatory response. However, the second hypothesis was proven to be partially false. While we did see a more pronounced effect on the mTOR pathway in injured spinal cords after pp242 treatment, the increased inflammatory cytokine levels and decreased axonal sprouting have shown, that pp242 did not lead to more pronounced outcomes regarding recovery after SCI, compared to RAPA.

5.2. Treatment of ALS in SOD1^{G93A} rats with a repeated intrathecal and intramuscular application of MSCs

In this experiment, the effect of repeated application of bone-marrow-derived hMSC cell therapy on progression of SOD1^{G93A} rat model of ALS was investigated. Intrathecal and intramuscular deliveries of hMSC and their combination were performed three times at intervals of two weeks since disease onset. The lifespan of the animals increased

significantly in all groups that received cell therapy (Fig. 13), preservation of motor neurons (Fig. 14) and NMJ in the SC+M group and decreased cell death in SC+M and SC group (Fig. 14) all point to overwhelming positive effects of the therapy on ALS progression. These results are confirming previous studies about the effectiveness of MSC therapy in animal models of ALS (Kim et al., 2010; Boido et al., 2014; Forostyak et al., 2014). The majority of previous studies were focused on investigation of the effects of cell therapy applied intravenously, intrathecally or intraspinally, while intramuscular application was tested only in some studies (Gothelf et al., 2014) and combinatory application was tried by other groups only recently (Martínez-Muriana et al., 2020). The results from experiment 2 demonstrate, that combined intrathecal and intramuscular application of hMSCs is superior to other delivery methods, as it leads to structural preservation of MNs and NMJ. Interestingly, injection of cell therapy to the *quadriceps femoris* alone did not have any protective effect on NMJ degradation. Failure of achieving therapeutic effect with intramuscular therapy alone was confirmed in recent study as well (Martínez-Muriana et al., 2020). Given that the therapy was administered in already symptomatic animals, this result indicates that degeneration of NMJ in ALS starts early in symptomatic animals and its preservation is dependent on spinal MNs health. For the preservation of MNs and NMJ in ALS, trophic support of MNs in the spinal cord and their axonal targets in muscles is needed.

The stem cell therapy in ALS leads to decreased disease progression probably through the positive paracrine effect of grafted cells on resident MNs and glia. Factors BDNF, GDNF, VEGF and insulin-like growth factor-1 secreted by MSCs lead to overall reduction of inflammation and decreased apoptosis of MNs in ALS animals (Forostyak et al., 2014). The exact effect that these signaling molecules have on intracellular pathways in MNs and other cells in ALS is still not clear. As there is increasing evidence that autophagy pathway is involved in ALS pathology (Ramesh and Pandey, 2017; Vicencio et al., 2020), the effect of hMSC application on this pathway was investigated in experiment 2.

Beclin-1 an essential autophagy regulator was found to be downregulated in animals treated with the most effective form of hMSC application, the SC+M group (Fig. 12). Abnormal interaction between Beclin-1 and mutant SOD1 was previously reported, which may affect the threshold for autophagy induction (Nassif et al., 2014). The same group reported protection against ALS in $SOD1^{G86R}$ transgenic mice that also had *Becn1* haploinsufficiency. An increase of AP formation demonstrated by LC3b-II/LC3b-I ratio was seen in control $SOD1^{G93A}$ rats, while no elevated p62 expression was recorded.

This result demonstrated that although there is an upregulation of autophagy, no disfunction of autophagy flux is present in SOD1^{G93A} rat spinal cords. Previous study by Perera et al. (2018) also found similar upregulation of autophagy in spinal cords of SOD1^{G93A} mice. None of hMSC treatments led to change in LC3b or p62 levels compared to vehicle-treated rats. Although other studies showed that inhibition of autophagy can be neuroprotective in ALS (Hsueh et al., 2016; Zhou et al., 2017), other groups report that enhancement of autophagy, especially in mTOR- independent manner prolongs the lifespan of ALS mice (Castillo et al., 2013; Zhang et al., 2018, 2019). Moreover, Perera et al. (2018) pointed out that induction of autophagy by mTOR- independent mechanism leads to enhanced motor neuron degeneration contributing to disease progression. These publications draw attention to the complexity of autophagy and ALS relationship. Important aspect that needs to be explored further in the autophagy regulation in ALS is cell specificity (Massenzio et al., 2018). In case of hMSC treatment of ALS, Beclin-1 decrease in SC+M treatment group, indicates that the therapy modestly modifies autophagy pathway in SOD1^{G93A} rats, proving the hypothesis of the experiment 2 true.

5.3. Studying the effect of PHLDA3 overexpression in astrocytes

PHLDA3, a protein of interest discovered to be upregulated in aberrant ALS astrocytes (Tyzack et al., 2017) was overexpressed successfully in WT astrocytes in experiment 3. PHLDA3 overexpression did not seem to cause cytotoxicity or cell death in astrocytes. During transfection optimization, GFP transfected cells died at similar rates to those transfected with PHLDA3-GFP (Fig. 16). Absence of cytotoxicity was confirmed by lack of LDH activity upregulation (Fig. 17), which would be upregulated if the enzyme was released into the cell culture medium upon cell membrane damage (Kumar et al., 2018). Production of ROS, evaluated by H_2O_2 levels also did not increase in PHLDA3 overexpressing astrocytes. Even in the cells treated with thapsigargin, a known ER-stress inducer (Sanchez et al., 2019) did not produce more ROS, indicating that WT astrocytes do not produce much ROS even under ER stress. Overexpression of PHLDA3 however, led to upregulation of p-eIF2α, a protein that is activated upon induction of PERK branch of ER stress. This could be a new, alternative mechanism of action of PHLDA3. PHLDA3 overexpression has been shown to lead to ER stress through IRE1-XBP1 branch activation and induced cell death in hepatocytes (Han et al., 2016). Known mechanism of action of PHLDA3 is through repression of Akt (Takikawa and Ohki, 2017). The inhibition of p-Akt however, was not

accomplished by overexpression of studied protein in astrocytes. This result can be interpreted in various ways. It could be the case that non-transfected astrocytes (approximately 70-85% of analyzed cells) present in the culture increased the p-Akt levels enough to distort the decrease caused by PHDLA3 overexpression. The slightly lower, but not significant p-Akt/Akt ratio in PHLDA3-GFP transfected astrocytes indicates the possibility of this scenario. Another possibility is that Akt was not highly active in WT astrocytes in the first place, so inhibition by PHLDA3 did not affect the phosphorylation of this protein significantly. A recent study found that in primary cardiomyocyte culture, inhibition of PHLDA3 does not affect Akt phosphorylation or LDH activity in physiological conditions, but only in hypoxia/reoxygenation injury model settings (Liu et al., 2021).

Together, these results suggest that PHLDA3 upregulation in WT astrocytes induces ER stress, confirming the first hypothesis of experiment 3. The upregulation does not affect the viability, ROS buffering capacity, or Akt signaling in WT astrocytes. The true effect of PHLDA3 upregulation in astrocytes could lead to different outcomes in ALS disease models.

PHLDA3 overexpression in astrocytes impacted the survival of MNs in cultures treated with astrocyte-conditioned medium (Fig. 18), confirming the second hypothesis of the experiment. This result could mean that these astrocytes express some factors into their surrounding that cause death of MNs, or at least decrease their survival capacity *in vitro*. It's difficult to speculate about the nature of the secreted factors without closer analysis of astrocytic secretome, therefore further experiments are needed. Potentially secreted molecules include nitroxidative species (Rojas et al., 2014) or cytokines such as IL-6, TNF-α, transforming growth factor β1 (TGF- β1), IFNγ and others (Filipi et al., 2020). IL-6 expression was found to be increased in astrocytes derived from ALS patients (Wosiski-Kuhn et al., 2021), and is upregulated in astrocytes undergoing ER stress (Sanchez et al., 2019). IFNγ and TGF- β1 were also found to be upregulated in ALS patients (Aebischer et al., 2012; Tripathi et al., 2017) and cause death of MNs treated by astrocyte conditioned medium (Aebischer et al., 2011) or protein aggregation in MNs cultured together with astrocytes (Tripathi et al., 2017).

5.4. Establishing a robust *in vitro* model of spinal cord interneurons

In this experiment, a method of culturing spinal cord neurons was optimized, neuronal maturation and regenerative ability of neurons were investigated. The aim was to produce a

robust culture model of spinal cord neurons that represents the mature CNS and which could be used in upcoming experiments intended to boost the ability of the CNS neurons to regenerate. There is a great advantage in utilizing murine embryos for neuronal culture preparation due to their viability, but the immaturity of the neurons after seeding is an issue, as they exhibit characteristics that are entirely unlike the mature neurons, especially regarding their superior intrinsic regenerative ability (LaBarbera et al., 2021). To encourage maturation of neurons isolated from E14 spinal cords, the cultures were maintained long-term, usually for a month, but were able to survive even longer, up to 70 days (Fig. 19). Proliferation of glia was observed during longer cultivation, but it did not affect survival of neurons, and probably encouraged their maturation (Fig. 20). To assess the maturity of newly established cultures, electrophysiological properties, the immunoreactivity of NF70, DBC and synaptic connectivity of neurons was investigated during cultivation.

The changes in the electrophysiological properties are typical signs of neurodevelopment of CNS neurons, including spinal cord neurons (Durand et al., 2015). The cultured spinal cord neurons exhibited typical changes linked with maturation until DIV16, with the major shift in most analyzed parameters emerging before DIV9 (Fig. 21). After DIV16 there was no further change in the electrophysiological properties. Neurons in the culture were probably solely interneurons, as the IR, E_m and spontaneous activity were comparable to interneurons recorded on P6-10 spinal cord slices in a previous study (Sun and Harrington, 2019). The neurons in the culture likely possess electrical activity of early to late postnatal neurons, as they were comparable to properties of neurons recorded in spinal cord slices or whole spinal cords in other studies (Wilson et al., 2005; Zhong et al., 2006; Sun and Harrington, 2019).

Maturity markers of embryonic cortical neurons maturing *in vitro,* NF70 and DBC were discovered by Koseki et al., (2017). Developing, migrating neurons express DBC a microtubule-associated protein. It is regularly used as a neuronal precursor marker (Ayanlaja et al., 2017), while it's downregulated in mature neurons (Brown et al., 2003). A significant decrease in DBC immunoreactivity was observed in culture of spinal cord neurons after DIV6 (Fig. 22). NF70, a marker of mature axons (Lu et al., 2017) was sharply upregulated in analyzed culture at DIV20. Formation of neural networks, assessed by excitatory and inhibitory synapse development also confirmed maturity of the culture (Fig. 23). The quantity of inhibitory and excitatory synapses increased until DIV15, and plateaued after

that. Similar synapse formation pattern was previously described in primary cortical and striatal neuron co-cultures between DIV14 and DIV21 (Moutaux et al., 2018)

Various strategies have been utilized to classify the neurons of the adult spinal cord, even though there is no consensus in the scientific community (Zeng and Sanes, 2017; Hayashi et al., 2018; Dobrott et al., 2019). One efficient strategy includes classifying neurons according to transcription factors they express, because some transcription factors determine the neuronal specialization and subtype during development of the spinal cord, but can be expressed in adulthood as well (Del Barrio et al., 2013; Lu et al., 2015; Russ et al., 2021). Several such transcription factors, specifically Lbx1, Lmx1b, Chx10, Pax2 and Tlx3 were found to be expressed in the nuclei of the cultured spinal cord neurons (Fig. 24). Lbx1 transcription factor is expressed by mostly excitatory interneurons located laminae III-IV of the adult spinal cord (Müller et al., 2002). Some Lbx1+ neurons are also Lmx1b positive, but Lmx1b+ interneurons are exclusively excitatory and located in laminae I-III (Del Barrio et al., 2013). Lmx1b+ neurons were in majority also Tlx3+, which was already established *in vivo* previously (Dai et al., 2008). Tlx3 transcription factor, expressed mostly by laminae I-II is a marker of excitatory interneurons (Monteiro et al., 2021). Pax2, transcription factor commonly used as a marker of inhibitory interneurons of the dorsal horn (Larsson, 2017) was also expressed by the neurons in the culture. Ventral V2a interneurons, identified by Chx10 staining (Hayashi et al., 2018) were identified. On top of transcription factors, proteins such as PKCγ or parvalbumin that are commonly used for identification of lamina II excitatory interneurons or lamina II and III inhibitory interneurons respectively (Neumann et al., 2008; Petitjean et al., 2015) were also expressed *in vitro*. ChAT positive cells, marking MNs did not survive long in the analyzed culture. MNs are known to be exceptionally vulnerable and heavily depend for survival on trophic support of cells on the periphery, such as Schwann cells and muscle cells (Bucchia et al., 2018).

Morphology of cultured spinal cord neurons was analyzed in attempt to identify individual morphological groups of neurons. Morphology of spinal cord neurons is not fully established, although previous studies were classifying the neuronal morphology according to laminar location, geometry and orientation of neurites (Grudt and Perl, 2002; Hantman et al., 2004), which is not achievable *in vitro*. A previous study characterized neurites of spinal cord MNs during 48h *in vitro* cultivation (Gertz et al., 2010), but studies characterizing SpINs are lacking. In four time points of the culture, individual morphological groups were identified (Tab. 7; Fig. 26). Additionally, it was discovered that neurites continue to grow

even in mature cultures, at DIV28 (Fig. 27). Electrophysiological parameters C_m and IR, which correlate with cell size (Sun et al., 2018) did not change significantly after DIV9 (Fig. 21). This does not correspond with the result found in morphological analysis. This discrepancy could be due to the fact that morphological changes were discovered in cells at DIV28, which were older than oldest neurons (DIV24) analyzed by patch-clamp. On the other hand, increasing number of excitatory synapses observed at DIV28 (Fig. 23) could explain elongation of neurites at this time point due to formation of new connections in the culture.

Regenerative capacity of neurons in culture was lost by DIV23 (Fig. 28). Even at DIV16, axon regeneration was less common and the reaction to laser-induced injury was slower. These events coincided with the transition of neuronal maturity properties, indicating that spinal neurons lose their regenerative ability with maturation *in vitro*, as was previously shown on cortical cultures (Koseki et al., 2017). Developmental loss of regenerative ability and plasticity in neurons of the CNS is well established (Fawcett, 2020). In addition to suppressive environment created at the site of the injury, mature neurons lack intrinsic properties needed for regeneration. Maturing neurons undergo genetic and epigenetic changes that drive changes in expression of growth-related molecules, as they switch from motile and growing cells into more rigid, electrically active cells incorporated into complex neural networks that need to be maintained and diligently regulated. The changes affect axons particularly, as they lose growth-related receptors, retrograde vesicular trafficking and other mechanisms essential for regeneration (Kappagantula et al., 2014; Franssen et al., 2015; Cheah et al., 2016).

One of the most studied pathways lacking in non-regenerating axons is PI3K/Akt/mTOR pathway. Deletion of phosphatase and tensin homolog (PTEN), an enzyme converting PIP3 into PIP2, activates the PI3K/Akt/mTOR pathway (Fig. 4) in retinal ganglion cells and leads to robust regeneration (Park et al., 2008; Geoffroy et al., 2015). Overexpression of active form of PI3K also leads to regeneration and an upregulation of pS6, a product of mTORC1 activity in cortical neurons (Nieuwenhuis et al., 2020). Investigated spinal cord neurons seem to lose expression of pS6 in neurites and most neuronal somas during maturation *in vitro* (Fig. 28). There was no signal present in axons of the mature neurons, while a clear expression of pS6 in axon tips of immature cells was observed. This result indicates that spinal cord neurons lose pro-regenerative intracellular mechanisms during maturation in the described culture. It is known that mTOR is vital for

neurite development, axon growth and guidance (Morita and Sobue, 2009; Switon et al., 2017). Regarding it's role in adult CNS, it was previously reported that this pathway is involved in synaptic plasticity, adult neurogenesis, learning, and memory (Garza-Lombó and Gonsebatt, 2016). The mTOR pathway is known repressor of autophagy, but previous experiments reported, that this may not be the case in axons of primary cortical neurons (Maday and Holzbaur, 2016). This group indicated that autophagy in neurons may not be induced by starvation, therefore is not under control of mTOR as in other cells. Older studies, however dispute this result (Boland et al., 2008). It is possible that the maturity state of cortical neurons used in mentioned experiments influenced the results. As we saw, maturity of neurons in culture significantly influences autophagy flux in axons (Fig. 29), which was not been reported previously. Mature axons have more, static autophagic vesicles, while younger ones have less, but are highly mobile. RAPA treatment induced autophagy flux in older axons, which contradicts the findings by Maday and Holzbaur (2016) and therefore warrants further investigation into mTOR and autophagy relationship in axons.

The role of mTOR and autophagy in injury of adult spinal cord neurons remains to be poorly understood. Both downregulation (Zhang et al., 2013) and upregulation (Wang et al., 2016) of mTOR was reported in spinal cord tissue after SCI. Results presented in this thesis also reported that there is an upregulation of effector of mTOR pathway after SCI (Fig. 7). Due to heterogeneity of these results, there is a need of further investigation of mTOR and closely related autophagy involvement in function of individual spinal cord cell types after SCI as well as in the timing after the injury. Complex intracellular pathways and their interactions can be effectively explored in an *in vitro* model, such as the model described in this thesis.

6. CONCLUSION

In conclusion, the results of this thesis demonstrate that neuronal damage occurring in SCI and ALS possibly includes similar pathways, namely the mTOR pathway and intracellular processes in which it is involved, such as ER stress and autophagy. The complexity of the mature CNS and unique properties of neurons, being the most polarized and electrically active cells of the body, clearly makes them particularly vulnerable to the influences of their surroundings, their intrinsic defects, or alterations of intracellular pathways.

We demonstrated that there is upregulation of mTOR pathway and autophagy at the lesion site after SCI. These processes probably influence the extent of secondary injury because inhibition of the mTOR pathway by both RAPA and pp242 led to functional and structural improvement. Both RAPA and pp242 administration led to similar upregulation of autophagy at the lesion site, indicating that induction of this mechanism is helping in recovery from contusion type of acute SCI. Comparing the two inhibitors, we were able to conclude that mTORC1 inhibition by RAPA could be more favorable to the dual mTORC1 and mTORC2 inhibition by pp242 in SCI. Both inhibitors influenced the immune response at the lesion site, but the cytokine profile present in injured spinal cord tissue was more inflammatory in pp242 treated animals, compared to the RAPA group, which had more anti-inflammatory cytokine profile. Additionally, more axonal sprouting was present in RAPA treated animals, compared to pp242.

Even though mTOR inhibition can lead to recovery after SCI, its downregulation during maturation of spinal cord neurons could have influenced the loss of regeneration ability in development, as we saw in newly established culture of spinal cord neurons. Genetic stimulation of mTOR pathway had led to axon regeneration in previous studies, so it may look like at a glance, that both inhibition and stimulation of mTOR pathway can be used for SCI treatment. Still, it is important to distinguish gene therapy approaches, which can reprogram neurons into growth-competent cells and pharmacological treatments which influence the SCI lesion as a whole. The role of pathways as central as mTOR, therefore, needs to be explored further in relation to SCI and axon injury. For this purpose, we developed a new *in vitro* spinal cord neuron model. The described primary culture, isolated from E14 spinal cords, matures *in vitro* after approximately two weeks of cultivation, demonstrated by changes in electrophysiological properties, expression of maturity markers,

synapse development and morphology. This culture, comprising of a variety SpINs will be a valuable tool for future studies.

Similarly to SCI, we detected increased autophagic activity in spinal cords of SOD1^{G93A} ALS rats. Modest influence on autophagy was observed after application of experimental cell therapies, suggesting that this could be a new pathway through which hMSCs can influence ALS progression. Effectivity of different application methods was tested. Combination of intrathecal and intramuscular application of hMSCs had prolonged the lifespan of ALS rats, preserved MNs and protected them against apoptosis more effectively than separate intrathecal, intramuscular application of cell therapy or conditioned medium therapy.

Another aspect of the mTOR pathway involvement in ALS was explored in astrocytes. Astrocytes derived from ALS patients were showing aberrant activation phenotype and a new protein of interest, PHLDA3 was identified in a previous study. PHLDA3 was a recently identified as mTOR pathway repressor. We tested how the PHLDA3 overexpression influences WT astrocytes and their effect on MNs in culture. ER stress was induced in astrocytes transfected with PHLDA3 and conditioned medium from these cells led to decreased survival of MNs, pointing to a new possible mechanism of ALS pathology that needs to be explored further.

In summary, this thesis shows that neurodegeneration occurring in both SCI and ALS is an extremely complex and multifaceted process. Because of this, it is not fully understood despite the immense effort of the scientific community. Counteracting the damage to the CNS with effective therapies, therefore, requires multiple approaches, while focusing on one pathway is not enough. Regardless, exploration of individual pathways such as mTOR in these pathologies is a step required to make steady progress in the field.

7. SUMMARY

Pharmacological inhibition of the upregulated mTOR pathway after SCI was found to be a possible new therapy approach in acute SCI, as it can lead to functional and structural recovery. Inhibition of mTORC1 by RAPA was found to be superior, compared to dual inhibition of both mTORC1 and mTORC2 by inhibitor pp242. Positive effects of the treatment are probably mediated through upregulation of autophagy and modulation of inflammatory response at the lesion site.

In ALS, stem cell therapy has shown a great promise in recent years, even though it is not clear which pathological pathways it targets. We have explored multiple application methods, to find that the combination of intrathecal and intramuscular application of hMSCs has the most prominent effect in stunting ALS progression. One possible mechanism by which hMSC therapy affects ALS, as we identified, is modulation of autophagy.

The role of the mTOR pathway in motor neuron degeneration was investigated in relation to astrocytes. Astrocytes play an important role in ALS pathology. We explored PHLDA3, a repressor of mTOR pathway that was previously found to be upregulated in pathologically reactive ALS astrocytes. Overexpression of this protein in WT astrocytes led to induction of ER stress in these cells and negatively affected survival of MNs *in vitro*, revealing a new potential mechanism of ALS pathology, that needs to be explored further.

We described a new *in vitro* model of spinal cord interneurons. Described cultures, isolated from e14 mice, mature *in vitro,* and lose their regenerative ability, accurately modeling biology of the postnatal CNS. Furthermore, we have shown that mTOR pathway is downregulated in non-regenerating mature neurons in the culture, making the described model a valuable tool for future exploration of related pathways during axonal injury.

8. SOUHRN

Farmakologická inhibice mTOR dráhy zvýšené po MP byla prokázaná jako možná nová terapie akutního MP jelikož může vést k funkční a strukturální obnově. Bylo zjištěno, že inhibice mTORC1 pomocí RAPA je účinnější ve srovnání s duální inhibicí mTORC1 i mTORC2 inhibitorem pp242. Pozitivní účinky léčby jsou pravděpodobně zprostředkovány zvýšenou autofagií a modulací zánětlivé odpovědi v místě léze.

U ALS se terapie kmenovými buňkami v posledních letech ukázala jako velmi slibná, i když není zcela jasné, které patologické dráhy přesně ovlivňuje. Prozkoumali jsme různé způsoby podání, a zjistili jsme, že na zastavení progrese ALS má nejvýraznější účinek kombinace intratekální a intramuskulární aplikace hMSC. Jeden z možných mechanismů ALS, který hMSCs terapie může ovlivnit, je modulace autofagie.

Role dráhy mTOR v degeneraci motorických neuronů byla zkoumána ve vztahu k astrocytům. Astrocyty hrají důležitou roli v patologii ALS. Prozkoumali jsme úlohu proteinu PHLDA3, represoru mTOR dráhy, který je prokázaně zvýšen v patologicky reaktivních astrocytech v ALS. Nadměrná exprese tohoto proteinu ve astrocytech divokého typu vedla k indukci stresu ER v těchto buňkách a negativně ovlivnila přežití motorických neuronů *in vitro*, což odhalilo další potenciální mechanismus patologie ALS.

Charakterizovali jsme nový *in vitro* model míšních interneuronů. Kultury, izolované z e14 myší, dozrávají *in vitro* a ztrácejí svou regenerační schopnost, a přesně tak modelují biologii postnatálního CNS. Dále jsme ukázali, že exprese dráhy mTOR se snižuje v neregenerujících, zralých neuronech v kultuře, díky čemuž je popsaný model cenným nástrojem pro budoucí zkoumání drah souvisejících s axonálním poškozením.

9. LITERATURE REFERENCES

1. Abe, K., Itoyama, Y., Sobue, G., Tsuji, S., Aoki, M., Doyu, M., et al. (2014). Confirmatory double-blind, parallel-group, placebo-controlled study of efficacy and safety of edaravone (MCI-186) in amyotrophic lateral sclerosis patients. *Amyotroph Lateral Scler Frontotemporal Degener* 15, 610–617. doi: 10.3109/21678421.2014.959024.

2. Abu-Rub, M., McMahon, S., Zeugolis, D. I., Windebank, A., and Pandit, A. (2010). Spinal cord injury in vitro: modelling axon growth inhibition. *Drug Discovery Today* 15, 436–443. doi: 10.1016/j.drudis.2010.03.008.

3. Aebischer, J., Cassina, P., Otsmane, B., Moumen, A., Seilhean, D., Meininger, V., et al. (2011). IFNγ triggers a LIGHT-dependent selective death of motoneurons contributing to the non-cell-autonomous effects of mutant SOD1. *Cell Death Differ* 18, 754–768. doi: 10.1038/cdd.2010.143.

4. Aebischer, J., Moumen, A., Sazdovitch, V., Seilhean, D., Meininger, V., and Raoul, C. (2012). Elevated levels of IFNγ and LIGHT in the spinal cord of patients with sporadic amyotrophic lateral sclerosis. *Eur J Neurol* 19, 752–759, e45-46. doi: 10.1111/j.1468-1331.2011.03623.x.

5. Ahuja, C. S., Wilson, J. R., Nori, S., Kotter, M. R. N., Druschel, C., Curt, A., et al. (2017). Traumatic spinal cord injury. *Nat Rev Dis Primers* 3, 17018. doi: 10.1038/nrdp.2017.18.

6. Alaynick, W. A., Jessell, T. M., and Pfaff, S. L. (2011). SnapShot: Spinal Cord Development. *Cell* 146, 178-178.e1. doi: 10.1016/j.cell.2011.06.038.

7. Alberts, B., Johnson, A., Lewis, J., Raff, M., Roberts, K., and Walter, P. (2002). Intracellular Compartments and Protein Sorting. *Molecular Biology of the Cell. 4th edition*. Available at: https://www.ncbi.nlm.nih.gov/books/NBK21053/ [Accessed September 20, 2021].

8. Amin, A., Perera, N. D., Beart, P. M., Turner, B. J., and Shabanpoor, F. (2020). Amyotrophic Lateral Sclerosis and Autophagy: Dysfunction and Therapeutic Targeting. *Cells* 9, 2413. doi: 10.3390/cells9112413.

9. Anderson, M. A., Burda, J. E., Ren, Y., Ao, Y., O'Shea, T. M., Kawaguchi, R., et al. (2016). Astrocyte scar formation aids central nervous system axon regeneration. *Nature* 532, 195–200. doi: 10.1038/nature17623.

10. Ankeny, D. P., Lucin, K. M., Sanders, V. M., McGaughy, V. M., and Popovich, P. G. (2006). Spinal cord injury triggers systemic autoimmunity: evidence for chronic B lymphocyte activation and lupus-like autoantibody synthesis. *J Neurochem* 99, 1073–1087. doi: 10.1111/j.1471-4159.2006.04147.x.

11. Appel, S. H., Engelhardt, J. I., Henkel, J. S., Siklos, L., Beers, D. R., Yen, A. A., et al. (2008). Hematopoietic stem cell transplantation in patients with sporadic amyotrophic lateral sclerosis. *Neurology* 71, 1326–1334. doi: 10.1212/01.wnl.0000327668.43541.22.

12. Arakawa, S., Tsujioka, M., Yoshida, T., Tajima-Sakurai, H., Nishida, Y., Matsuoka, Y., et al. (2017). Role of Atg5-dependent cell death in the embryonic development of Bax/Bak double-knockout mice. *Cell Death Differ* 24, 1598–1608. doi: 10.1038/cdd.2017.84.

13. Arshadi, C., Günther, U., Eddison, M., Harrington, K. I. S., and Ferreira, T. A. (2020). SNT: A Unifying Toolbox for Quantification of Neuronal Anatomy. Neuroscience doi: 10.1101/2020.07.13.179325.

14. Ashammakhi, N., Kim, H.-J., Ehsanipour, A., Bierman, R. D., Kaarela, O., Xue, C., et al. (2019). Regenerative Therapies for Spinal Cord Injury. *Tissue Engineering Part B: Reviews* 25, 471–491. doi: 10.1089/ten.teb.2019.0182.

15. Ayanlaja, A. A., Xiong, Y., Gao, Y., Ji, G., Tang, C., Abdikani Abdullah, Z., et al. (2017). Distinct Features of Doublecortin as a Marker of Neuronal Migration and Its Implications in Cancer Cell Mobility. *Frontiers in Molecular Neuroscience* 10, 199. doi: 10.3389/fnmol.2017.00199.

16. Bahar, E., Kim, H., and Yoon, H. (2016). ER Stress-Mediated Signaling: Action Potential and Ca2+ as Key Players. *Int J Mol Sci* 17, 1558. doi: 10.3390/ijms17091558.

17. Bao, F., Chen, Y., Dekaban, G. A., and Weaver, L. C. (2004). Early anti-inflammatory treatment reduces lipid peroxidation and protein nitration after spinal cord injury in rats. *J Neurochem* 88, 1335–1344. doi: 10.1046/j.1471-4159.2003.02240.x.

18. Barbati, A. C., Fang, C., Banker, G. A., and Kirby, B. J. (2013). Culture of Primary Rat Hippocampal Neurons: Design, Analysis, and Optimization of a Microfluidic Device for Cell Seeding, Coherent Growth, and Solute Delivery. *Biomed Microdevices* 15, 97–108. doi: 10.1007/s10544-012-9691-2.

19. Bareyre, F. M., Kerschensteiner, M., Raineteau, O., Mettenleiter, T. C., Weinmann, O., and Schwab, M. E. (2004). The injured spinal cord spontaneously forms a new intraspinal circuit in adult rats. *Nat Neurosci* 7, 269–277. doi: 10.1038/nn1195.

20. Baroja-Mazo, A., Revilla-Nuin, B., Ramírez, P., and Pons, J. A. (2016). Immunosuppressive potency of mechanistic target of rapamycin inhibitors in solid-organ transplantation. *World J Transplant* 6, 183–192. doi: 10.5500/wjt.v6.i1.183.

21. Basso, D. M., Beattie, M. S., and Bresnahan, J. C. (1995). A sensitive and reliable locomotor rating scale for open field testing in rats. *J Neurotrauma* 12, 1–21. doi: 10.1089/neu.1995.12.1.

22. B'chir, W., Maurin, A.-C., Carraro, V., Averous, J., Jousse, C., Muranishi, Y., et al. (2013). The eIF2α/ATF4 pathway is essential for stress-induced autophagy gene expression. *Nucleic Acids Research* 41, 7683–7699. doi: 10.1093/nar/gkt563.

23. Beattie, M. S., Hermann, G. E., Rogers, R. C., and Bresnahan, J. C. (2002). Cell death in models of spinal cord injury. *Prog Brain Res* 137, 37–47. doi: 10.1016/s0079-6123(02)37006-7.

24. Beck, K. D., Nguyen, H. X., Galvan, M. D., Salazar, D. L., Woodruff, T. M., and Anderson, A. J. (2010). Quantitative analysis of cellular inflammation after traumatic spinal cord injury: evidence for a multiphasic inflammatory response in the acute to chronic environment. *Brain* 133, 433–447. doi: 10.1093/brain/awp322.

25. Becker, L. A., Huang, B., Bieri, G., Ma, R., Knowles, D. A., Jafar-Nejad, P., et al. (2017). Therapeutic reduction of ataxin-2 extends lifespan and reduces pathology in TDP-43 mice. *Nature* 544, 367–371. doi: 10.1038/nature22038.

26. Bell, K. F. S., and Hardingham, G. E. (2011). The influence of synaptic activity on neuronal health. *Curr Opin Neurobiol* 21, 299–305. doi: 10.1016/j.conb.2011.01.002.

27. Benevento, B. T., and Sipski, M. L. (2002). Neurogenic bladder, neurogenic bowel, and sexual dysfunction in people with spinal cord injury. *Phys Ther* 82, 601–612.

28. Bento, C. F., Renna, M., Ghislat, G., Puri, C., Ashkenazi, A., Vicinanza, M., et al. (2016). Mammalian Autophagy: How Does It Work? *Annual Review of Biochemistry* 85, 685–713. doi: 10.1146/annurev-biochem-060815-014556.

29. Bergmann, O., Spalding, K. L., and Frisén, J. (2015). Adult Neurogenesis in Humans. *Cold Spring Harb Perspect Biol* 7, a018994. doi: 10.1101/cshperspect.a018994.

30. Bertolotti, A., Zhang, Y., Hendershot, L. M., Harding, H. P., and Ron, D. (2000). Dynamic interaction of BiP and ER stress transducers in the unfolded-protein response. *Nat Cell Biol* 2, 326–332. doi: 10.1038/35014014.

31. Bialik, S., Dasari, S. K., and Kimchi, A. (2018). Autophagy-dependent cell death – where, how and why a cell eats itself to death. *Journal of Cell Science* 131, jcs215152. doi: 10.1242/jcs.215152.

32. Biazik, J., Ylä-Anttila, P., Vihinen, H., Jokitalo, E., and Eskelinen, E.-L. (2015). Ultrastructural relationship of the phagophore with surrounding organelles. *Autophagy* 11, 439–451. doi: 10.1080/15548627.2015.1017178.

33. Boido, M., Piras, A., Valsecchi, V., Spigolon, G., Mareschi, K., Ferrero, I., et al. (2014). Human mesenchymal stromal cell transplantation modulates neuroinflammatory milieu in a mouse model of amyotrophic lateral sclerosis. *Cytotherapy* 16, 1059–1072. doi: 10.1016/j.jcyt.2014.02.003.

34. Boillée, S., Vande Velde, C., and Cleveland, D. W. (2006). ALS: A Disease of Motor Neurons and Their Nonneuronal Neighbors. *Neuron* 52, 39–59. doi: 10.1016/j.neuron.2006.09.018.

35. Boland, B., Kumar, A., Lee, S., Platt, F. M., Wegiel, J., Yu, W. H., et al. (2008). Autophagy Induction and Autophagosome Clearance in Neurons: Relationship to Autophagic Pathology in Alzheimer's Disease. *J. Neurosci.* 28, 6926–6937. doi: 10.1523/JNEUROSCI.0800-08.2008.

36. Boulis, N. M., Federici, T., Glass, J. D., Lunn, J. S., Sakowski, S. A., and Feldman, E. L. (2011). Translational stem cell therapy for amyotrophic lateral sclerosis. *Nat Rev Neurol* 8, 172–176. doi: 10.1038/nrneurol.2011.191.

37. Brennan, F. H., Kurniawan, N. D., Vukovic, J., Bartlett, P. F., Käsermann, F., Arumugam, T. V., et al. (2016). IVIg attenuates complement and improves spinal cord injury outcomes in mice. *Ann Clin Transl Neurol* 3, 495–511. doi: 10.1002/acn3.318.

38. Brommer, B., Engel, O., Kopp, M. A., Watzlawick, R., Müller, S., Prüss, H., et al. (2016). Spinal cord injury-induced immune deficiency syndrome enhances infection susceptibility dependent on lesion level. *Brain* 139, 692–707. doi: 10.1093/brain/awv375.

39. Brown, E. J., Beal, P. A., Keith, C. T., Chen, J., Bum Shin, T., and Schreiber, S. L. (1995). Control of p70 S6 kinase by kinase activity of FRAP in vivo. *Nature* 377, 441–446. doi: 10.1038/377441a0.

40. Brown, J. P., Couillard-Després, S., Cooper-Kuhn, C. M., Winkler, J., Aigner, L., and Kuhn, H. G. (2003). Transient expression of doublecortin during adult neurogenesis. *Journal of Comparative Neurology* 467, 1–10. doi: 10.1002/cne.10874.

41. Bucchia, M., Merwin, S. J., Re, D. B., and Kariya, S. (2018). Limitations and Challenges in Modeling Diseases Involving Spinal Motor Neuron Degeneration in Vitro. *Frontiers in Cellular Neuroscience* 12, 61. doi: 10.3389/fncel.2018.00061.

42. Cai, Y., Arikkath, J., Yang, L., Guo, M.-L., Periyasamy, P., and Buch, S. (2016). Interplay of endoplasmic reticulum stress and autophagy in neurodegenerative disorders. *Autophagy* 12, 225–244. doi: 10.1080/15548627.2015.1121360.

43. Cajal, S. R. y (1991). Cajal's Degeneration and Regeneration of the Nervous System. Oxford University Press.

44. Calfon, M., Zeng, H., Urano, F., Till, J. H., Hubbard, S. R., Harding, H. P., et al. (2002). IRE1 couples endoplasmic reticulum load to secretory capacity by processing the XBP-1 mRNA. *Nature* 415, 92–96. doi: 10.1038/415092a.

45. Cardenas, D. D., and Felix, E. R. (2009). Pain after spinal cord injury: a review of classification, treatment approaches, and treatment assessment. *PM R* 1, 1077–1090. doi: 10.1016/j.pmrj.2009.07.002.

46. Castillo, K., Nassif, M., Valenzuela, V., Rojas, F., Matus, S., Mercado, G., et al. (2013). Trehalose delays the progression of amyotrophic lateral sclerosis by enhancing autophagy in motoneurons. *Autophagy* 9, 1308–1320. doi: 10.4161/auto.25188.

47. Cekanaviciute, E., and Buckwalter, M. (2016). Astrocytes: Integrative Regulators of Neuroinflammation in Stroke and Other Neurological Diseases. *Neurotherapeutics*. doi: 10.1007/s13311-016-0477-8.

48. Cheah, M., Andrews, M. R., Chew, D. J., Moloney, E. B., Verhaagen, J., Fassler, R., et al. (2016). Expression of an Activated Integrin Promotes Long-Distance Sensory Axon Regeneration in the Spinal Cord. *Journal of Neuroscience* 36, 7283–7297. doi: 10.1523/JNEUROSCI.0901-16.2016.

49. Chen, H.-C., Fong, T.-H., Hsu, P.-W., and Chiu, W.-T. (2013). Multifaceted effects of rapamycin on functional recovery after spinal cord injury in rats through autophagy promotion, anti-inflammation, and neuroprotection. *J Surg Res* 179:e203-210. doi: 10.1016/j.jss.2012.02.023.

50. Chen, H.-C., Fong, T.-H., Lee, A.-W., and Chiu, W.-T. (2012). Autophagy Is Activated in Injured Neurons and Inhibited by Methylprednisolone After Experimental Spinal Cord Injury. *Spine* 37, 470–475. doi: 10.1097/BRS.0b013e318221e859.

51. Chen, P.-C., Hsieh, Y.-C., Huang, C.-C., and Hu, C.-J. (2020). Tamoxifen for amyotrophic lateral sclerosis: A randomized double-blind clinical trial. *Medicine* 99, e20423. doi: 10.1097/MD.0000000000020423.

52. Chen, W., Lu, N., Ding, Y., Wang, Y., Chan, L. T., Wang, X., et al. (2016). Rapamycin-Resistant mTOR Activity Is Required for Sensory Axon Regeneration Induced by a Conditioning Lesion. *eNeuro* 3. doi: 10.1523/ENEURO.0358-16.2016.

53. Cheriyan, T., Ryan, D. J., Weinreb, J. H., Cheriyan, J., Paul, J. C., Lafage, V., et al. (2014). Spinal cord injury models: a review. *Spinal Cord* 52, 588–595. doi: 10.1038/sc.2014.91.

54. Chiò, A., Battistini, S., Calvo, A., Caponnetto, C., Conforti, F. L., Corbo, M., et al. (2014). Genetic counselling in ALS: facts, uncertainties and clinical suggestions. *J Neurol Neurosurg Psychiatry* 85, 478–485. doi: 10.1136/jnnp-2013-305546.

55. Chio, J. C. T., Xu, K. J., Popovich, P., David, S., and Fehlings, M. G. (2021). Neuroimmunological therapies for treating spinal cord injury: Evidence and future perspectives. *Experimental Neurology* 341, 113704. doi: 10.1016/j.expneurol.2021.113704.

56. Claydon, V. E., Steeves, J. D., and Krassioukov, A. (2006). Orthostatic hypotension following spinal cord injury: understanding clinical pathophysiology. *Spinal Cord* 44, 341–351. doi: 10.1038/sj.sc.3101855.

57. Clement, A. M., Nguyen, M. D., Roberts, E. A., Garcia, M. L., Boillée, S., Rule, M., et al. (2003). Wild-Type Nonneuronal Cells Extend Survival of SOD1 Mutant Motor Neurons in ALS Mice. *Science*. doi: 10.1126/science.1086071.

58. Codeluppi, S., Svensson, C. I., Hefferan, M. P., Valencia, F., Silldorff, M. D., Oshiro, M., et al. (2009). The Rheb-mTOR Pathway Is Upregulated in Reactive Astrocytes of the Injured Spinal Cord. *J Neurosci* 29, 1093–1104. doi: 10.1523/JNEUROSCI.4103-08.2009.

59. Coelho, D. S., and Domingos, P. M. (2014). Physiological roles of regulated Ire1 dependent decay. *Front Genet* 5, 76. doi: 10.3389/fgene.2014.00076.

60. Cordaro, M., Paterniti, I., Siracusa, R., Impellizzeri, D., Esposito, E., and Cuzzocrea, S. (2017). KU0063794, a Dual mTORC1 and mTORC2 Inhibitor, Reduces Neural Tissue Damage and Locomotor Impairment After Spinal Cord Injury in Mice. *Mol Neurobiol* 54, 2415–2427. doi: 10.1007/s12035-016-9827-0.

61. Courtine, G., Song, B., Roy, R. R., Zhong, H., Herrmann, J. E., Ao, Y., et al. (2008). Recovery of supraspinal control of stepping via indirect propriospinal relay connections after spinal cord injury. *Nat Med* 14, 69–74. doi: 10.1038/nm1682.

62. Dai, J.-X., Hu, Z.-L., Shi, M., Guo, C., and Ding, Y.-Q. (2008). Postnatal ontogeny of the transcription factor Lmx1b in the mouse central nervous system. *Journal of Comparative Neurology* 509, 341–355. doi: 10.1002/cne.21759.

63. Darian-Smith, C. (2009). Synaptic Plasticity, Neurogenesis, and Functional Recovery after Spinal Cord Injury. *Neuroscientist* 15, 149–165. doi: 10.1177/1073858408331372.

64. David, S., Greenhalgh, A. D., and Kroner, A. (2015). Macrophage and microglial plasticity in the injured spinal cord. *Neuroscience* 307, 311–318. doi: 10.1016/j.neuroscience.2015.08.064.

65. David, S., and Kroner, A. (2011). Repertoire of microglial and macrophage responses after spinal cord injury. *Nat Rev Neurosci* 12, 388–399. doi: 10.1038/nrn3053.

66. David, S., and Kroner, A. (2015). "Chapter 16 - Inflammation and Secondary Damage after Spinal Cord Injury," in *Neural Regeneration*, eds. K.-F. So and X.-M. Xu (Oxford: Academic Press), 245–261. doi: 10.1016/B978-0-12-801732-6.00016-1.

67. de Mena, L., Lopez-Scarim, J., and Rincon-Limas, D. E. (2021). TDP-43 and ER Stress in Neurodegeneration: Friends or Foes? *Front Mol Neurosci* 14, 772226. doi: 10.3389/fnmol.2021.772226.

68. Del Barrio, M. G., Bourane, S., Grossmann, K., Schüle, R., Britsch, S., O'Leary, D. D. M., et al. (2013). A Transcription Factor Code Defines Nine Sensory Interneuron Subtypes in the Mechanosensory Area of the Spinal Cord. *PLoS ONE* 8, e77928. doi: 10.1371/journal.pone.0077928.

69. Denton, D., and Kumar, S. (2019). Autophagy-dependent cell death. *Cell Death Differ* 26, 605–616. doi: 10.1038/s41418-018-0252-y.

70. Dobrott, C. I., Sathyamurthy, A., and Levine, A. J. (2019). Decoding cell type diversity within the spinal cord. *Current Opinion in Physiology* 8, 1–6. doi: 10.1016/j.cophys.2018.11.006.

71. Donaldson, K., and Höke, A. (2014). Studying axonal degeneration and regeneration using *in vitro* and *in vivo* models: the translational potential. *Future Neurology* 9, 461–473. doi: 10.2217/fnl.14.29.

72. Dong, L., Krewson, E. A., and Yang, L. V. (2017). Acidosis Activates Endoplasmic Reticulum Stress Pathways through GPR4 in Human Vascular Endothelial Cells. *International Journal of Molecular Sciences* 18, 278. doi: 10.3390/ijms18020278.

73. Dooley, H. C., Razi, M., Polson, H. E. J., Girardin, S. E., Wilson, M. I., and Tooze, S. A. (2014). WIPI2 links LC3 conjugation with PI3P, autophagosome formation, and pathogen clearance by recruiting Atg12-5-16L1. *Mol Cell* 55, 238–252. doi: 10.1016/j.molcel.2014.05.021.

74. Dossou, A. S., and Basu, A. (2019). The Emerging Roles of mTORC1 in Macromanaging Autophagy. *Cancers (Basel)* 11, 1422. doi: 10.3390/cancers11101422.

75. Du, J., Li, X., Lin, X., Lu, Y., and Chen, B. (2017). A Rapamycin-Enhanced Autophagy Reduces Neural Apoptosis by Blocking Bax Mitochondral Translation and Cytochrome C Release in Acute Spinal Cord Injury in Rats. *Med Case Rep*, 3. doi: 10.21767/2471-8041.100075.

76. Durand, J., Filipchuk, A., Pambo-Pambo, A., Amendola, J., Borisovna Kulagina, I., and Guéritaud, J.-P. (2015). Developing electrical properties of postnatal mouse lumbar motoneurons. *Frontiers in Cellular Neuroscience* 9, 349. doi: 10.3389/fncel.2015.00349.

77. Eckert, M. J., and Martin, M. J. (2017). Trauma: Spinal Cord Injury. *Surg Clin North Am* 97, 1031–1045. doi: 10.1016/j.suc.2017.06.008.

78. Eldeiry, M., Yamanaka, K., Reece, T. B., and Aftab, M. (2017). Spinal Cord Neurons Isolation and Culture from Neonatal Mice. *JoVE*, 55856. doi: 10.3791/55856.

79. Elkabes, S., DiCicco-Bloom, E. M., and Black, I. B. (1996). Brain microglia/macrophages express neurotrophins that selectively regulate microglial proliferation and function. *J Neurosci* 16, 2508–2521.

80. Farg, M. A., Soo, K. Y., Walker, A. K., Pham, H., Orian, J., Horne, M. K., et al. (2012). Mutant FUS induces endoplasmic reticulum stress in amyotrophic lateral sclerosis and interacts with

protein disulfide-isomerase. *Neurobiol Aging* 33, 2855–2868. doi: 10.1016/j.neurobiolaging.2012.02.009.

81. Fawcett, J. W. (2020). The Struggle to Make CNS Axons Regenerate: Why Has It Been so Difficult? *Neurochem Res* 45, 144–158. doi: 10.1007/s11064-019-02844-y.

82. Feldman, M. E., Apsel, B., Uotila, A., Loewith, R., Knight, Z. A., Ruggero, D., et al. (2009). Active-Site Inhibitors of mTOR Target Rapamycin-Resistant Outputs of mTORC1 and mTORC2. doi: 10.1371/journal.pbio.1000038.

83. Filipi, T., Hermanova, Z., Tureckova, J., Vanatko, O., and Anderova, A. M. (2020). Glial Cells-The Strategic Targets in Amyotrophic Lateral Sclerosis Treatment. *J Clin Med* 9, E261. doi: 10.3390/jcm9010261.

84. Filomeni, G., De Zio, D., and Cecconi, F. (2015). Oxidative stress and autophagy: the clash between damage and metabolic needs. *Cell Death Differ* 22, 377–388. doi: 10.1038/cdd.2014.150.

85. Forostyak, S., Homola, A., Turnovcova, K., Svitil, P., Jendelova, P., and Sykova, E. (2014). Intrathecal delivery of mesenchymal stromal cells protects the structure of altered perineuronal nets in SOD1 rats and amends the course of ALS. *Stem Cells* 32, 3163–3172. doi: 10.1002/stem.1812.

86. Forostyak, S., Jendelova, P., Kapcalova, M., Arboleda, D., and Sykova, E. (2011). Mesenchymal stromal cells prolong the lifespan in a rat model of amyotrophic lateral sclerosis. *Cytotherapy* 13, 1036–1046. doi: 10.3109/14653249.2011.592521.

87. Forostyak, S., Jendelova, P., and Sykova, E. (2013). The role of mesenchymal stromal cells in spinal cord injury, regenerative medicine and possible clinical applications. *Biochimie* 95, 2257–2270. doi: 10.1016/j.biochi.2013.08.004.

88. Franssen, E. H. P., Zhao, R.-R., Koseki, H., Kanamarlapudi, V., Hoogenraad, C. C., Eva, R., et al. (2015). Exclusion of integrins from CNS axons is regulated by Arf6 activation and the AIS. *J Neurosci* 35, 8359–8375. doi: 10.1523/JNEUROSCI.2850-14.2015.

89. Fritz, E., Izaurieta, P., Weiss, A., Mir, F. R., Rojas, P., Gonzalez, D., et al. (2013). Mutant SOD1-expressing astrocytes release toxic factors that trigger motoneuron death by inducing hyperexcitability. *J Neurophysiol* 109, 2803–2814. doi: 10.1152/jn.00500.2012.

90. Fujikake, N., Shin, M., and Shimizu, S. (2018). Association Between Autophagy and Neurodegenerative Diseases. *Front Neurosci* 12, 255. doi: 10.3389/fnins.2018.00255.

91. Füllgrabe, J., Lynch-Day, M. A., Heldring, N., Li, W., Struijk, R. B., Ma, Q., et al. (2013). The histone H4 lysine 16 acetyltransferase hMOF regulates the outcome of autophagy. *Nature* 500, 468–471. doi: 10.1038/nature12313.

92. Gade, P., Manjegowda, S. B., Nallar, S. C., Maachani, U. B., Cross, A. S., and Kalvakolanu, D. V. (2014). Regulation of the death-associated protein kinase 1 expression and autophagy via ATF6 requires apoptosis signal-regulating kinase 1. *Mol Cell Biol* 34, 4033–4048. doi: 10.1128/MCB.00397-14.

93. Gaj, T., Ojala, D. S., Ekman, F. K., Byrne, L. C., Limsirichai, P., and Schaffer, D. V. (2017). In vivo genome editing improves motor function and extends survival in a mouse model of ALS. *Sci Adv* 3, eaar3952. doi: 10.1126/sciadv.aar3952.

94. Garcia, E., Aguilar-Cevallos, J., Silva-Garcia, R., and Ibarra, A. (2016). Cytokine and Growth Factor Activation In Vivo and In Vitro after Spinal Cord Injury. *Mediators of Inflammation* 2016, e9476020. doi: 10.1155/2016/9476020.

95. Garza-Lombó, C., and Gonsebatt, M. E. (2016). Mammalian Target of Rapamycin: Its Role in Early Neural Development and in Adult and Aged Brain Function. *Frontiers in Cellular Neuroscience* 10. Available at: https://www.frontiersin.org/article/10.3389/fncel.2016.00157 [Accessed May 23, 2022].

96. Geoffroy, C. G., Lorenzana, A. O., Kwan, J. P., Lin, K., Ghassemi, O., Ma, A., et al. (2015). Effects of PTEN and Nogo Codeletion on Corticospinal Axon Sprouting and Regeneration in Mice. *J Neurosci* 35, 6413–6428. doi: 10.1523/JNEUROSCI.4013-14.2015.

97. Geoffroy, C. G., and Zheng, B. (2014). Myelin-Associated Inhibitors in Axonal Growth After CNS Injury. *Curr Opin Neurobiol* 0, 31–38. doi: 10.1016/j.conb.2014.02.012.

98. Gertz, C. C., Leach, M. K., Birrell, L. K., Martin, D. C., Feldman, E. L., and Corey, J. M. (2010). Accelerated neuritogenesis and maturation of primary spinal motor neurons in response to nanofibers. *Dev Neurobiol* 70, 589–603. doi: 10.1002/dneu.20792.

99. Glick, D., Barth, S., and Macleod, K. F. (2010). Autophagy: cellular and molecular mechanisms. *J Pathol* 221, 3–12. doi: 10.1002/path.2697.

100. Golowasch, J., Thomas, G., Taylor, A. L., Patel, A., Pineda, A., Khalil, C., et al. (2009). Membrane Capacitance Measurements Revisited: Dependence of Capacitance Value on Measurement Method in Nonisopotential Neurons. *J Neurophysiol* 102, 2161–2175. doi: 10.1152/jn.00160.2009.

101. Gordeev, S. A., Bykova, T. V., Zubova, S. G., Bystrova, O. A., Martynova, M. G., Pospelov, V. A., et al. (2015). mTOR kinase inhibitor pp242 causes mitophagy terminated by apoptotic cell death in E1A-Ras transformed cells. *Oncotarget* 6, 44905–44926. doi: 10.18632/oncotarget.6457.

102. Gothelf, Y., Abramov, N., Harel, A., and Offen, D. (2014). Safety of repeated transplantations of neurotrophic factors-secreting human mesenchymal stromal stem cells. *Clinical and Translational Medicine* 3, e21. doi: 10.1186/2001-1326-3-21.

103. Graber, D. J., and Harris, B. T. (2013). Purification and Culture of Spinal Motor Neurons from Rat Embryos. *Cold Spring Harb Protoc* 2013, pdb.prot074161. doi: 10.1101/pdb.prot074161.

104. Gris, D., Marsh, D. R., Oatway, M. A., Chen, Y., Hamilton, E. F., Dekaban, G. A., et al. (2004). Transient Blockade of the CD11d/CD18 Integrin Reduces Secondary Damage after Spinal Cord Injury, Improving Sensory, Autonomic, and Motor Function. *Journal of Neuroscience* 24, 4043–4051. doi: 10.1523/JNEUROSCI.5343-03.2004.

105. Grudt, T. J., and Perl, E. R. (2002). Correlations between neuronal morphology and electrophysiological features in the rodent superficial dorsal horn. *J Physiol* 540, 189–207. doi: 10.1113/jphysiol.2001.012890.

106. Guo, Y., Liu, S., Zhang, X., Wang, L., Gao, J., Han, A., et al. (2015). G-CSF promotes autophagy and reduces neural tissue damage after spinal cord injury in mice. *Lab Invest* 95, 1439–1449. doi: 10.1038/labinvest.2015.120.

107. Hailey, D. W., Rambold, A. S., Satpute-Krishnan, P., Mitra, K., Sougrat, R., Kim, P. K., et al. (2010). Mitochondria supply membranes for autophagosome biogenesis during starvation. *Cell* 141, 656–667. doi: 10.1016/j.cell.2010.04.009.

108. Han, C. Y., Lim, S. W., Koo, J. H., Kim, W., and Kim, S. G. (2016). PHLDA3 overexpression in hepatocytes by endoplasmic reticulum stress via IRE1–Xbp1s pathway expedites liver injury. *Gut* 65, 1377–1388. doi: 10.1136/gutjnl-2014-308506.

109. Hantman, A. W., Pol, A. N. van den, and Perl, E. R. (2004). Morphological and Physiological Features of a Set of Spinal Substantia Gelatinosa Neurons Defined by Green Fluorescent Protein Expression. *J. Neurosci.* 24, 836–842. doi: 10.1523/JNEUROSCI.4221-03.2004.

110. Hardiman, O., Al-Chalabi, A., Chio, A., Corr, E. M., Logroscino, G., Robberecht, W., et al. (2017). Amyotrophic lateral sclerosis. *Nat Rev Dis Primers* 3, 17071. doi: 10.1038/nrdp.2017.71.

111. Harding, H. P., Zhang, Y., and Ron, D. (1999). Protein translation and folding are coupled by an endoplasmic-reticulum-resident kinase. *Nature* 397, 271–274. doi: 10.1038/16729.

112. Harding, H. P., Zhang, Y., Zeng, H., Novoa, I., Lu, P. D., Calfon, M., et al. (2003). An integrated stress response regulates amino acid metabolism and resistance to oxidative stress. *Mol Cell* 11, 619–633. doi: 10.1016/s1097-2765(03)00105-9.

113. Hayashi, M., Hinckley, C. A., Driscoll, S. P., Moore, N. J., Levine, A. J., Hilde, K. L., et al. (2018). Graded Arrays of Spinal and Supraspinal V2a Interneuron Subtypes Underlie Forelimb and Hindlimb Motor Control. *Neuron* 97, 869-884.e5. doi: 10.1016/j.neuron.2018.01.023.

114. Haze, K., Yoshida, H., Yanagi, H., Yura, T., and Mori, K. (1999). Mammalian Transcription Factor ATF6 Is Synthesized as a Transmembrane Protein and Activated by Proteolysis in Response to Endoplasmic Reticulum Stress. *MBoC* 10, 3787–3799. doi: 10.1091/mbc.10.11.3787.

115. Hetz, C., and Saxena, S. (2017). ER stress and the unfolded protein response in neurodegeneration. *Nat Rev Neurol* 13, 477–491. doi: 10.1038/nrneurol.2017.99.

116. Hetz, C., Thielen, P., Matus, S., Nassif, M., Court, F., Kiffin, R., et al. (2009). XBP-1 deficiency in the nervous system protects against amyotrophic lateral sclerosis by increasing autophagy. *Genes Dev* 23, 2294–2306. doi: 10.1101/gad.1830709.

117. Hinchcliffe, M., and Smith, A. (2017). Riluzole: real-world evidence supports significant extension of median survival times in patients with amyotrophic lateral sclerosis. *Degener Neurol Neuromuscul Dis* 7, 61–70. doi: 10.2147/DNND.S135748.

118. Hines, D. J., Hines, R. M., Mulligan, S. J., and Macvicar, B. A. (2009). Microglia processes block the spread of damage in the brain and require functional chloride channels. *Glia* 57, 1610–1618. doi: 10.1002/glia.20874.

119. Hsueh, K.-W., Chiou, T.-W., Chiang, S.-F., Yamashita, T., Abe, K., Borlongan, C. V., et al. (2016). Autophagic down-regulation in motor neurons remarkably prolongs the survival of ALS mice. *Neuropharmacology* 108, 152–160. doi: 10.1016/j.neuropharm.2016.03.035.

120. Ikeda, K., Iwasaki, Y., and Kaji, R. (2015). Neuroprotective effect of ultra-high dose methylcobalamin in wobbler mouse model of amyotrophic lateral sclerosis. *J Neurol Sci* 354, 70–74. doi: 10.1016/j.jns.2015.04.052.

121. Ilieva, E. V., Ayala, V., Jové, M., Dalfó, E., Cacabelos, D., Povedano, M., et al. (2007). Oxidative and endoplasmic reticulum stress interplay in sporadic amyotrophic lateral sclerosis. *Brain* 130, 3111–3123. doi: 10.1093/brain/awm190.

122. Ito, Y., Yamada, M., Tanaka, H., Aida, K., Tsuruma, K., Shimazawa, M., et al. (2009). Involvement of CHOP, an ER-stress apoptotic mediator, in both human sporadic ALS and ALS model mice. *Neurobiol Dis* 36, 470–476. doi: 10.1016/j.nbd.2009.08.013.

123. Jack J. Chen, P. (2020). Overview of Current and Emerging Therapies for Amyotrophic Lateral Sclerosis. Available at: https://www.ajmc.com/view/overview-of-current-and-emerging-therapies-for-amyotrophic-lateral-sclerosis [Accessed January 11, 2022].

124. Jaiswal, M. K. (2016). Riluzole But Not Melatonin Ameliorates Acute Motor Neuron Degeneration and Moderately Inhibits SOD1-Mediated Excitotoxicity Induced Disrupted Mitochondrial Ca2+ Signaling in Amyotrophic Lateral Sclerosis. *Front Cell Neurosci* 10, 295. doi: 10.3389/fncel.2016.00295.

125. Jellinger, K. A. (2010). Basic mechanisms of neurodegeneration: a critical update. *J Cell Mol Med* 14, 457–487. doi: 10.1111/j.1582-4934.2010.01010.x.

126. Jhanwar-Uniyal, M., Amin, A. G., Cooper, J. B., Das, K., Schmidt, M. H., and Murali, R. (2017). Discrete signaling mechanisms of mTORC1 and mTORC2: Connected yet apart in cellular and molecular aspects. *Advances in Biological Regulation* 64, 39–48. doi: 10.1016/j.jbior.2016.12.001.

127. Jhanwar-Uniyal, M., Wainwright, J. V., Mohan, A. L., Tobias, M. E., Murali, R., Gandhi, C. D., et al. (2019). Diverse signaling mechanisms of mTOR complexes: mTORC1 and mTORC2 in forming a formidable relationship. *Adv Biol Regul* 72, 51–62. doi: 10.1016/j.jbior.2019.03.003.

128. Jiao, P., Ma, J., Feng, B., Zhang, H., Diehl, J. A., Chin, Y. E., et al. (2011). FFA-induced adipocyte inflammation and insulin resistance: involvement of ER stress and IKKβ pathways. *Obesity (Silver Spring)* 19, 483–491. doi: 10.1038/oby.2010.200.

129. Johnson, J. O., Mandrioli, J., Benatar, M., Abramzon, Y., Van Deerlin, V. M., Trojanowski, J. Q., et al. (2010). Exome sequencing reveals VCP mutations as a cause of familial ALS. *Neuron* 68, 857–864. doi: 10.1016/j.neuron.2010.11.036.

130. Jones, T. B., McDaniel, E. E., and Popovich, P. G. (2005). Inflammatory-Mediated Injury and Repair in the Traumatically Injured Spinal Cord. *Current Pharmaceutical Design* 11, 1223–1236. doi: 10.2174/1381612053507468.

131. Kadowaki, H., and Nishitoh, H. (2013). Signaling Pathways from the Endoplasmic Reticulum and Their Roles in Disease. *Genes* 4, 306–333. doi: 10.3390/genes4030306.

132. Kaech, S., and Banker, G. (2006). Culturing hippocampal neurons. *Nat Protoc* 1, 2406–2415. doi: 10.1038/nprot.2006.356.

133. Kaji, R., Imai, T., Iwasaki, Y., Okamoto, K., Nakagawa, M., Ohashi, Y., et al. (2019). Ultra-high-dose methylcobalamin in amyotrophic lateral sclerosis: a long-term phase II/III randomised controlled study. *J Neurol Neurosurg Psychiatry* 90, 451–457. doi: 10.1136/jnnp-2018-319294.

134. Kanno, H., Ozawa, H., Sekiguchi, A., Yamaya, S., and Itoi, E. (2011). Induction of autophagy and autophagic cell death in damaged neural tissue after acute spinal cord injury in mice. *Spine (Phila Pa 1976)* 36, E1427-1434. doi: 10.1097/BRS.0b013e3182028c3a.

135. Kanno, H., Ozawa, H., Sekiguchi, A., Yamaya, S., Tateda, S., Yahata, K., et al. (2012). The role of mTOR signaling pathway in spinal cord injury. *Cell Cycle* 11, 3175–3179. doi: 10.4161/cc.21262.

136. Kappagantula, S., Andrews, M. R., Cheah, M., Abad-Rodriguez, J., Dotti, C. G., and Fawcett, J. W. (2014). Neu3 Sialidase-Mediated Ganglioside Conversion Is Necessary for Axon Regeneration and Is Blocked in CNS Axons. *J Neurosci* 34, 2477–2492. doi: 10.1523/JNEUROSCI.4432-13.2014.

137. Karanasios, E., Walker, S. A., Okkenhaug, H., Manifava, M., Hummel, E., Zimmermann, H., et al. (2016). Autophagy initiation by ULK complex assembly on ER tubulovesicular regions marked by ATG9 vesicles. *Nat Commun* 7, 12420. doi: 10.1038/ncomms12420.

138. Kedersha, N. L., Gupta, M., Li, W., Miller, I., and Anderson, P. (1999). RNA-Binding Proteins Tia-1 and Tiar Link the Phosphorylation of Eif-2α to the Assembly of Mammalian Stress Granules. *Journal of Cell Biology* 147, 1431–1442. doi: 10.1083/jcb.147.7.1431.

139. Kim, H., Kim, H. Y., Choi, M. R., Hwang, S., Nam, K.-H., Kim, H.-C., et al. (2010). Dose-dependent efficacy of ALS-human mesenchymal stem cells transplantation into cisterna magna in SOD1-G93A ALS mice. *Neurosci Lett* 468, 190–194. doi: 10.1016/j.neulet.2009.10.074.

140. Kim, Y. C., and Guan, K.-L. (2015). mTOR: a pharmacologic target for autophagy regulation. *J Clin Invest* 125, 25–32. doi: 10.1172/JCI73939.

141. Kipnis, J., Mizrahi, T., Hauben, E., Shaked, I., Shevach, E., and Schwartz, M. (2002). Neuroprotective autoimmunity: naturally occurring CD4+CD25+ regulatory T cells suppress the ability to withstand injury to the central nervous system. *Proc Natl Acad Sci U S A* 99, 15620–15625. doi: 10.1073/pnas.232565399.

142. Klionsky, D. J., Abdel-Aziz, A. K., Abdelfatah, S., Abdellatif, M., Abdoli, A., Abel, S., et al. (2021). Guidelines for the use and interpretation of assays for monitoring autophagy (4th edition)1. *Autophagy* 17, 1–382. doi: 10.1080/15548627.2020.1797280.

143. Kopach, O., Esteras, N., Wray, S., Rusakov, D. A., and Abramov, A. Y. (2020). Maturation and phenotype of pathophysiological neuronal excitability of human cells in tau-related dementia. *J Cell Sci* 133. doi: 10.1242/jcs.241687.

144. Koseki, H., Donegá, M., Lam, B. Y., Petrova, V., van Erp, S., Yeo, G. S., et al. (2017). Selective rab11 transport and the intrinsic regenerative ability of CNS axons. *Elife* 6. doi: 10.7554/eLife.26956.

145. Kroner, A., Greenhalgh, A. D., Zarruk, J. G., Passos Dos Santos, R., Gaestel, M., and David, S. (2014). TNF and increased intracellular iron alter macrophage polarization to a detrimental M1 phenotype in the injured spinal cord. *Neuron* 83, 1098–1116. doi: 10.1016/j.neuron.2014.07.027.

146. Kumar, P., Nagarajan, A., and Uchil, P. D. (2018). Analysis of Cell Viability by the Lactate Dehydrogenase Assay. *Cold Spring Harb Protoc* 2018. doi: 10.1101/pdb.prot095497.

147. LaBarbera, K. M., Limegrover, C., Rehak, C., Yurko, R., Izzo, N. J., Knezovich, N., et al. (2021). Modeling the mature CNS: A predictive screening platform for neurodegenerative disease drug discovery. *J Neurosci Methods* 358, 109180. doi: 10.1016/j.jneumeth.2021.109180.

148. Laplante, M., and Sabatini, D. M. (2012). mTOR Signaling in Growth Control and Disease. *Cell* 149, 274–293. doi: 10.1016/j.cell.2012.03.017.

149. Larsson, M. (2017). Pax2 is persistently expressed by GABAergic neurons throughout the adult rat dorsal horn. *Neuroscience Letters* 638, 96–101. doi: 10.1016/j.neulet.2016.12.015.

150. Lee, A.-H., Iwakoshi, N. N., and Glimcher, L. H. (2003). XBP-1 regulates a subset of endoplasmic reticulum resident chaperone genes in the unfolded protein response. *Mol Cell Biol* 23, 7448–7459. doi: 10.1128/MCB.23.21.7448-7459.2003.

151. Lee, J.-A., and Gao, F.-B. (2009). Inhibition of autophagy induction delays neuronal cell loss caused by dysfunctional ESCRT-III in frontotemporal dementia. *J Neurosci* 29, 8506–8511. doi: 10.1523/JNEUROSCI.0924-09.2009.

152. Li, A., Song, N.-J., Riesenberg, B. P., and Li, Z. (2020). The Emerging Roles of Endoplasmic Reticulum Stress in Balancing Immunity and Tolerance in Health and Diseases: Mechanisms and Opportunities. *Frontiers in Immunology* 10, 3154. doi: 10.3389/fimmu.2019.03154.

153. Li, L., Zhang, X., and Le, W. (2008). Altered macroautophagy in the spinal cord of SOD1 mutant mice. *Autophagy* 4, 290–293. doi: 10.4161/auto.5524.

154. Li, X.-G., Du, J.-H., Lu, Y., and Lin, X.-J. (2019a). Neuroprotective effects of rapamycin on spinal cord injury in rats by increasing autophagy and Akt signaling. *Neural Regen Res* 14. doi: 10.4103/1673-5374.247476.

155. Li, Z., lingling, N., Chen, L., Sun, Y., and Li, G. (2019b). Rapamycin relieves inflammation of experimental autoimmune encephalomyelitis by altering the balance of Treg/Th17 in a mouse model. *Neurosci Lett* 705, 39–45. doi: 10.1016/j.neulet.2019.04.035.

156. Lian, H., Yang, L., Cole, A., Sun, L., Chiang, A. C.-A., Fowler, S. W., et al. (2015). NFκB-Activated Astroglial Release of Complement C3 Compromises Neuronal Morphology and Function Associated with Alzheimer's Disease. *Neuron* 85, 101–115. doi: 10.1016/j.neuron.2014.11.018.

157. Liddelow, S. A., and Barres, B. A. (2017). Reactive Astrocytes: Production, Function, and Therapeutic Potential. *Immunity* 46, 957–967. doi: 10.1016/j.immuni.2017.06.006.

158. Linn, W. S., Adkins, R. H., Gong, H., and Waters, R. L. (2000). Pulmonary function in chronic spinal cord injury: a cross-sectional survey of 222 southern California adult outpatients. *Arch Phys Med Rehabil* 81, 757–763. doi: 10.1016/s0003-9993(00)90107-2.

159. Lipinski, M. M., Wu, J., Faden, A. I., and Sarkar, C. (2015). Function and Mechanisms of Autophagy in Brain and Spinal Cord Trauma. *Antioxidants & Redox Signaling* 23, 565–577. doi: 10.1089/ars.2015.6306.

160. Liu, J., and Du, L. (2015). PERK pathway is involved in oxygen-glucose-serum deprivation-induced NF-kB activation via ROS generation in spinal cord astrocytes. *Biochem Biophys Res Commun* 467, 197–203. doi: 10.1016/j.bbrc.2015.10.007.

161. Liu, K., Chen, Y., Ai, F., Li, Y.-Q., Zhang, K., and Zhang, W.-T. (2021). PHLDA3 inhibition attenuates endoplasmic reticulum stress-induced apoptosis in myocardial hypoxia/reoxygenation injury by activating the PI3K/AKT signaling pathway. *Experimental and Therapeutic Medicine* 21, 1–9. doi: 10.3892/etm.2021.10045.

162. Liu, S., Sarkar, C., Dinizo, M., Faden, A. I., Koh, E. Y., Lipinski, M. M., et al. (2015). Disrupted autophagy after spinal cord injury is associated with ER stress and neuronal cell death. *Cell Death Dis* 6, e1582–e1582. doi: 10.1038/cddis.2014.527.

163. Liu, S., Xu, G.-Y., Johnson, K. M., Echetebu, C., Z, Y., Hulsebosch, C. E., et al. (2008). Regulation of interleukin-1β by the interleukin-1 receptor antagonist in the glutamate-injured spinal cord: Endogenous neuroprotection. *Brain Res* 1231, 63–74. doi: 10.1016/j.brainres.2008.07.035.

164. Liu, Z., Yang, Y., He, L., Pang, M., Luo, C., Liu, B., et al. (2019). High-dose methylprednisolone for acute traumatic spinal cord injury: A meta-analysis. *Neurology* 93, e841–e850. doi: 10.1212/WNL.0000000000007998.

165. Lu, D. C., Niu, T., and Alaynick, W. A. (2015). Molecular and cellular development of spinal cord locomotor circuitry. *Front. Mol. Neurosci.* 8. doi: 10.3389/fnmol.2015.00025.

166. Lu, P., Ceto, S., Wang, Y., Graham, L., Wu, D., Kumamaru, H., et al. (2017). Prolonged human neural stem cell maturation supports recovery in injured rodent CNS. *J Clin Invest* 127, 3287–3299. doi: 10.1172/JCI92955.

167. Machova Urdzikova, L., Karova, K., Ruzicka, J., Kloudova, A., Shannon, C., Dubisova, J., et al. (2015). The Anti-Inflammatory Compound Curcumin Enhances Locomotor and Sensory Recovery after Spinal Cord Injury in Rats by Immunomodulation. *Int J Mol Sci* 17, E49. doi: 10.3390/ijms17010049.

168. Machova Urdzikova, L., Ruzicka, J., Karova, K., Kloudova, A., Svobodova, B., Amin, A., et al. (2017). A green tea polyphenol epigallocatechin-3-gallate enhances neuroregeneration after spinal cord injury by altering levels of inflammatory cytokines. *Neuropharmacology* 126, 213–223. doi: 10.1016/j.neuropharm.2017.09.006.

169. Machová Urdzíková, L., Růžička, J., LaBagnara, M., Kárová, K., Kubinová, Š., Jiráková, K., et al. (2014). Human Mesenchymal Stem Cells Modulate Inflammatory Cytokines after Spinal Cord Injury in Rat. *Int J Mol Sci* 15, 11275–11293. doi: 10.3390/ijms150711275.

170. Machova Urdzikova, L., Sedlacek, R., Suchy, T., Amemori, T., Ruzicka, J., Lesny, P., et al. (2014). Human multipotent mesenchymal stem cells improve healing after collagenase tendon injury in the rat. *Biomed Eng Online* 13, 42. doi: 10.1186/1475-925X-13-42.

171. Mackenzie, I. R., Rademakers, R., and Neumann, M. (2010). TDP-43 and FUS in amyotrophic lateral sclerosis and frontotemporal dementia. *Lancet Neurol* 9, 995–1007. doi: 10.1016/S1474-4422(10)70195-2.

172. Maday, S. (2016). Mechanisms of neuronal homeostasis: autophagy in the axon. *Brain Res* 1649, 143–150. doi: 10.1016/j.brainres.2016.03.047.

173. Maday, S., and Holzbaur, E. L. F. (2016). Compartment-Specific Regulation of Autophagy in Primary Neurons. *J Neurosci* 36, 5933–5945. doi: 10.1523/JNEUROSCI.4401-15.2016.

174. Maday, S., Wallace, K. E., and Holzbaur, E. L. F. (2012). Autophagosomes initiate distally and mature during transport toward the cell soma in primary neurons. *J Cell Biol* 196, 407–417. doi: 10.1083/jcb.201106120.

175. Malhotra, J. D., and Kaufman, R. J. (2007). Endoplasmic reticulum stress and oxidative stress: a vicious cycle or a double-edged sword? *Antioxid Redox Signal* 9, 2277–2293. doi: 10.1089/ars.2007.1782.

176. Mannack, L. V., and Lane, J. D. (2015). The autophagosome: current understanding of formation and maturation. *RRBC* 5, 39–58. doi: 10.2147/RRBC.S57405.

177. Martier, R., Liefhebber, J. M., Miniarikova, J., van der Zon, T., Snapper, J., Kolder, I., et al. (2019). Artificial MicroRNAs Targeting C9orf72 Can Reduce Accumulation of Intra-nuclear Transcripts in ALS and FTD Patients. *Mol Ther Nucleic Acids* 14, 593–608. doi: 10.1016/j.omtn.2019.01.010.

178. Martina, J. A., Chen, Y., Gucek, M., and Puertollano, R. (2012). MTORC1 functions as a transcriptional regulator of autophagy by preventing nuclear transport of TFEB. *Autophagy* 8, 903–914. doi: 10.4161/auto.19653.

179. Martinez, M., Delivet-Mongrain, H., Leblond, H., and Rossignol, S. (2012). Incomplete spinal cord injury promotes durable functional changes within the spinal locomotor circuitry. *Journal of Neurophysiology* 108, 124–134. doi: 10.1152/jn.00073.2012.

180. Martínez-Muriana, A., Pastor, D., Mancuso, R., Rando, A., Osta, R., Martínez, S., et al. (2020). Combined intramuscular and intraspinal transplant of bone marrow cells improves neuromuscular function in the SOD1G93A mice. *Stem Cell Research & Therapy* 11, 53. doi: 10.1186/s13287-020-1573-6.

181. Masrori, P., and Van Damme, P. (2020). Amyotrophic lateral sclerosis: a clinical review. *Eur J Neurol* 27, 1918–1929. doi: 10.1111/ene.14393.

182. Massenzio, F., Peña-Altamira, E., Petralla, S., Virgili, M., Zuccheri, G., Miti, A., et al. (2018). Microglial overexpression of fALS-linked mutant SOD1 induces SOD1 processing impairment, activation and neurotoxicity and is counteracted by the autophagy inducer trehalose. *Biochim Biophys Acta Mol Basis Dis* 1864, 3771–3785. doi: 10.1016/j.bbadis.2018.10.013.

183. May, Z., Fenrich, K. K., Dahlby, J., Batty, N. J., Torres-Espín, A., and Fouad, K. (2017). Following Spinal Cord Injury Transected Reticulospinal Tract Axons Develop New Collateral Inputs to Spinal Interneurons in Parallel with Locomotor Recovery. *Neural Plasticity* 2017, 1–15. doi: 10.1155/2017/1932875.

184. McKeon, R. J., Schreiber, R. C., Rudge, J. S., and Silver, J. (1991). Reduction of neurite outgrowth in a model of glial scarring following CNS injury is correlated with the expression of inhibitory molecules on reactive astrocytes. *J Neurosci* 11, 3398–3411.

185. Meares, G. P., Liu, Y., Rajbhandari, R., Qin, H., Nozell, S. E., Mobley, J. A., et al. (2014). PERK-dependent activation of JAK1 and STAT3 contributes to endoplasmic reticulum stress-induced inflammation. *Mol Cell Biol* 34, 3911–3925. doi: 10.1128/MCB.00980-14.

186. Medinas, D. B., Cabral-Miranda, F., and Hetz, C. (2019). ER stress links aging to sporadic ALS. *Aging (Albany NY)* 11, 5–6. doi: 10.18632/aging.101705.

187. Medinas, D. B., Rozas, P., Martínez Traub, F., Woehlbier, U., Brown, R. H., Bosco, D. A., et al. (2018). Endoplasmic reticulum stress leads to accumulation of wild-type SOD1 aggregates associated with sporadic amyotrophic lateral sclerosis. *Proc Natl Acad Sci U S A* 115, 8209–8214. doi: 10.1073/pnas.1801109115.

188. Mejzini, R., Flynn, L. L., Pitout, I. L., Fletcher, S., Wilton, S. D., and Akkari, P. A. (2019). ALS Genetics, Mechanisms, and Therapeutics: Where Are We Now? *Frontiers in Neuroscience* 13, 1310. doi: 10.3389/fnins.2019.01310.

189. Milhorat, T. H., Capocelli, A. L., Anzil, A. P., Kotzen, R. M., and Milhorat, R. H. (1995). Pathological basis of spinal cord cavitation in syringomyelia: analysis of 105 autopsy cases. *J Neurosurg* 82, 802–812. doi: 10.3171/jns.1995.82.5.0802.

190. Miller, T., Cudkowicz, M., Shaw, P. J., Andersen, P. M., Atassi, N., Bucelli, R. C., et al. (2020). Phase 1-2 Trial of Antisense Oligonucleotide Tofersen for SOD1 ALS. *N Engl J Med* 383, 109–119. doi: 10.1056/NEJMoa2003715.

191. Miller, T. M., Pestronk, A., David, W., Rothstein, J., Simpson, E., Appel, S. H., et al. (2013). An antisense oligonucleotide against SOD1 delivered intrathecally for patients with SOD1 familial amyotrophic lateral sclerosis: a phase 1, randomised, first-in-man study. *Lancet Neurol* 12, 435–442. doi: 10.1016/S1474-4422(13)70061-9.

192. Miquel, E., Cassina, A., Martínez-Palma, L., Souza, J. M., Bolatto, C., Rodríguez-Bottero, S., et al. (2014). Neuroprotective effects of the mitochondria-targeted antioxidant MitoQ in a model of inherited amyotrophic lateral sclerosis. *Free Radic Biol Med* 70, 204–213. doi: 10.1016/j.freeradbiomed.2014.02.019.

193. Miron, V. E., and Franklin, R. J. M. (2014). Macrophages and CNS remyelination. *J Neurochem* 130, 165–171. doi: 10.1111/jnc.12705.

194. Monteiro, F. A., Miranda, R. M., Samina, M. C., Dias, A. F., Raposo, A. A. S. F., Oliveira, P., et al. (2021). Tlx3 Exerts Direct Control in Specifying Excitatory Over Inhibitory Neurons in the Dorsal Spinal Cord. *Front Cell Dev Biol* 9, 642697. doi: 10.3389/fcell.2021.642697.

195. Moore, D. L., Blackmore, M. G., Hu, Y., Kaestner, K. H., Bixby, J. L., Lemmon, V. P., et al. (2009). KLF Family Members Regulate Intrinsic Axon Regeneration Ability. *Science* 326, 298–301. doi: 10.1126/science.1175737.

196. Morata-Tarifa, C., Azkona, G., Glass, J., Mazzini, L., and Sanchez-Pernaute, R. (2021). Looking backward to move forward: a meta-analysis of stem cell therapy in amyotrophic lateral sclerosis. *npj Regen Med* 6, 1–10. doi: 10.1038/s41536-021-00131-5.

197. Morimoto, N., Nagai, M., Ohta, Y., Miyazaki, K., Kurata, T., Morimoto, M., et al. (2007). Increased autophagy in transgenic mice with a G93A mutant SOD1 gene. *Brain Res* 1167, 112–117. doi: 10.1016/j.brainres.2007.06.045.

198. Morita, T., and Sobue, K. (2009). Specification of Neuronal Polarity Regulated by Local Translation of CRMP2 and Tau via the mTOR-p70S6K Pathway*. *Journal of Biological Chemistry* 284, 27734–27745. doi: 10.1074/jbc.M109.008177.

199. Moutaux, E., Christaller, W., Scaramuzzino, C., Genoux, A., Charlot, B., Cazorla, M., et al. (2018). Neuronal network maturation differently affects secretory vesicles and mitochondria transport in axons. *Sci Rep* 8, 13429. doi: 10.1038/s41598-018-31759-x.

200. Mueller, C., Berry, J. D., McKenna-Yasek, D. M., Gernoux, G., Owegi, M. A., Pothier, L. M., et al. (2020). SOD1 Suppression with Adeno-Associated Virus and MicroRNA in Familial ALS. *N Engl J Med* 383, 151–158. doi: 10.1056/NEJMoa2005056.

201. Mukaino, M., Nakamura, M., Yamada, O., Okada, S., Morikawa, S., Renault-Mihara, F., et al. (2010). Anti-IL-6-receptor antibody promotes repair of spinal cord injury by inducing microglia-dominant inflammation. *Exp Neurol* 224, 403–414. doi: 10.1016/j.expneurol.2010.04.020.

202. Müller, T., Brohmann, H., Pierani, A., Heppenstall, P. A., Lewin, G. R., Jessell, T. M., et al. (2002). The homeodomain factor lbx1 distinguishes two major programs of neuronal differentiation in the dorsal spinal cord. *Neuron* 34, 551–562. doi: 10.1016/s0896-6273(02)00689-x.

203. Muñoz-Galdeano, T., Reigada, D., Del Águila, Á., Velez, I., Caballero-López, M. J., Maza, R. M., et al. (2018). Cell Specific Changes of Autophagy in a Mouse Model of Contusive Spinal Cord Injury. *Front Cell Neurosci* 12, 164. doi: 10.3389/fncel.2018.00164.

204. Nabavi, S. M., Arab, L., Jarooghi, N., Bolurieh, T., Abbasi, F., Mardpour, S., et al. (2019). Safety, Feasibility of Intravenous and Intrathecal Injection of Autologous Bone Marrow Derived Mesenchymal Stromal Cells in Patients with Amyotrophic Lateral Sclerosis: An Open Label Phase I Clinical Trial. *Cell J* 20, 592–598. doi: 10.22074/cellj.2019.5370.

205. Nassif, M., Valenzuela, V., Rojas-Rivera, D., Vidal, R., Matus, S., Castillo, K., et al. (2014). Pathogenic role of BECN1/Beclin 1 in the development of amyotrophic lateral sclerosis. *Autophagy* 10, 1256–1271. doi: 10.4161/auto.28784.

206. Neumann, S., Braz, J. M., Skinner, K., Llewellyn-Smith, I. J., and Basbaum, A. I. (2008). Innocuous, not noxious, input activates PKCgamma interneurons of the spinal dorsal horn via myelinated afferent fibers. *J Neurosci* 28, 7936–7944. doi: 10.1523/JNEUROSCI.1259-08.2008.

207. Nicholls, J., and Saunders, N. (1996). Regeneration of immature mammalian spinal cord after injury. *Trends Neurosci* 19, 229–234. doi: 10.1016/0166-2236(96)10021-7.

208. Nieuwenhuis, B., Barber, A. C., Evans, R. S., Pearson, C. S., Fuchs, J., MacQueen, A. R., et al. (2020). PI 3-kinase delta enhances axonal PIP 3 to support axon regeneration in the adult CNS. *EMBO Mol Med* 12, e11674. doi: 10.15252/emmm.201911674.

209. Nishitoh, H., Matsuzawa, A., Tobiume, K., Saegusa, K., Takeda, K., Inoue, K., et al. (2002). ASK1 is essential for endoplasmic reticulum stress-induced neuronal cell death triggered by expanded polyglutamine repeats. *Genes Dev* 16, 1345–1355. doi: 10.1101/gad.992302.

210. Nixon, R. A., and Yang, D.-S. (2012). Autophagy and Neuronal Cell Death in Neurological Disorders. *Cold Spring Harb Perspect Biol* 4, a008839. doi: 10.1101/cshperspect.a008839.

211. Noguchi, M., Hirata, N., Tanaka, T., Suizu, F., Nakajima, H., and Chiorini, J. A. (2020). Autophagy as a modulator of cell death machinery. *Cell Death Dis* 11, 1–12. doi: 10.1038/s41419-020-2724-5.

212. Norris, C. M., Blalock, E. M., Thibault, O., Brewer, L. D., Clodfelter, G. V., Porter, N. M., et al. (2006). Electrophysiological Mechanisms of Delayed Excitotoxicity: Positive Feedback Loop Between NMDA Receptor Current and Depolarization-Mediated Glutamate Release. *J Neurophysiol* 96, 2488–2500. doi: 10.1152/jn.00593.2005.

213. Novak, I., Kirkin, V., McEwan, D. G., Zhang, J., Wild, P., Rozenknop, A., et al. (2010). Nix is a selective autophagy receptor for mitochondrial clearance. *EMBO Rep* 11, 45–51. doi: 10.1038/embor.2009.256.

214. Okada, S., Nakamura, M., Mikami, Y., Shimazaki, T., Mihara, M., Ohsugi, Y., et al. (2004). Blockade of Interleukin-6 Receptor Suppresses Reactive Astrogliosis and Ameliorates Functional Recovery in Experimental Spinal Cord Injury. *J Neurosci Res* 76, 265–276. doi: 10.1002/jnr.20044.

215. O'Reilly, K. E., Rojo, F., She, Q.-B., Solit, D., Mills, G. B., Smith, D., et al. (2006). mTOR Inhibition Induces Upstream Receptor Tyrosine Kinase Signaling and Activates Akt. *Cancer Res* 66, 1500–1508. doi: 10.1158/0008-5472.CAN-05-2925.

216. Oyanagi, K., Yamazaki, M., Takahashi, H., Watabe, K., Wada, M., Komori, T., et al. (2008). Spinal anterior horn cells in sporadic amyotrophic lateral sclerosis show ribosomal detachment from, and cisternal distention of the rough endoplasmic reticulum. *Neuropathology and Applied Neurobiology* 34, 650–658. doi: 10.1111/j.1365-2990.2008.00941.x.

217. Oyinbo, C. A. (2011). Secondary injury mechanisms in traumatic spinal cord injury: a nugget of this multiply cascade. *Acta Neurobiol Exp (Wars)* 71, 281–299.

218. Paganoni, S., Macklin, E. A., Hendrix, S., Berry, J. D., Elliott, M. A., Maiser, S., et al. (2020). Trial of Sodium Phenylbutyrate-Taurursodiol for Amyotrophic Lateral Sclerosis. *N Engl J Med* 383, 919–930. doi: 10.1056/NEJMoa1916945.

219. Pankiv, S., Clausen, T. H., Lamark, T., Brech, A., Bruun, J.-A., Outzen, H., et al. (2007). p62/SQSTM1 binds directly to Atg8/LC3 to facilitate degradation of ubiquitinated protein aggregates by autophagy. *J Biol Chem* 282, 24131–24145. doi: 10.1074/jbc.M702824200.

220. Park, C.-H., Joa, K.-L., Lee, M.-O., Yoon, S.-H., and Kim, M.-O. (2020). The combined effect of granulocyte-colony stimulating factor (G-CSF) treatment and exercise in rats with spinal cord injury. *The Journal of Spinal Cord Medicine* 43, 339–346. doi: 10.1080/10790268.2018.1521567.

221. Park, K. K., Liu, K., Hu, Y., Smith, P. D., Wang, C., Cai, B., et al. (2008). Promoting axon regeneration in the adult CNS by modulation of the PTEN/mTOR pathway. *Science* 322, 963–966. doi: 10.1126/science.1161566.

222. Pelisch, N., Rosas Almanza, J., Stehlik, K. E., Aperi, B. V., and Kroner, A. (2020). CCL3 contributes to secondary damage after spinal cord injury. *J Neuroinflammation* 17. doi: 10.1186/s12974-020-02037-3.

223. Perera, N. D., Sheean, R. K., Lau, C. L., Shin, Y. S., Beart, P. M., Horne, M. K., et al. (2018). Rilmenidine promotes MTOR-independent autophagy in the mutant SOD1 mouse model of amyotrophic lateral sclerosis without slowing disease progression. *Autophagy* 14, 534–551. doi: 10.1080/15548627.2017.1385674.

224. Petitjean, H., Pawlowski, S. A., Fraine, S. L., Sharif, B., Hamad, D., Fatima, T., et al. (2015). Dorsal Horn Parvalbumin Neurons Are Gate-Keepers of Touch-Evoked Pain after Nerve Injury. *Cell Rep* 13, 1246–1257. doi: 10.1016/j.celrep.2015.09.080.

225. Petrova, V., and Eva, R. (2018). The Virtuous Cycle of Axon Growth: Axonal Transport of Growth-Promoting Machinery as an Intrinsic Determinant of Axon Regeneration. *Developmental Neurobiology* 78, 898–925. doi: https://doi.org/10.1002/dneu.22608.

226. Petrova, V., Nieuwenhuis, B., Fawcett, J. W., and Eva, R. (2021). Axonal Organelles as Molecular Platforms for Axon Growth and Regeneration after Injury. *Int J Mol Sci* 22, 1798. doi: 10.3390/ijms22041798.

227. Petrova, V., Pearson, C. S., Ching, J., Tribble, J. R., Solano, A. G., Yang, Y., et al. (2020). Protrudin functions from the endoplasmic reticulum to support axon regeneration in the adult CNS. *Nat Commun* 11. doi: 10.1038/s41467-020-19436-y.

228. Pineau, I., Sun, L., Bastien, D., and Lacroix, S. (2010). Astrocytes initiate inflammation in the injured mouse spinal cord by promoting the entry of neutrophils and inflammatory monocytes in an IL-1 receptor/MyD88-dependent fashion. *Brain Behav Immun* 24, 540–553. doi: 10.1016/j.bbi.2009.11.007.

229. Polymenidou, M., and Cleveland, D. W. (2011). The seeds of neurodegeneration: prion-like spreading in ALS. *Cell* 147, 498–508. doi: 10.1016/j.cell.2011.10.011.

230. Popovich, P. G., and Jones, T. B. (2003). Manipulating neuroinflammatory reactions in the injured spinal cord: back to basics. *Trends Pharmacol Sci* 24, 13–17. doi: 10.1016/s0165-6147(02)00006-8.

231. Przedborski, S., Vila, M., and Jackson-Lewis, V. (2003). Series Introduction: Neurodegeneration: What is it and where are we? *J Clin Invest* 111, 3–10. doi: 10.1172/JCI200317522.

232. Qian, K., Huang, H., Peterson, A., Hu, B., Maragakis, N. J., Ming, G.-L., et al. (2017a). Sporadic ALS Astrocytes Induce Neuronal Degeneration In Vivo. *Stem Cell Reports* 8, 843–855. doi: 10.1016/j.stemcr.2017.03.003.

233. Qian, M., Fang, X., and Wang, X. (2017b). Autophagy and inflammation. *Clin Transl Med* 6, 24. doi: 10.1186/s40169-017-0154-5.

234. Ramesh, G., MacLean, A. G., and Philipp, M. T. (2013). Cytokines and chemokines at the crossroads of neuroinflammation, neurodegeneration, and neuropathic pain. *Mediators Inflamm* 2013, 480739. doi: 10.1155/2013/480739.

235. Ramesh, N., and Pandey, U. B. (2017). Autophagy Dysregulation in ALS: When Protein Aggregates Get Out of Hand. *Frontiers in Molecular Neuroscience* 10, 263. doi: 10.3389/fnmol.2017.00263.

236. Ravikumar, B., Moreau, K., Jahreiss, L., Puri, C., and Rubinsztein, D. C. (2010). Plasma membrane contributes to the formation of pre-autophagosomal structures. *Nat Cell Biol* 12, 747–757. doi: 10.1038/ncb2078.

237. Řehořová, M., Vargová, I., Forostyak, S., Vacková, I., Turnovcová, K., Kupcová Skalníková, H., et al. (2019). A Combination of Intrathecal and Intramuscular Application of Human Mesenchymal Stem Cells Partly Reduces the Activation of Necroptosis in the Spinal Cord of SOD1G93A Rats. *Stem Cells Transl Med* 8, 535–547. doi: 10.1002/sctm.18-0223.

238. Ren, H., Chen, X., Tian, M., Zhou, J., Ouyang, H., and Zhang, Z. (2018). Regulation of Inflammatory Cytokines for Spinal Cord Injury Repair Through Local Delivery of Therapeutic Agents. *Adv. Sci.* 5, 1800529. doi: 10.1002/advs.201800529.

239. Ribas, V. T., Schnepf, B., Challagundla, M., Koch, J. C., Bähr, M., and Lingor, P. (2015). Early and sustained activation of autophagy in degenerating axons after spinal cord injury. *Brain Pathol* 25, 157–170. doi: 10.1111/bpa.12170.

240. Richter, B., Sliter, D. A., Herhaus, L., Stolz, A., Wang, C., Beli, P., et al. (2016). Phosphorylation of OPTN by TBK1 enhances its binding to Ub chains and promotes selective autophagy of damaged mitochondria. *Proc Natl Acad Sci U S A* 113, 4039–4044. doi: 10.1073/pnas.1523926113.

241. Rojas, F., Cortes, N., Abarzua, S., Dyrda, A., and van Zundert, B. (2014). Astrocytes expressing mutant SOD1 and TDP43 trigger motoneuron death that is mediated via sodium channels and nitroxidative stress. *Front Cell Neurosci* 8, 24. doi: 10.3389/fncel.2014.00024.

242. Rowland, J. W., Hawryluk, G. W. J., Kwon, B., and Fehlings, M. G. (2008). Current status of acute spinal cord injury pathophysiology and emerging therapies: promise on the horizon. *Neurosurg Focus* 25, E2. doi: 10.3171/FOC.2008.25.11.E2.

243. Russ, D. E., Cross, R. B. P., Li, L., Koch, S. C., Matson, K. J. E., Yadav, A., et al. (2021). A harmonized atlas of mouse spinal cord cell types and their spatial organization. *Nat Commun* 12, 5722. doi: 10.1038/s41467-021-25125-1.

244. Russell, R. C., Tian, Y., Yuan, H., Park, H. W., Chang, Y.-Y., Kim, J., et al. (2013). ULK1 induces autophagy by phosphorylating Beclin-1 and activating VPS34 lipid kinase. *Nat Cell Biol* 15, 741–750. doi: 10.1038/ncb2757.

245. Ruzicka, J., Machova-Urdzikova, L., Gillick, J., Amemori, T., Romanyuk, N., Karova, K., et al. (2017). A Comparative Study of Three Different Types of Stem Cells for Treatment of Rat Spinal Cord Injury. *Cell Transplant* 26, 585–603. doi: 10.3727/096368916X693671.

246. Saitoh, T., and Akira, S. (2010). Regulation of innate immune responses by autophagy-related proteins. *J Cell Biol* 189, 925–935. doi: 10.1083/jcb.201002021.

247. Sanchez, C. L., Sims, S. G., Nowery, J. D., and Meares, G. P. (2019). Endoplasmic reticulum stress differentially modulates the IL-6 family of cytokines in murine astrocytes and macrophages. *Sci Rep* 9, 14931. doi: 10.1038/s41598-019-51481-6.

248. Sarbassov, D. D. (2005). Phosphorylation and Regulation of Akt/PKB by the Rictor-mTOR Complex. *Science* 307, 1098–1101. doi: 10.1126/science.1106148.

249. Sasaki, S. (2010). Endoplasmic reticulum stress in motor neurons of the spinal cord in sporadic amyotrophic lateral sclerosis. *J Neuropathol Exp Neurol* 69, 346–355. doi: 10.1097/NEN.0b013e3181d44992.

250. Sasaki, S., Takeda, T., Shibata, N., and Kobayashi, M. (2010). Alterations in subcellular localization of TDP-43 immunoreactivity in the anterior horns in sporadic amyotrophic lateral sclerosis. *Neurosci Lett* 478, 72–76. doi: 10.1016/j.neulet.2010.04.068.

251. Schindelin, J., Arganda-Carreras, I., Frise, E., Kaynig, V., Longair, M., Pietzsch, T., et al. (2012). Fiji: an open-source platform for biological-image analysis. *Nature Methods* 9, 676–682. doi: 10.1038/nmeth.2019.

252. Sekiguchi, A., Kanno, H., Ozawa, H., Yamaya, S., and Itoi, E. (2012). Rapamycin Promotes Autophagy and Reduces Neural Tissue Damage and Locomotor Impairment after Spinal Cord Injury in Mice. *J Neurotrauma* 29, 946–956. doi: 10.1089/neu.2011.1919.

253. Shah, M., Peterson, C., Yilmaz, E., Halalmeh, D. R., and Moisi, M. (2020). Current advancements in the management of spinal cord injury: A comprehensive review of literature. *Surgical Neurology International* 11, 2. doi: 10.25259/SNI_568_2019.

254. Shen, J., Snapp, E. L., Lippincott-Schwartz, J., and Prywes, R. (2005). Stable Binding of ATF6 to BiP in the Endoplasmic Reticulum Stress Response. *Molecular and Cellular Biology* 25, 921–932. doi: 10.1128/MCB.25.3.921-932.2005.

255. Song, M., Mohamad, O., Chen, D., and Yu, S. P. (2013). Coordinated Development of Voltage-Gated Na+ and K+ Currents Regulates Functional Maturation of Forebrain Neurons Derived from Human Induced Pluripotent Stem Cells. *Stem Cells Dev* 22, 1551–1563. doi: 10.1089/scd.2012.0556.

256. Spilman, P., Podlutskaya, N., Hart, M. J., Debnath, J., Gorostiza, O., Bredesen, D., et al. (2010). Inhibition of mTOR by rapamycin abolishes cognitive deficits and reduces amyloid-beta levels in a mouse model of Alzheimer's disease. *PLoS One* 5, e9979. doi: 10.1371/journal.pone.0009979.

257. Srivastava, I. N., Shperdheja, J., Baybis, M., Ferguson, T., and Crino, P. B. (2016). mTOR pathway inhibition prevents neuroinflammation and neuronal death in a mouse model of cerebral palsy. *Neurobiol Dis* 85, 144–154. doi: 10.1016/j.nbd.2015.10.001.

258. Stavoe, A. K. H., and Holzbaur, E. L. F. (2019). Autophagy in Neurons. *Annu Rev Cell Dev Biol* 35, 477–500. doi: 10.1146/annurev-cellbio-100818-125242.

259. Stoica, L., Todeasa, S. H., Cabrera, G. T., Salameh, J. S., ElMallah, M. K., Mueller, C., et al. (2016). Adeno-associated virus-delivered artificial microRNA extends survival and delays paralysis in an amyotrophic lateral sclerosis mouse model. *Ann Neurol* 79, 687–700. doi: 10.1002/ana.24618.

260. Sun, J., and Harrington, M. A. (2019). The Alteration of Intrinsic Excitability and Synaptic Transmission in Lumbar Spinal Motor Neurons and Interneurons of Severe Spinal Muscular Atrophy Mice. *Frontiers in Cellular Neuroscience* 13, 15. doi: 10.3389/fncel.2019.00015.

261. Sun, Z., Williams, D. J., Xu, B., and Gogos, J. A. (2018). Altered function and maturation of primary cortical neurons from a 22q11.2 deletion mouse model of schizophrenia. *Transl Psychiatry* 8, 85. doi: 10.1038/s41398-018-0132-8.

262. Switon, K., Kotulska, K., Janusz-Kaminska, A., Zmorzynska, J., and Jaworski, J. (2017). Molecular neurobiology of mTOR. *Neuroscience* 341, 112–153. doi: 10.1016/j.neuroscience.2016.11.017.

263. Takazawa, T., Croft, G. F., Amoroso, M. W., Studer, L., Wichterle, H., and MacDermott, A. B. (2012). Maturation of Spinal Motor Neurons Derived from Human Embryonic Stem Cells. *PLOS ONE* 7, e40154. doi: 10.1371/journal.pone.0040154.

264. Takikawa, M., and Ohki, R. (2017). A vicious partnership between AKT and PHLDA3 to facilitate neuroendocrine tumors. *Cancer Science* 108, 1101–1108. doi: 10.1111/cas.13235.

265. Tanabe, F., Yone, K., Kawabata, N., Sakakima, H., Matsuda, F., Ishidou, Y., et al. (2011). Accumulation of p62 in degenerated spinal cord under chronic mechanical compression: functional analysis of p62 and autophagy in hypoxic neuronal cells. *Autophagy* 7, 1462–1471. doi: 10.4161/auto.7.12.17892.

266. Tanaka, M., Sakata, T., Palumbo, J., and Akimoto, M. (2016). A 24-Week, Phase III, Double-Blind, Parallel-Group Study of Edaravone (MCI-186) for Treatment of Amyotrophic Lateral Sclerosis (ALS) (P3.189). *Neurology* 86. Available at: https://n.neurology.org/content/86/16_Supplement/P3.189 [Accessed January 11, 2022].

267. Tang, P., Hou, H., Zhang, L., Lan, X., Mao, Z., Liu, D., et al. (2014). Autophagy reduces neuronal damage and promotes locomotor recovery via inhibition of apoptosis after spinal cord injury in rats. *Mol Neurobiol* 49, 276–287. doi: 10.1007/s12035-013-8518-3.

268. Tanida, I., Ueno, T., and Kominami, E. (2008). LC3 and Autophagy. *Methods Mol Biol* 445, 77–88. doi: 10.1007/978-1-59745-157-4_4.

269. Taoka, Y., Okajima, K., Murakami, K., Johno, M., and Naruo, M. (1998). Role of neutrophil elastase in compression-induced spinal cord injury in rats. *Brain Res* 799, 264–269. doi: 10.1016/s0006-8993(98)00459-4.

270. Taylor, J. P., Brown, R. H., and Cleveland, D. W. (2016). Decoding ALS: From Genes to Mechanism. *Nature* 539, 197–206. doi: 10.1038/nature20413.

271. Thomson, C. E., McCulloch, M., Sorenson, A., Barnett, S. C., Seed, B. V., Griffiths, I. R., et al. (2008). Myelinated, synapsing cultures of murine spinal cord – validation as an in vitro model of the central nervous system. *Eur J Neurosci* 28, 1518–1535. doi: 10.1111/j.1460-9568.2008.06415.x.

272. Thoreen, C. C., Kang, S. A., Chang, J. W., Liu, Q., Zhang, J., Gao, Y., et al. (2009). An ATP-competitive Mammalian Target of Rapamycin Inhibitor Reveals Rapamycin-resistant Functions of mTORC1. *J Biol Chem* 284, 8023–8032. doi: 10.1074/jbc.M900301200.

273. Tian, F., Morimoto, N., Liu, W., Ohta, Y., Deguchi, K., Miyazaki, K., et al. (2011). In vivo optical imaging of motor neuron autophagy in a mouse model of amyotrophic lateral sclerosis. *Autophagy* 7, 985–992. doi: 10.4161/auto.7.9.16012.

274. Tirasophon, W., Welihinda, A. A., and Kaufman, R. J. (1998). A stress response pathway from the endoplasmic reticulum to the nucleus requires a novel bifunctional protein kinase/endoribonuclease (Ire1p) in mammalian cells. *Genes Dev.* 12, 1812–1824. doi: 10.1101/gad.12.12.1812.

275. Torregrossa, F., Sallì, M., and Grasso, G. (2020). Emerging Therapeutic Strategies for Traumatic Spinal Cord Injury. *World Neurosurgery* 140, 591–601. doi: 10.1016/j.wneu.2020.03.199.

276. Tripathi, P., Rodriguez-Muela, N., Klim, J. R., de Boer, A. S., Agrawal, S., Sandoe, J., et al. (2017). Reactive Astrocytes Promote ALS-like Degeneration and Intracellular Protein Aggregation in Human Motor Neurons by Disrupting Autophagy through TGF-β1. *Stem Cell Reports* 9, 667–680. doi: 10.1016/j.stemcr.2017.06.008.

277. Tsuboyama, K., Koyama-Honda, I., Sakamaki, Y., Koike, M., Morishita, H., and Mizushima, N. (2016). The ATG conjugation systems are important for degradation of the inner autophagosomal membrane. *Science* 354, 1036–1041. doi: 10.1126/science.aaf6136.

278. Tsvetkov, A. S., Miller, J., Arrasate, M., Wong, J. S., Pleiss, M. A., and Finkbeiner, S. (2010). A small-molecule scaffold induces autophagy in primary neurons and protects against toxicity in a Huntington disease model. *Proc Natl Acad Sci U S A* 107, 16982–16987. doi: 10.1073/pnas.1004498107.

279. Turnovcova, K., Ruzickova, K., Vanecek, V., Sykova, E., and Jendelova, P. (2009). Properties and growth of human bone marrow mesenchymal stromal cells cultivated in different media. *Cytotherapy* 11, 874–885. doi: 10.3109/14653240903188947.

280. Tyzack, G. E., Hall, C. E., Sibley, C. R., Cymes, T., Forostyak, S., Carlino, G., et al. (2017). A neuroprotective astrocyte state is induced by neuronal signal EphB1 but fails in ALS models. *Nat Commun* 8, 1164. doi: 10.1038/s41467-017-01283-z.

281. Tyzack, G. E., Sitnikov, S., Barson, D., Adams-Carr, K. L., Lau, N. K., Kwok, J. C., et al. (2014). Astrocyte response to motor neuron injury promotes structural synaptic plasticity via STAT3-regulated TSP-1 expression. *Nat Commun* 5, 4294. doi: 10.1038/ncomms5294.

282. Van Deerlin, V. M., Leverenz, J. B., Bekris, L. M., Bird, T. D., Yuan, W., Elman, L. B., et al. (2008). TARDBP mutations in amyotrophic lateral sclerosis with TDP-43 neuropathology: a genetic and histopathological analysis. *Lancet Neurol* 7, 409–416. doi: 10.1016/S1474-4422(08)70071-1.

283. van der Vaart, A., Griffith, J., and Reggiori, F. (2010). Exit from the Golgi Is Required for the Expansion of the Autophagosomal Phagophore in Yeast Saccharomyces cerevisiae. *Mol Biol Cell* 21, 2270–2284. doi: 10.1091/mbc.E09-04-0345.

284. van Niekerk, E. A., Tuszynski, M. H., Lu, P., and Dulin, J. N. (2016). Molecular and Cellular Mechanisms of Axonal Regeneration After Spinal Cord Injury. *Mol Cell Proteomics* 15, 394–408. doi: 10.1074/mcp.R115.053751.

285. Vanický, I., Urdzíková, L., Saganová, K., Čízková, D., and Gálik, J. (2001). A Simple and Reproducible Model of Spinal Cord Injury Induced by Epidural Balloon Inflation in the Rat. *Journal of Neurotrauma* 18, 1399–1407. doi: 10.1089/08977150152725687.

286. Vargova, I., Machova Urdzikova, L., Karova, K., Smejkalova, B., Sursal, T., Cimermanova, V., et al. (2021). Involvement of mTOR Pathways in Recovery from Spinal Cord Injury by Modulation of Autophagy and Immune Response. *Biomedicines* 9, 593. doi: 10.3390/biomedicines9060593.

287. Vattem, K. M., and Wek, R. C. (2004). Reinitiation involving upstream ORFs regulates ATF4 mRNA translation in mammalian cells. *PNAS* 101, 11269–11274. doi: 10.1073/pnas.0400541101.

288. Venkatesh, K., Ghosh, S. K., Mullick, M., Manivasagam, G., and Sen, D. (2019). Spinal cord injury: pathophysiology, treatment strategies, associated challenges, and future implications. *Cell Tissue Res* 377, 125–151. doi: 10.1007/s00441-019-03039-1.

289. Vercelli, A., Mereuta, O. M., Garbossa, D., Muraca, G., Mareschi, K., Rustichelli, D., et al. (2008). Human mesenchymal stem cell transplantation extends survival, improves motor performance and decreases neuroinflammation in mouse model of amyotrophic lateral sclerosis. *Neurobiol Dis* 31, 395–405. doi: 10.1016/j.nbd.2008.05.016.

290. Vicencio, E., Beltrán, S., Labrador, L., Manque, P., Nassif, M., and Woehlbier, U. (2020). Implications of Selective Autophagy Dysfunction for ALS Pathology. *Cells* 9, 381. doi: 10.3390/cells9020381.

291. Walker, A. K., Soo, K. Y., Sundaramoorthy, V., Parakh, S., Ma, Y., Farg, M. A., et al. (2013). ALS-Associated TDP-43 Induces Endoplasmic Reticulum Stress, Which Drives Cytoplasmic TDP-43 Accumulation and Stress Granule Formation. *PLOS ONE* 8, e81170. doi: 10.1371/journal.pone.0081170.

292. Walsh, J. T., Zheng, J., Smirnov, I., Lorenz, U., Tung, K., and Kipnis, J. (2014). Regulatory T cells in central nervous system injury: a double-edged sword. *J Immunol* 193, 5013–5022. doi: 10.4049/jimmunol.1302401.

293. Wang, S., and Kaufman, R. J. (2012). The impact of the unfolded protein response on human disease. *Journal of Cell Biology* 197, 857–867. doi: 10.1083/jcb.201110131.

294. Wang, X., Li, X., Huang, B., and Ma, S. (2016). Blocking mammalian target of rapamycin (mTOR) improves neuropathic pain evoked by spinal cord injury. *Transl Neurosci*, 7. doi: 10.1515/tnsci-2016-0008.

295. Wilson, J. M., Hartley, R., Maxwell, D. J., Todd, A. J., Lieberam, I., Kaltschmidt, J. A., et al. (2005). Conditional Rhythmicity of Ventral Spinal Interneurons Defined by Expression of the Hb9 Homeodomain Protein. *J. Neurosci.* 25, 5710–5719. doi: 10.1523/JNEUROSCI.0274-05.2005.

296. Wolfe, M. S. (2018). "Chapter 1 - Solving the Puzzle of Neurodegeneration," in *The Molecular and Cellular Basis of Neurodegenerative Diseases*, ed. M. S. Wolfe (Academic Press), 1–22. doi: 10.1016/B978-0-12-811304-2.00001-8.

297. Wong, Y. C., and Holzbaur, E. L. F. (2015). Autophagosome dynamics in neurodegeneration at a glance. *J Cell Sci* 128, 1259–1267. doi: 10.1242/jcs.161216.

298. Wosiski-Kuhn, M., Caress, J. B., Cartwright, M. S., Hawkins, G. A., and Milligan, C. (2021). Interleukin 6 (IL6) level is a biomarker for functional disease progression within IL6R358Ala variant groups in amyotrophic lateral sclerosis patients. *Amyotroph Lateral Scler Frontotemporal Degener* 22, 248–259. doi: 10.1080/21678421.2020.1813310.

299. Wu, J., and Lipinski, M. M. (2019). Autophagy in Neurotrauma: Good, Bad, or Dysregulated. *Cells* 8, 693. doi: 10.3390/cells8070693.

300. Wu, S.-T., Sun, G.-H., Cha, T.-L., Kao, C.-C., Chang, S.-Y., Kuo, S.-C., et al. (2016). CSC-3436 switched tamoxifen-induced autophagy to apoptosis through the inhibition of AMPK/mTOR pathway. *J Biomed Sci* 23, 60. doi: 10.1186/s12929-016-0275-y.

301. Wullschleger, S., Loewith, R., and Hall, M. N. (2006). TOR signaling in growth and metabolism. *Cell* 124, 471–484. doi: 10.1016/j.cell.2006.01.016.

302. Xie, L., Sun, F., Wang, J., Mao, X., Xie, L., Yang, S.-H., et al. (2014). mTOR signaling inhibition modulates macrophages/microglia-mediated neuroinflammation and secondary injury via regulatory T cells after focal ischemia. *J Immunol* 192, 6009–6019. doi: 10.4049/jimmunol.1303492.

303. Xu, X., Shen, D., Gao, Y., Zhou, Q., Ni, Y., Meng, H., et al. (2021). A perspective on therapies for amyotrophic lateral sclerosis: can disease progression be curbed? *Translational Neurodegeneration* 10, 29. doi: 10.1186/s40035-021-00250-5.

304. Yan, P., Bai, L., Lu, W., Gao, Y., Bi, Y., and Lv, G. (2017). Regulation of autophagy by AMP-activated protein kinase/sirtuin 1 pathway reduces spinal cord neurons damage. *Iran J Basic Med Sci* 20, 1029–1036. doi: 10.22038/IJBMS.2017.9272.

305. Yao, Y. (2021). Mutant Genes in Amyotrophic Lateral sclerosis Associated with Autophagy. *BJSTR* 33. doi: 10.26717/BJSTR.2021.33.005339.

306. Yoshida, H., Okada, T., Haze, K., Yanagi, H., Yura, T., Negishi, M., et al. (2000). ATF6 Activated by Proteolysis Binds in the Presence of NF-Y (CBF) Directly to the cis-Acting Element Responsible for the Mammalian Unfolded Protein Response. *Molecular and Cellular Biology* 20, 6755–6767. doi: 10.1128/MCB.20.18.6755-6767.2000.

307. Yoshii, S. R., and Mizushima, N. (2017). Monitoring and Measuring Autophagy. *Int J Mol Sci* 18, 1865. doi: 10.3390/ijms18091865.

308. Yoshino, H., and Kimura, A. (2006). Investigation of the therapeutic effects of edaravone, a free radical scavenger, on amyotrophic lateral sclerosis (Phase II study). *Amyotroph Lateral Scler* 7, 241–245. doi: 10.1080/17482960600881870.

309. Zalfa, C., Rota Nodari, L., Vacchi, E., Gelati, M., Profico, D., Boido, M., et al. (2019). Transplantation of clinical-grade human neural stem cells reduces neuroinflammation, prolongs survival and delays disease progression in the SOD1 rats. *Cell Death Dis* 10, 345. doi: 10.1038/s41419-019-1582-5.

310. Zamanian, J. L., Xu, L., Foo, L. C., Nouri, N., Zhou, L., Giffard, R. G., et al. (2012). Genomic Analysis of Reactive Astrogliosis. *J Neurosci* 32, 6391–6410. doi: 10.1523/JNEUROSCI.6221-11.2012.

311. Zarei, S., Carr, K., Reiley, L., Diaz, K., Guerra, O., Altamirano, P., et al. (2015). A comprehensive review of amyotrophic lateral sclerosis. *Surg Neurol Int* 6, 171. doi: 10.4103/2152-7806.169561.

312. Zeng, H., and Sanes, J. R. (2017). Neuronal cell-type classification: challenges, opportunities and the path forward. *Nat Rev Neurosci* 18, 530–546. doi: 10.1038/nrn.2017.85.

313. Zhang, D., Zhu, D., Wang, F., Zhu, J.-C., Zhai, X., Yuan, Y., et al. (2020). Therapeutic effect of regulating autophagy in spinal cord injury: a network meta-analysis of direct and indirect comparisons. *Neural Regen Res* 15, 1120–1132. doi: 10.4103/1673-5374.270419.

314. Zhang, H.-Y., Wang, Z.-G., Wu, F.-Z., Kong, X.-X., Yang, J., Lin, B.-B., et al. (2013). Regulation of autophagy and ubiquitinated protein accumulation by bFGF promotes functional recovery and neural protection in a rat model of spinal cord injury. *Mol Neurobiol* 48, 452–464. doi: 10.1007/s12035-013-8432-8.

315. Zhang, J., Zhou, Q., Chen, S., and Le, W. (2018). Repurposing carbamazepine for the treatment of amyotrophic lateral sclerosis in SOD1-G93A mouse model. *CNS Neurosci Ther* 24, 1163–1174. doi: 10.1111/cns.12855.

316. Zhang, X., Chen, S., Lu, K., Wang, F., Deng, J., Xu, Z., et al. (2019). Verapamil Ameliorates Motor Neuron Degeneration and Improves Lifespan in the SOD1G93A Mouse Model of ALS by Enhancing Autophagic Flux. *Aging Dis* 10, 1159–1173. doi: 10.14336/AD.2019.0228.

317. Zhong, G., Díaz-Ríos, M., and Harris-Warrick, R. M. (2006). Intrinsic and Functional Differences among Commissural Interneurons during Fictive Locomotion and Serotonergic Modulation in the Neonatal Mouse. *J. Neurosci.* 26, 6509–6517. doi: 10.1523/JNEUROSCI.1410-06.2006.

318. Zhou, Q., Zhang, J., Li, S., Chen, S., and Le, W. (2017). n-butylidenephthalide treatment prolongs life span and attenuates motor neuron loss in SOD1G93A mouse model of amyotrophic lateral sclerosis. *CNS Neurosci Ther* 23, 375–385. doi: 10.1111/cns.12681.

319. Zhou, X., He, X., and Ren, Y. (2014). Function of microglia and macrophages in secondary damage after spinal cord injury. *Neural Regen Res* 9, 1787–1795. doi: 10.4103/1673-5374.143423.

10. LIST OF PUBLICATIONS

Original scientific works in extenso, which are the basis of the dissertation

Řehořová, M., **Vargová, I**., Forostyak, S., Vacková, I., Turnovcová, K., Kupcová Skalníková, H., Vodička, P., Kubinová, Š., Syková, E., Jendelová, P. (2019). A Combination of Intrathecal and Intramuscular Application of Human Mesenchymal Stem Cells Partly Reduces the Activation of Necroptosis in the Spinal Cord of SOD1G93A Rats. *Stem Cells Transl Med* 8, 535–547. doi:10.1002/sctm.18-0223. IF 2019: **6.429**

Vargova, I., Machova Urdzikova, L., Karova, K., Smejkalova, B., Sursal, T., Cimermanova, V., Turnovcova, K., Gandhi, C.D., Jhanwar-Uniyal, M., Jendelova, P. (2021). Involvement of mTOR Pathways in Recovery from Spinal Cord Injury by Modulation of Autophagy and Immune Response. *Biomedicines* 9, 593. doi:10.3390/biomedicines9060593. IF 2021: **5.612**

Vargova, I., Kriska, J., Kwok, J.C.F., Fawcett, J.W., Jendelova, P. (2022) Long-Term Cultures of Spinal Cord Interneurons. *Front Cell Neurosci* 16:827628. doi: 10.3389/fncel.2022.827628. IF 2021: **5.505**

11. APPENDIX